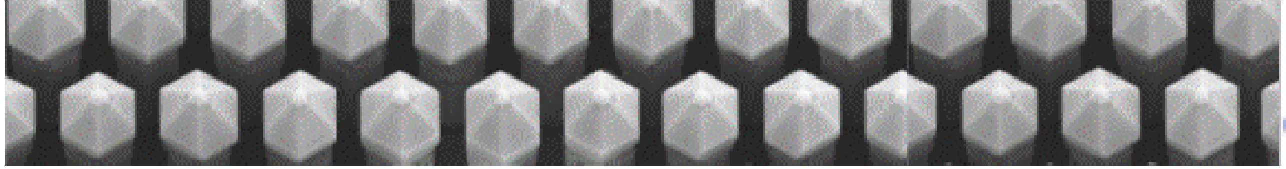

Nanowires

of III-nitride compounds

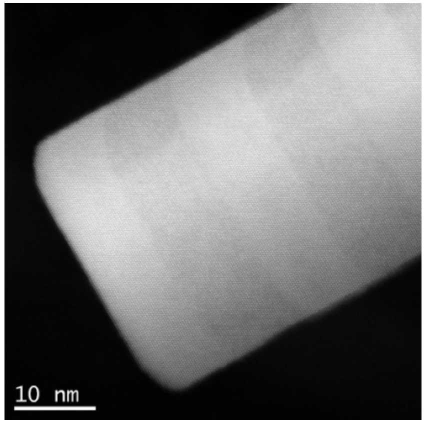

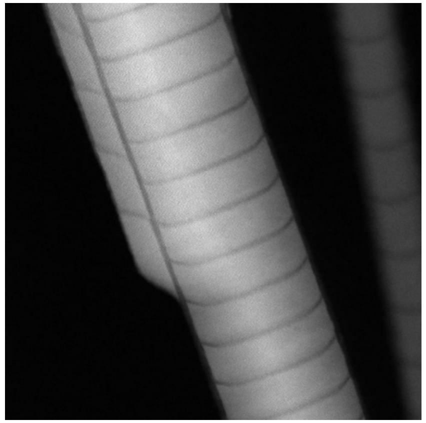

Jean-Christophe Harmand

Laboratoire de Photonique et de Nanostructures
CNRS
Route de Nozay, 91640 Marcoussis, France

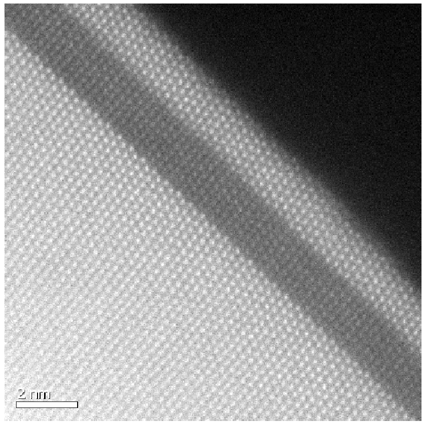

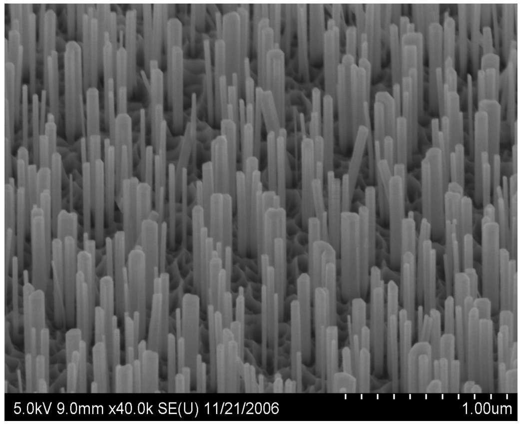

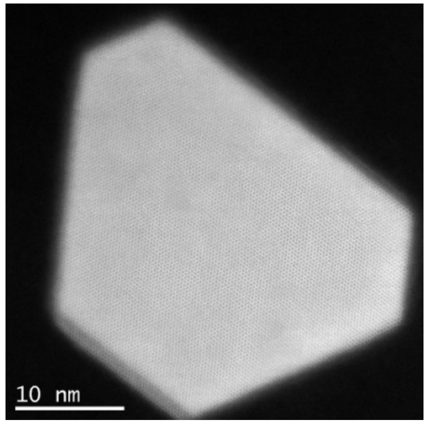

Summer school on the physics and applications of nitrides
23-28 June 2013, Montpellier , La Grande Motte

- Introduction
- GaN nanowire growth mechanisms
- Critical dimensions of nanowire heterostructures
- Nanowire characterization
- Nanowire applications

Scientific activity on semiconductor nanowires

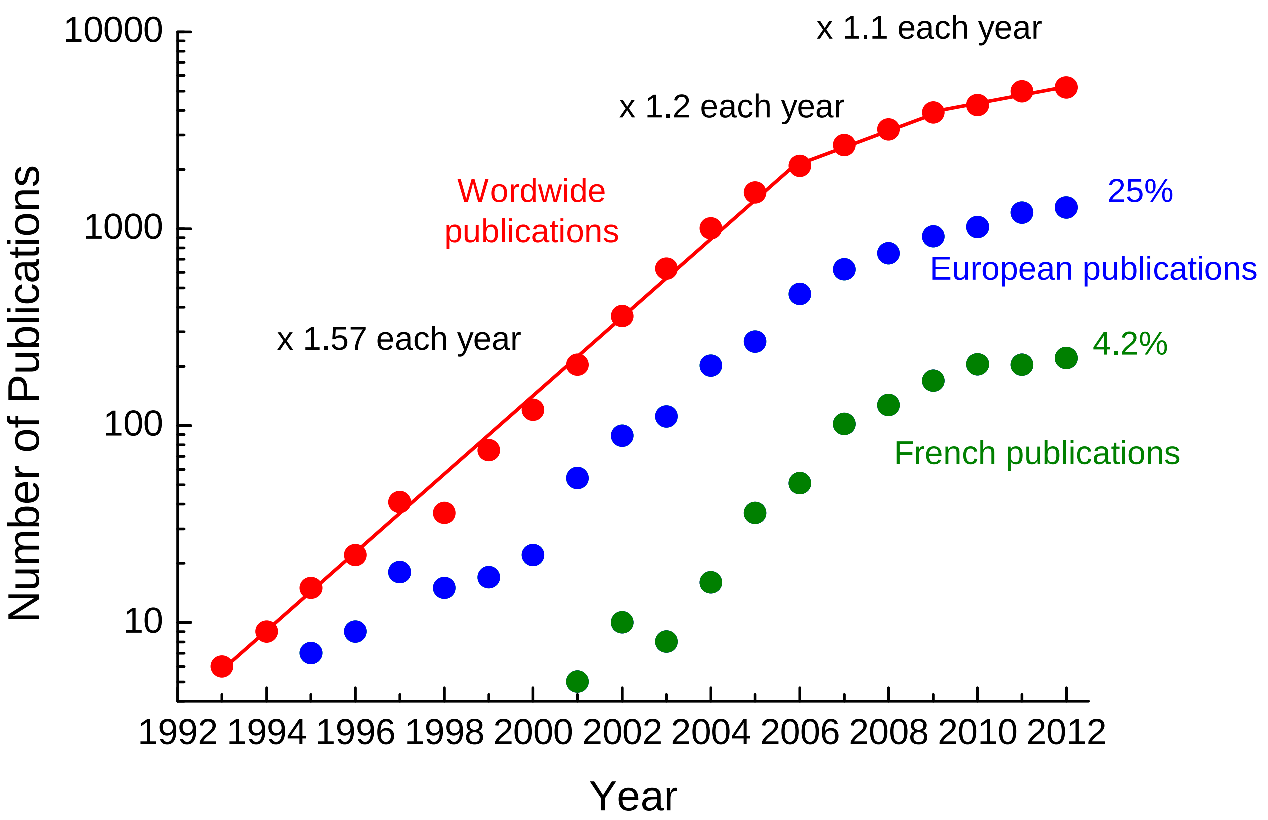

Source : Web of Sciences
TS=((nanowire OR nanowhisker* OR nanorod* OR nanocolumn* OR nanotube*) AND (semiconductor OR III-V OR II-VI OR Si OR Ge OR GaN OR GaP OR GaAs OR GaSb OR InN OR InAs OR InP OR InSb OR CdSe OR CdS OR ZnS OR ZnSe OR ZnO))*
NOT TS=(carbon AND nanotube)*

Part of these publications related to III-nitrides nanowires

10 %

Contributions per country for III-N NWs

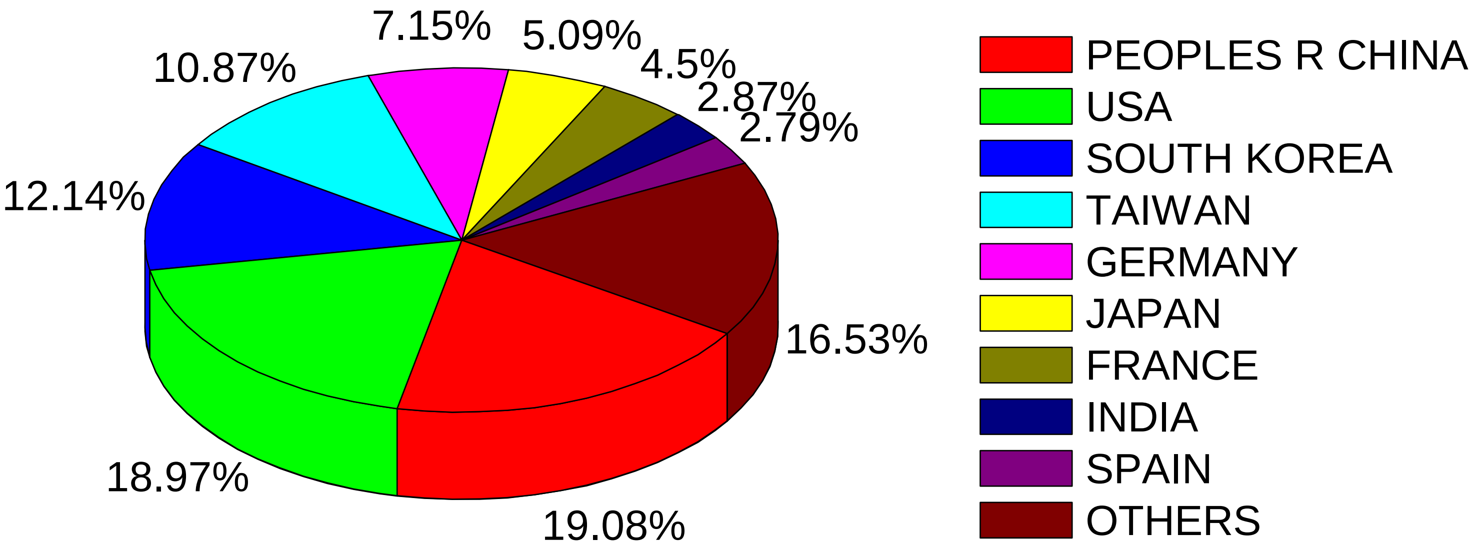

Where does the enthusiasm for NWs come from?

- A general interest for nanosciences which really started in the 90's
- 1D character (after quantum wells and quantum dots)
- Possibility to elaborate NWs on various substrates and by various methods
  (both chemists and physicists got involved in their elaboration)
- Flexibility to form original heterostructures (radial, axial, combination of both)
- Easy manipulation
  (possibility to isolate , address and study a single nano-object, fabrication of nanodevices)
- Collective effects of NWs ensembles (light trapping, light extraction)
- Exploitation of their high surface to volume ration in specific devices
  (sensors, thermoelectric devices)

Where does the enthusiasm for NWs come from?

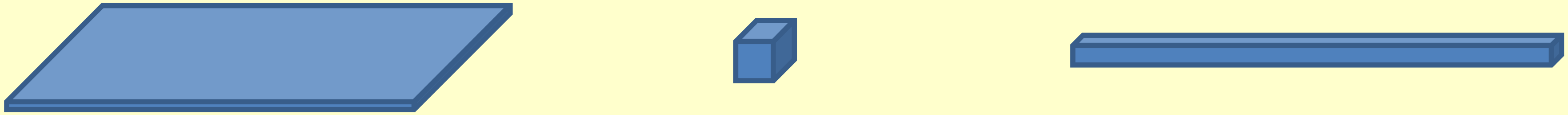

Quantum wells: 1970s

Quantum dots: 1985

Quantum wires: 1988

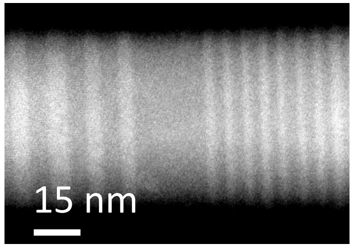

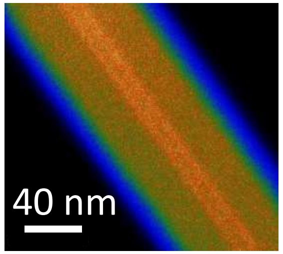

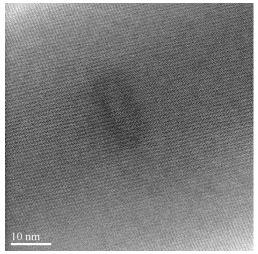

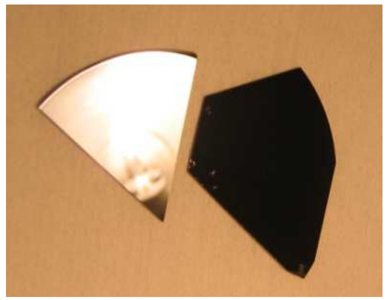

What are the specific advantages of elaborating III-nitrides in the form of NWs?

- Integration of III-N on various substrates:
  Lattice mismatch and difference of thermal expansion are much less critical
  → Strain is relieved by elastic relaxation (free surfaces)
  → Crystal quality better than that of 2D layers (no threading dislocations, no cracks)

- Expected impact on strategic markets: solid state lighting at low cost (white LEDs)

- To overcome the non-miscibility gap in strategic alloys (InGaN)

- High surface/volume + inertness of GaN (does not degrade easily) → good for bio-sensing

What about 1D confinement?

- Not really sought in III-N NWs
  Exciton Bohr radius in GaN is small (~3 nm)
  Thin GaN NWs are rarely elaborated (the typical range of diameters is 50 nm - 1 µm)

Elaboration: pioneering works

Growth of Self-Organized GaN Nanostructures on $Al_2O_3(0001)$ by RF-Radical Source Molecular Beam Epitaxy

Jpn. J. Appl. Phys. Vol. 36 (1997) pp. L 459–L 462
Part 2, No. 4B, 15 April 1997

Masaki YOSHIZAWA, Akihiko KIKUCHI, Masashi MORI, Nobuhiko FUJITA and Katsumi KISHINO
Department of Electrical and Electronics Engineering, Sophia University, 7-1 Kioi-cho, Chiyoda-ku, Tokyo 102, Japan

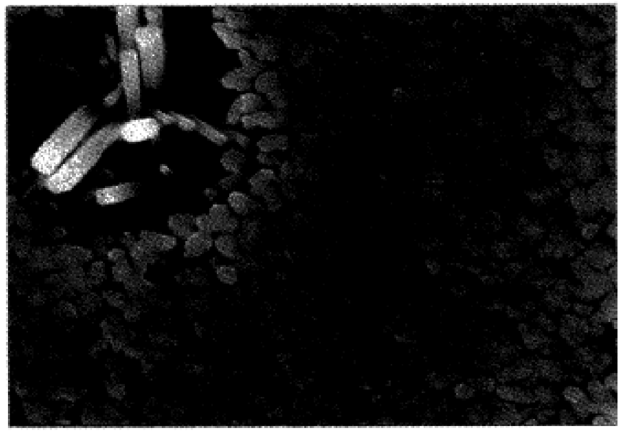

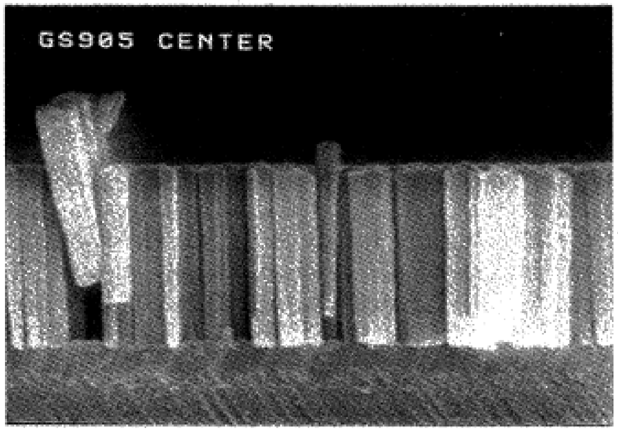

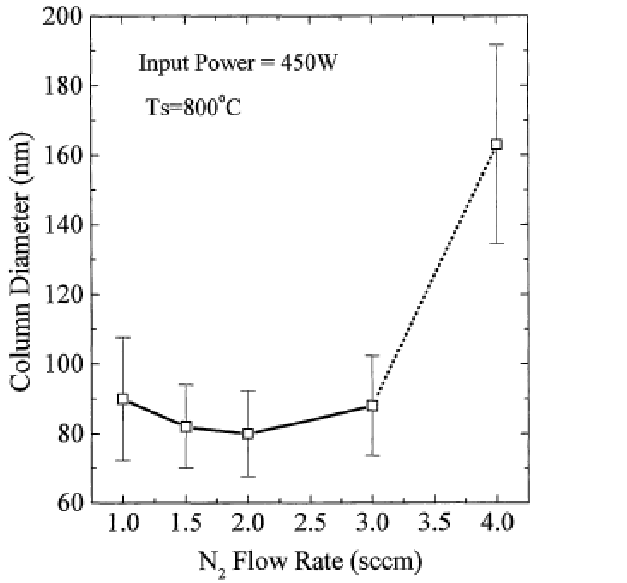

MBE growth, N radicals, T=800°C

Elaboration: pioneering works

The effect of the III/V ratio and substrate temperature on the morphology and properties of GaN- and AlN-layers grown by molecular beam epitaxy on Si(1 1 1)

Journal of Crystal Growth 183 (1998) 23–30

M.A. Sanchez-Garcia*, E. Calleja, E. Monroy, F.J. Sanchez, F. Calle, E. Muñoz, R. Beresford[1]

Departmento Ingeniería Electrónica, ETSI Telecomunicación, UPM, Ciudad Universitaria s/n, 28040 Madrid, Spain

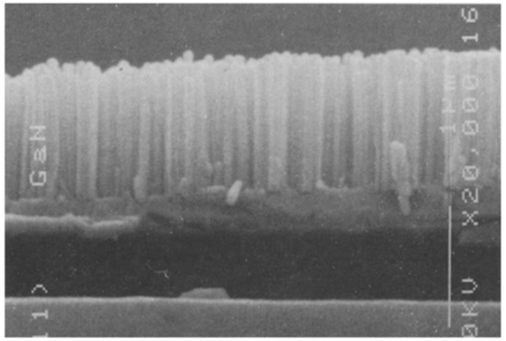

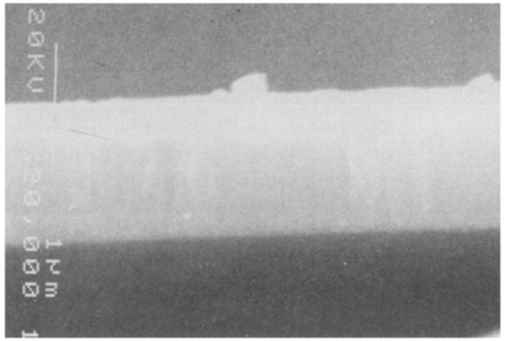

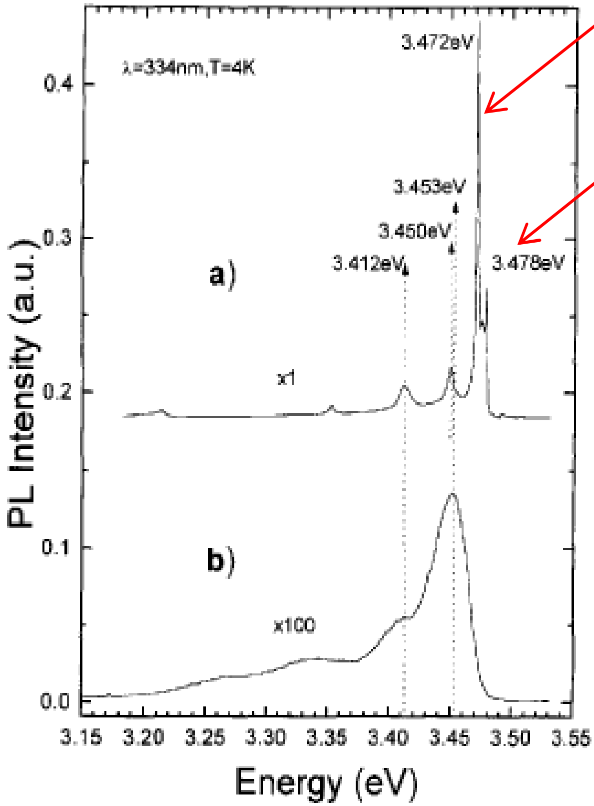

D^0X_A

FX_A

Fig. 7. PL spectra of two GaN layers grown directly on Si(1 1 1) substrates: (a) N-rich condition and (b) Ga-rich condition.

Later, it will be noticed that NW samples do not show defect-related emission in the yellow band

Observation of well defined excitonic peaks in the NW sample

Elaboration: pioneering works

APPLIED PHYSICS LETTERS VOLUME 75, NUMBER 16 18 OCTOBER 1999

Large-scale synthesis of single crystalline gallium nitride nanowires

G. S. Cheng,[a] L. D. Zhang,[b] Y. Zhu, G. T. Fei, and L. Li
Institute of Solid State Physics, Chinese Academy of Sciences, P.O. Box 1129, Hefei 230031, People's Republic of China

C. M. Mo
Department of Materials Science and Engineering, University of Science and Technology of China, Hefei 230026, People's Republic of China

Y. Q. Mao
Nanjing Institute of Geology and Palaeontology, Chinese Academy of Sciences, Nanjing 210008, People's Republic of China

Reaction of Ga_2O and NH_3 on anodic alumina membranes at T=1000°C

$$4\mathrm{Ga}(l) + \mathrm{Ga_2O_3}(s) \rightarrow 3\mathrm{Ga_2O}(g), \quad (1)$$

$$\mathrm{Ga_2O}(g) + 2\mathrm{NH_3}(g) \rightarrow 2\mathrm{GaN}(s) + \mathrm{H_2O}(g) + 2\mathrm{H_2}(g). \quad (2)$$

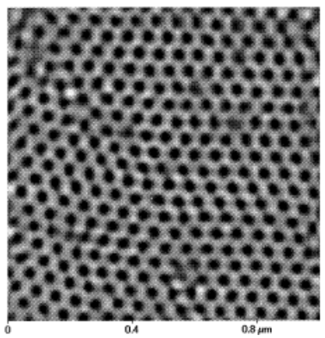

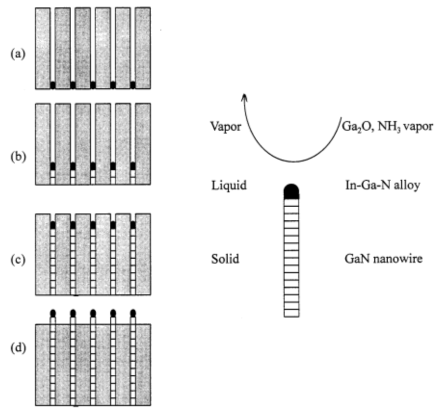

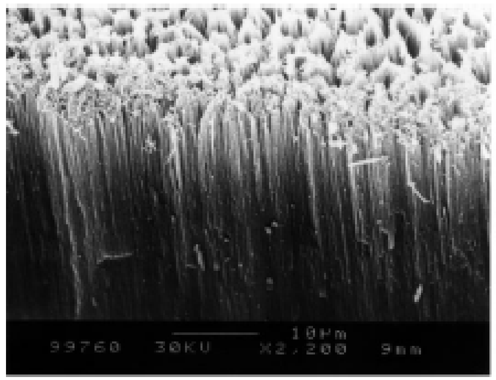

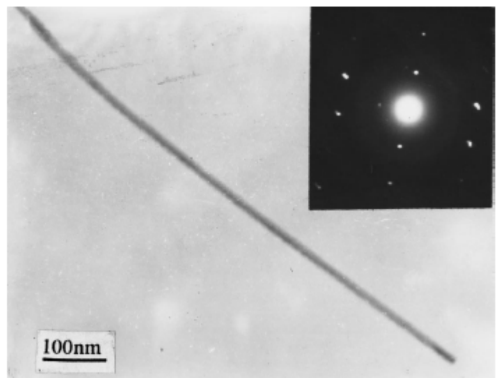

Template porous membrane

Mono-crystalline GaN NWs
WZ structure

Elaboration: pioneering works

Laser-Assisted Catalytic Growth of Single Crystal GaN Nanowires

Xiangfeng Duan and Charles M. Lieber*

Department of Chemistry and Chemical Biology
Harvard University, Cambridge, Massachusetts 02138

J. Am. Chem. Soc. **2000**, *122*, 188–189

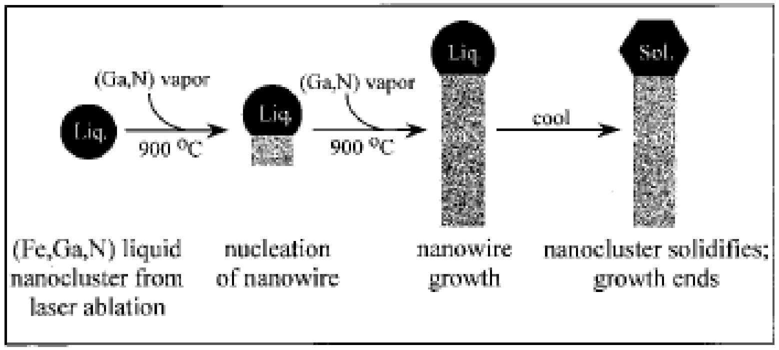

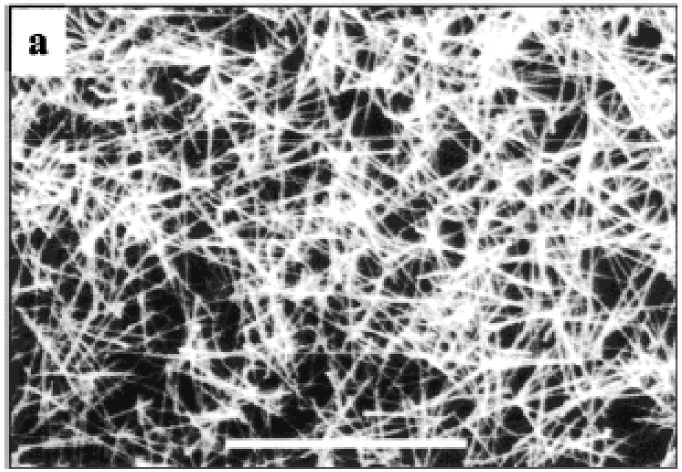

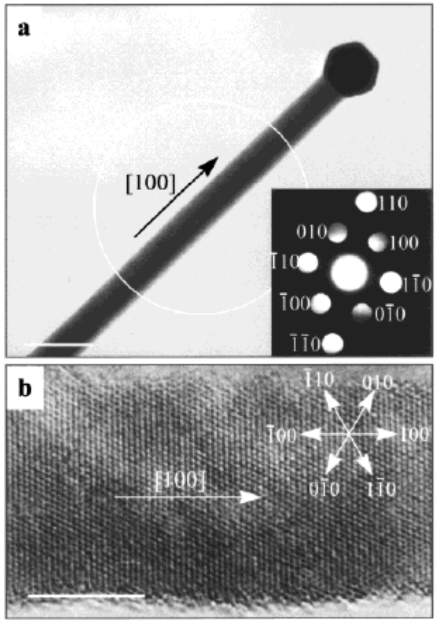

Laser ablation
GaN/Fe target is vaporized
Catalyst-assisted VLS growth
No epitaxial relationship with a substrate

Elaboration: pioneering works

Formation of GaN nanorods by a sublimation method

J.Y. Li[a,b,*], X.L. Chen[a], Z.Y. Qiao[b], Y.G. Cao[a], Y.C. Lan[a]

[a]Institute of Physics and Center for Condensed Matter Physics, Group 401, Chinese Academy of Sciences, P.O. Box 603-33, Beijing 100080, People's Republic of China
[b]Department of Physical Chemistry, University of Science and Technology Beijing, Beijing 100083, People's Republic of China

Journal of Crystal Growth 213 (2000) 408–410

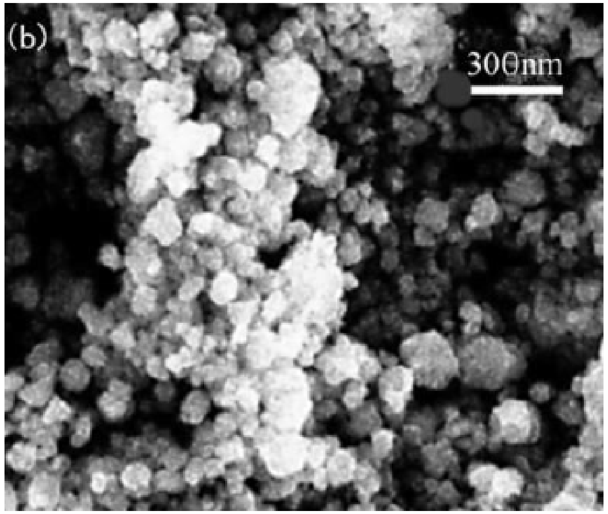

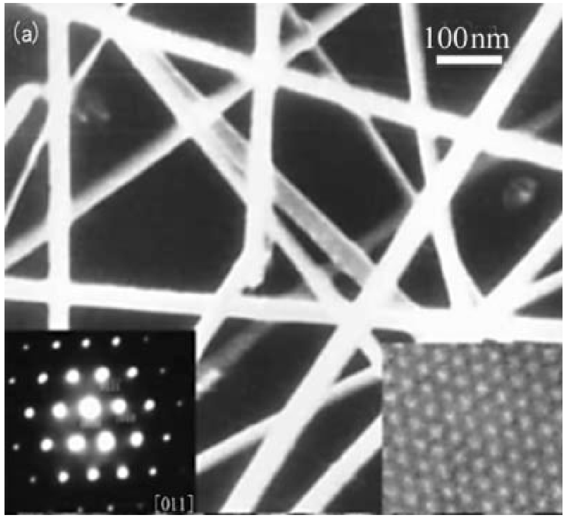

Sublimation of ball-milled GaN in ammonia at 930°C
straight and long NWs

A wide range of methods allow growing GaN nanowires

Molecular beam epitaxy

Vapor phase epitaxy

Chemical vapor deposition

In epitaxy with a substrate or not

Growth with templates

Various precursors

- Introduction
- GaN nanowire growth mechanisms
- Critical dimensions of nanowire heterostructures
- Nanowire characterization
- Nanowire applications

Crystallography of hexagonal systems

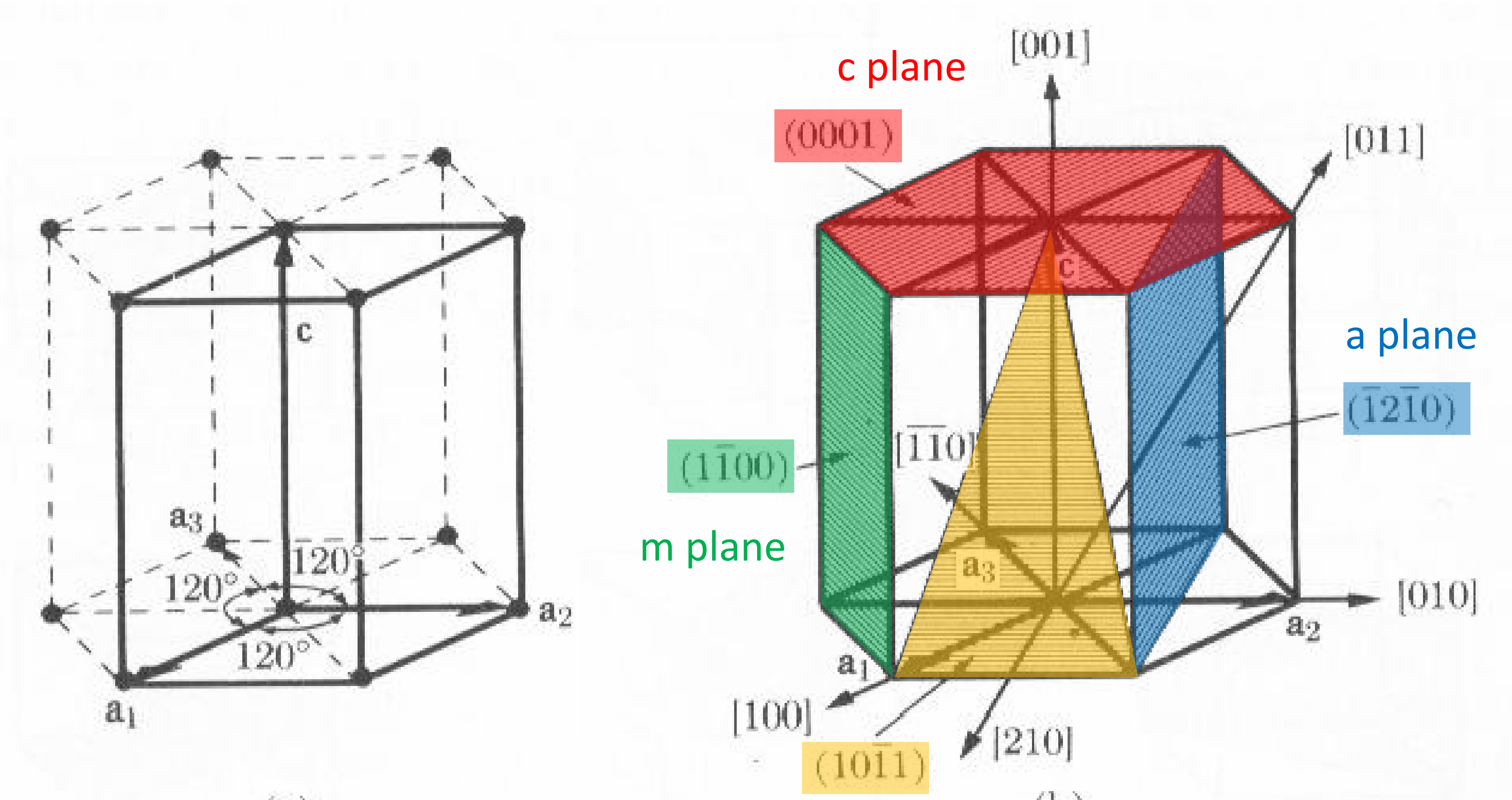

(a) (b)

The lower index planes

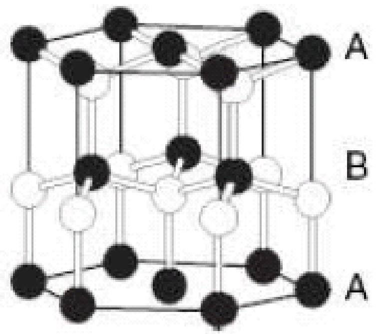

GaN
a = 0.3189 nm
c = 0.5185 nm

4-index notation: (h,k,i,l) coordinates in the (a_1, a_2, a_3, c) basis
h, k, i are not independent: h+k+i=0

Crystallography of hexagonal systems

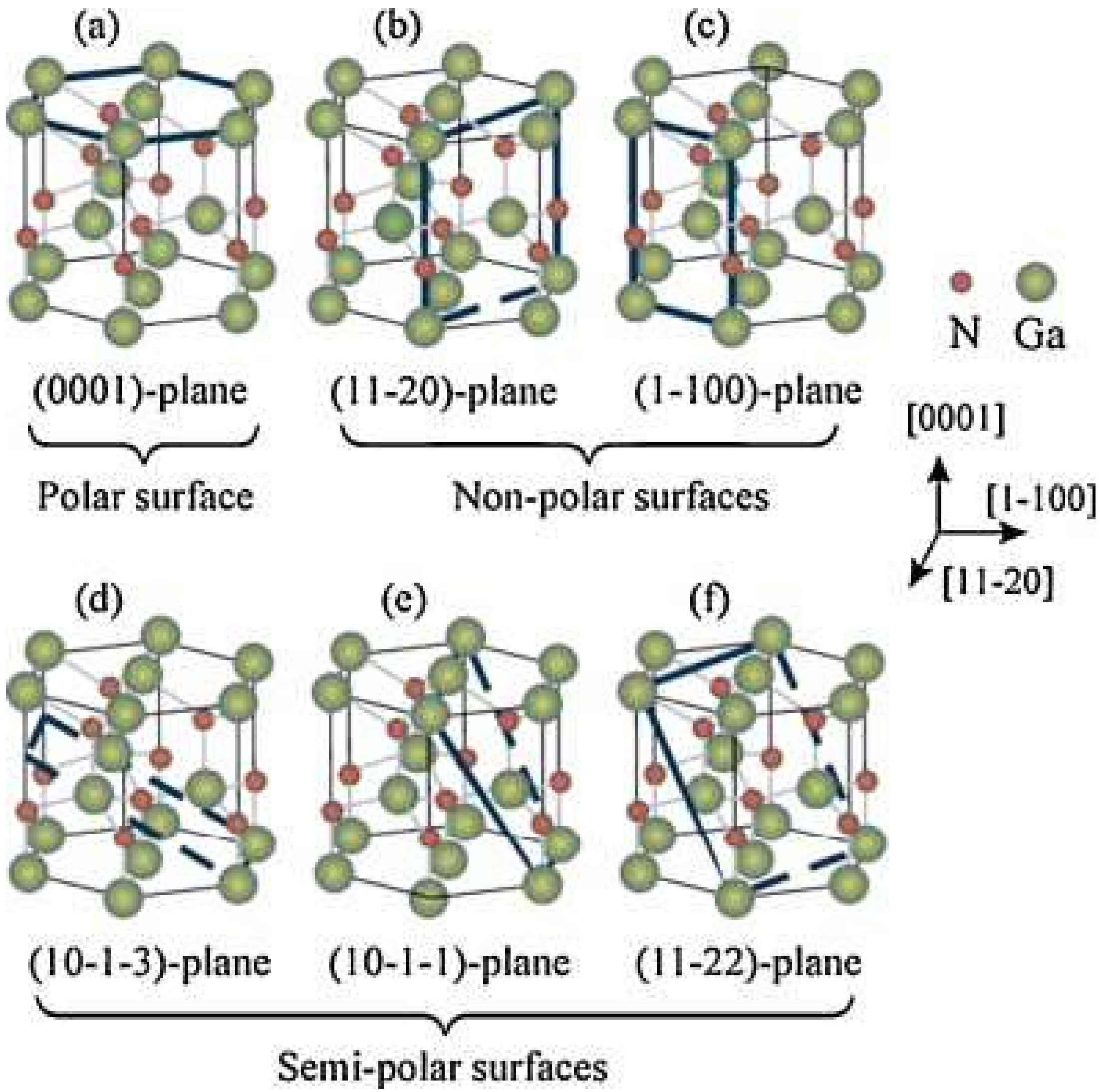

Polar planes:

c planes contain only one type of atoms
(0001): Ga atoms
(000-1): N atoms

Non-polar planes:

a planes and m planes contain equal numbers of N and Ga atoms

Semi-polar planes:

{10-11} planes contain the two types of atoms in inequal numbers

{ } : family of planes
( ) : particular plane
< >: family of directions
[ ]: particular direction

Various strategies to grow epitaxial GaN nanowires

Selective area growth
Masked substrate

Metallic or dielectric mask
Ti or SiO_2, Si_3N_4

Openings defined by lithography

Catalyst-assisted growth
Nanoparticle of catalyst

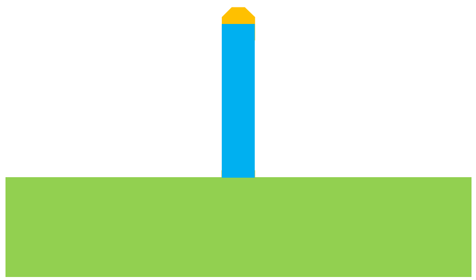

Good catalysts: Au, Ni
Does not need a substrate

Spontaneous NW growth

With specific growth
conditions

What determines the crystal shape ?
Situation at thermodynamic equilibrium: the Wulff construction

The GaN case

V. Jindal et al, J. Appl. Phys. 106, 083115 (2009)
University at Albany, New York

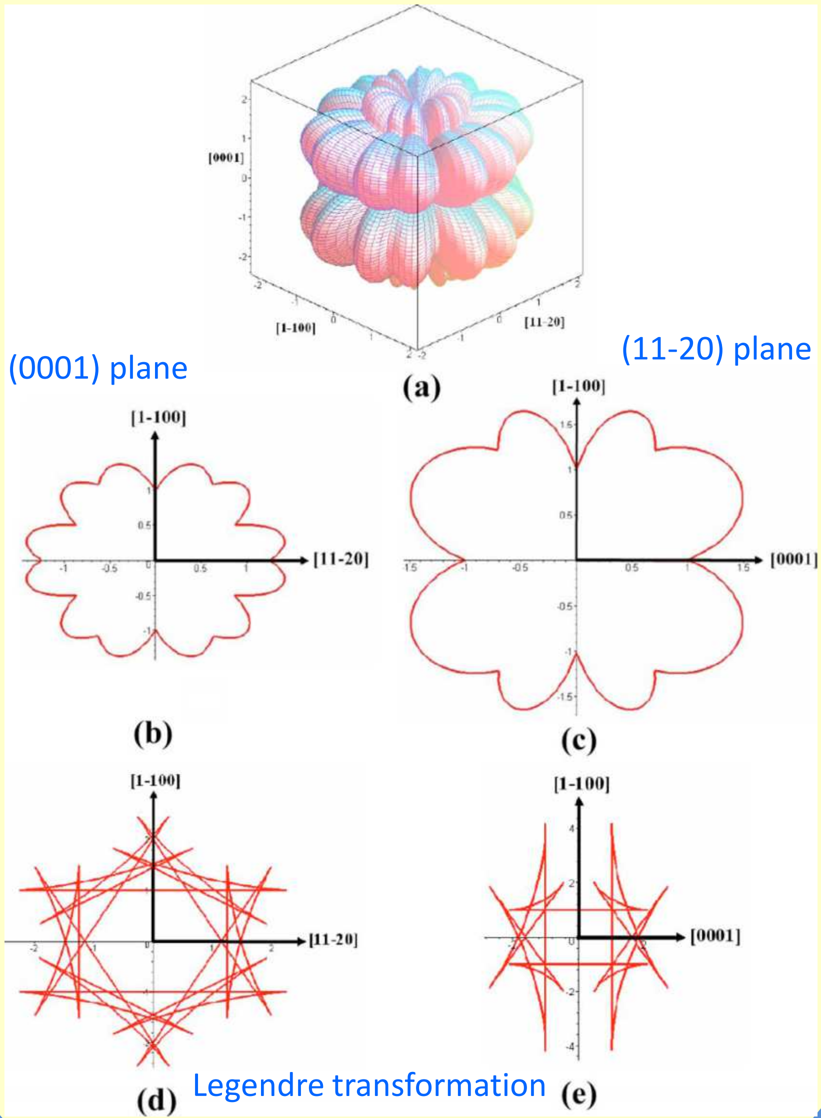

The energy of surfaces depend on their cristalline orientation.
At thermodynamic equilibrium, the crystal shape is related to the anisotropy of the surface energies.

This anisotropy is represented by the equilibrium Wulff plot (γ-plot)

Wulff, G. Z. Kristallogr. Mineral. 1901, 34, 449–530.

Broken-bond model:

relaxation, buckling and surface reconstruction are not considered

Type of surface	Broken bond meV/Å^2	*Ab initio* meV/Å^2
{1–100}	136.7	118[a]
{11–20}	158.8	123[a]
(Ga terminated (0001)+N terminated (000–1))/2	128.9	
(N terminated (0001)+Ga terminated (000–1))/2	386.9	
({1–101}+{1–10–1})/2	181.2	
({11–21}+{11–2–1})/2	201.5	

The facets of lower energy develops

What determines the crystal shape ?
Situation during growth: limitation by kinetics

V. Jindal et al, J. Appl. Phys. 106, 083115 (2009)
University at Albany, New York

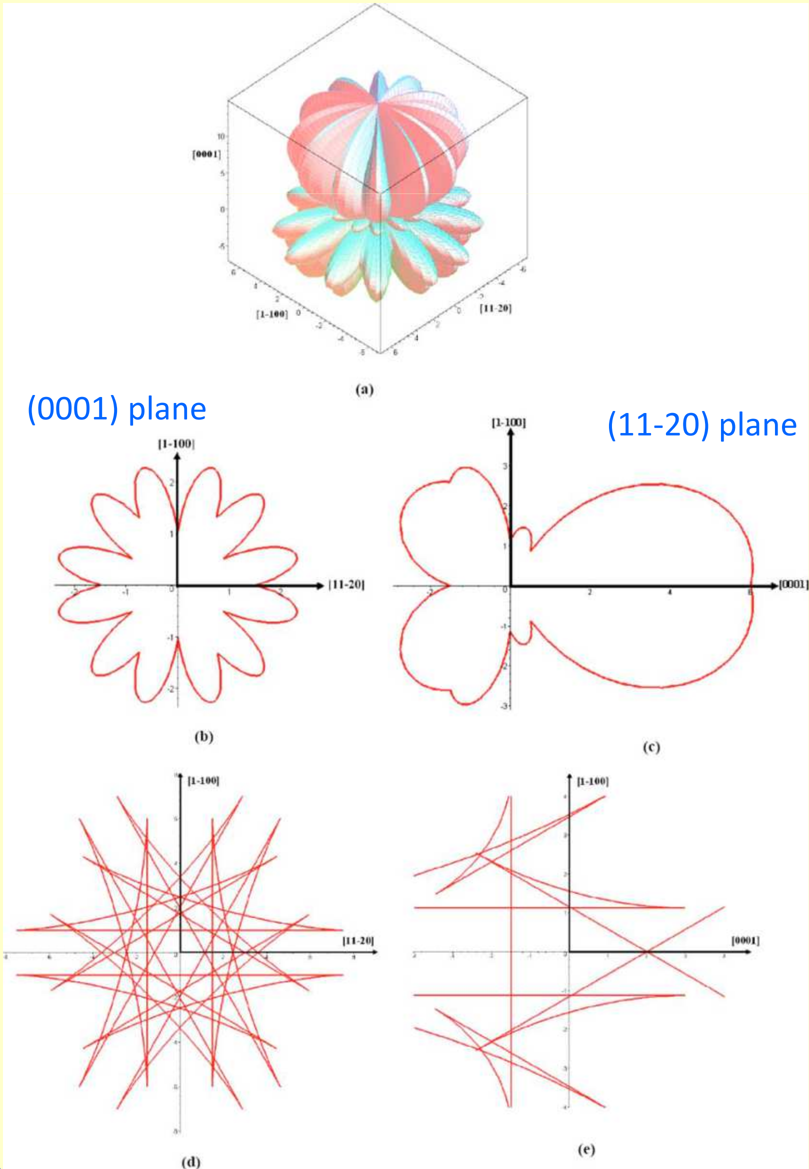

The different surfaces have:

→ different kinetic barriers for adsorption/desorption, surface diffusion, nucleation and incorporation of atoms
→ different chemical potential and growth velocities

The crystal shape is related to the anisotropy of the growth velocity
This anisotropy is represented by the kinetic Wulff plot (ν-plot)

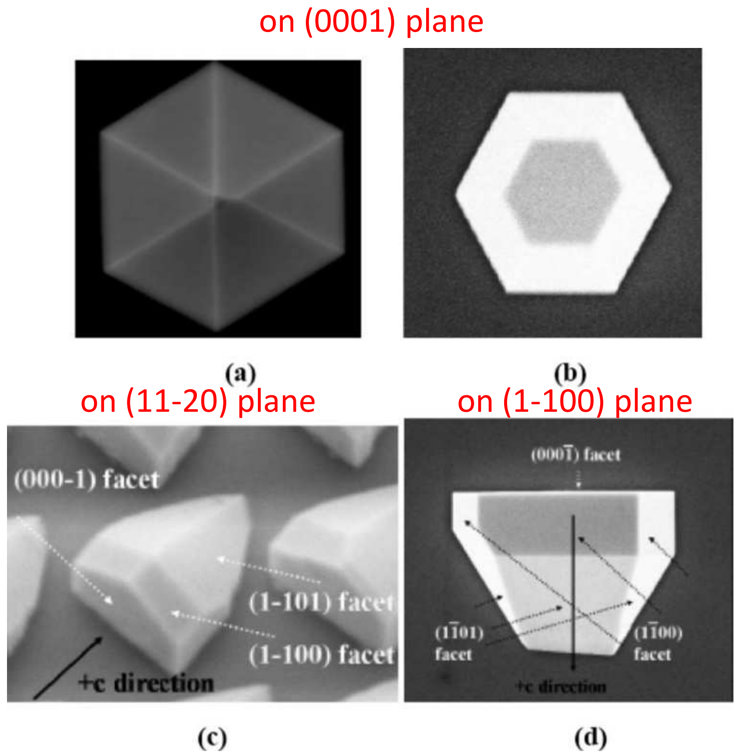

Growth velocities are determined on crystals obtained by SAG on various substrate orientations (MOVPE, TMGa and NH_3 sources)

The low velocity facets develops, the high velocity facets disappear.

The influence of growth conditions

Q. Sun et al, J. Appl. Phys. 104, 092523 (2008)
Yale University, New Haven

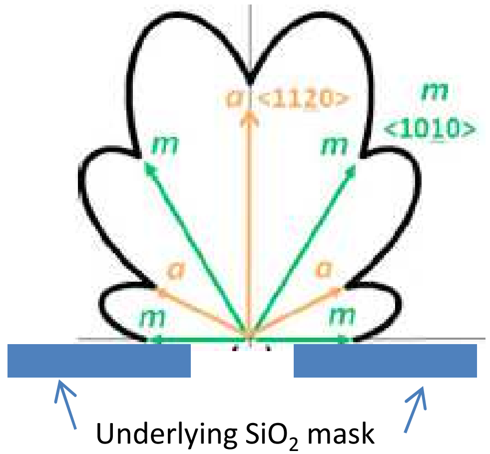

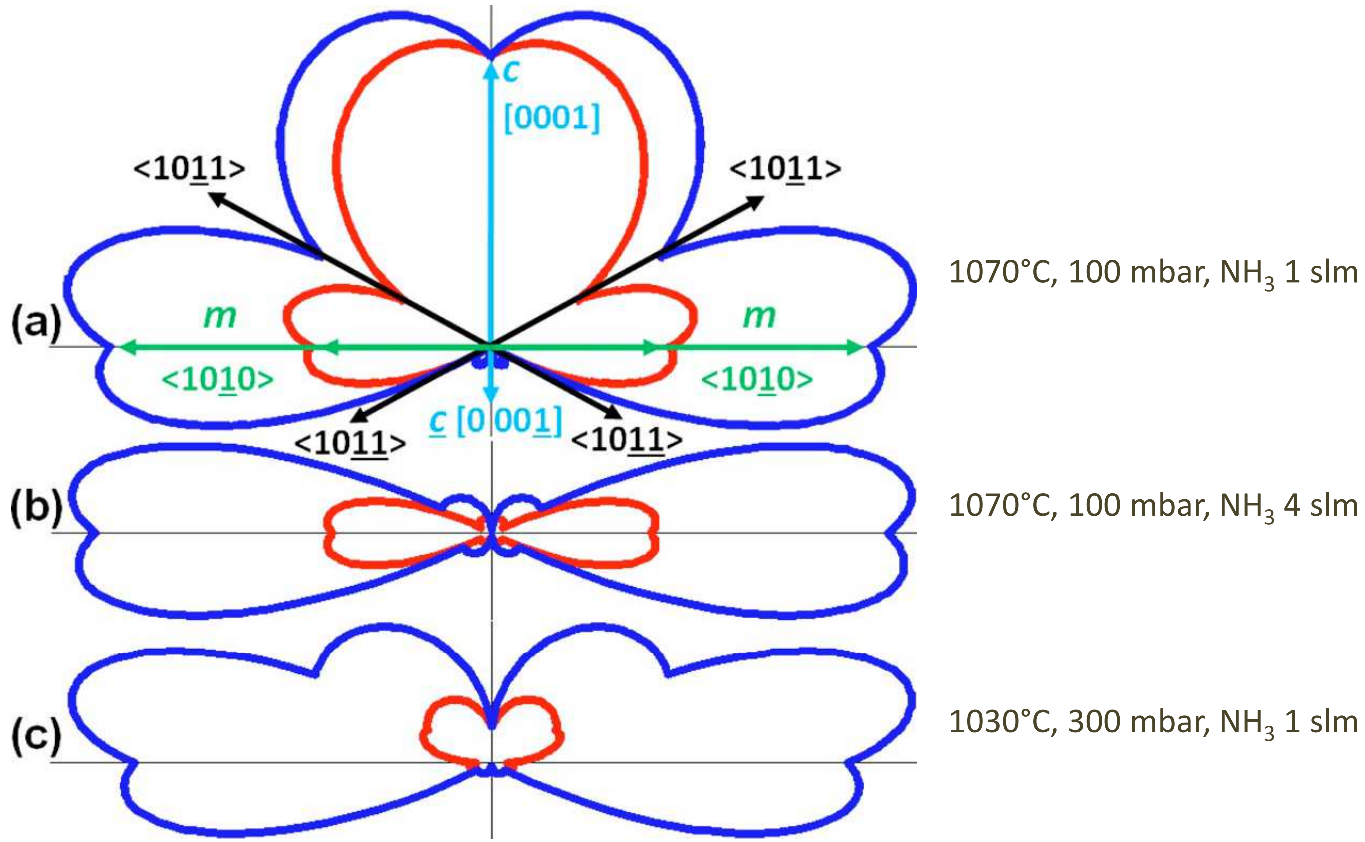

In SAG, the facets close to the dielectric mask can exhibit reduced growth velocities

MOVPE of GaN on masked r-sapphire substrates
The ν-plot is strongly dependent on growth conditions

Temperature: a key parameter

K. Kawasaki et al, J. Cryst. Growth 243, 129 (2002)
Tokyo Institute of Technology, Yokohama

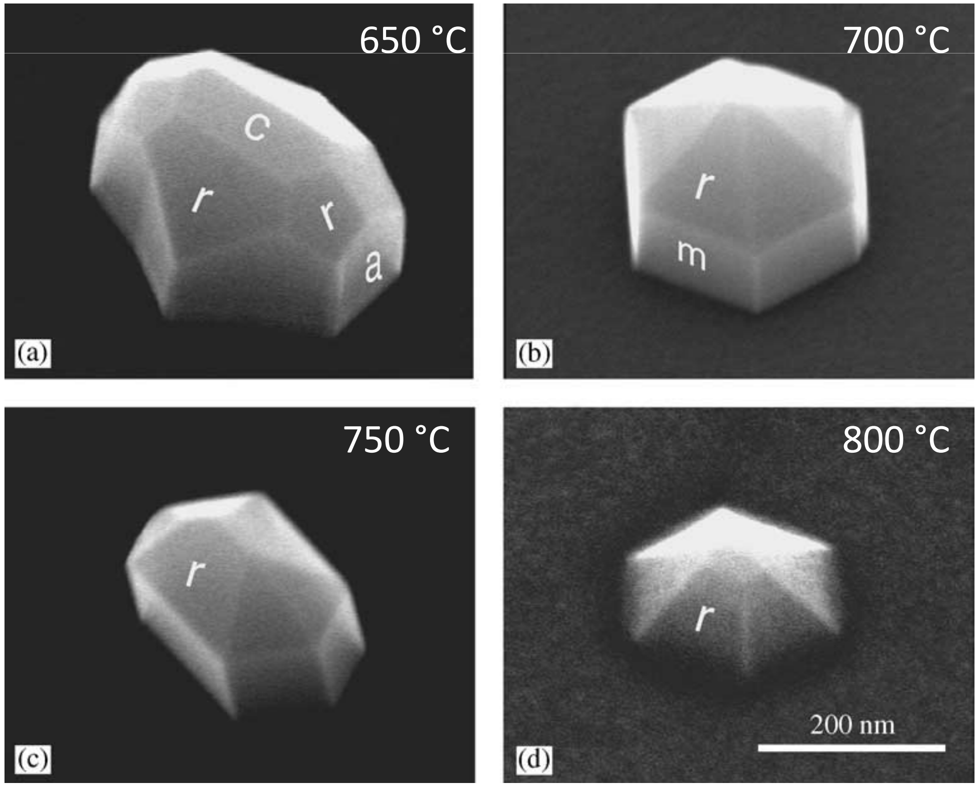

GSMBE of GaN nano-crystals on masked SiC (0001)
Ga and NH_3 sources
Effect of growth temperature on the crystal shape

Classification of typical growth regimes

V. Jindal et al, J. Appl. Phys. 106, 083115 (2009)
University at Albany, New York)

Cross-sections in the (11-20) plane, θ angle between (1-101) and (0001): 62°

$$V_{(000-1)} \ge \frac{V_{(1-10-1)}}{\cos\theta} \text{ and } V_{(1-100)} \ge \frac{V_{(1-10-1)} + V_{(1-101)}}{2\sin\theta}$$

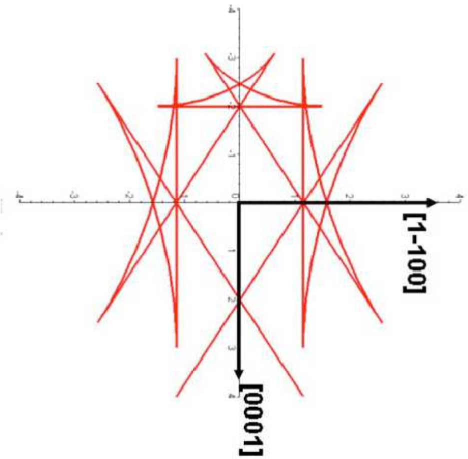

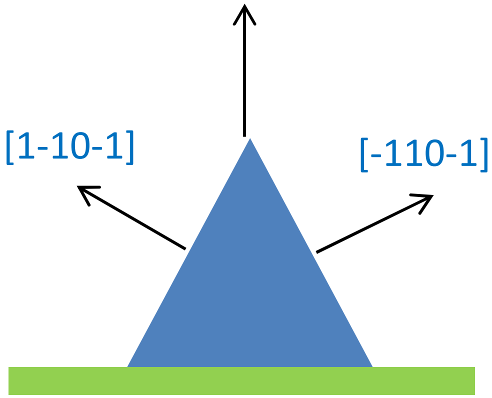

$$\frac{V_{(1-10-1)} - V_{(1-101)}}{2\cos\theta} \le V_{(000-1)} \le \frac{V_{(1-10-1)}}{\cos\theta} \text{ and}$$

$$V_{(1-100)} \ge \frac{V_{(1-10-1)} + V_{(1-101)}}{2\sin\theta}.$$

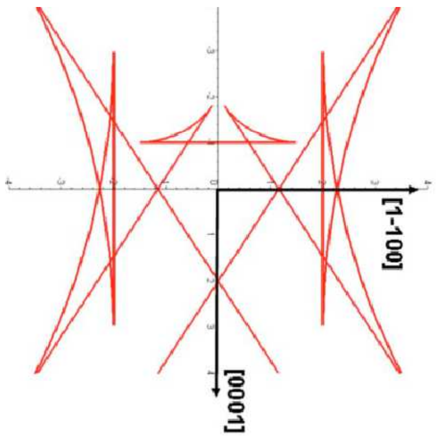

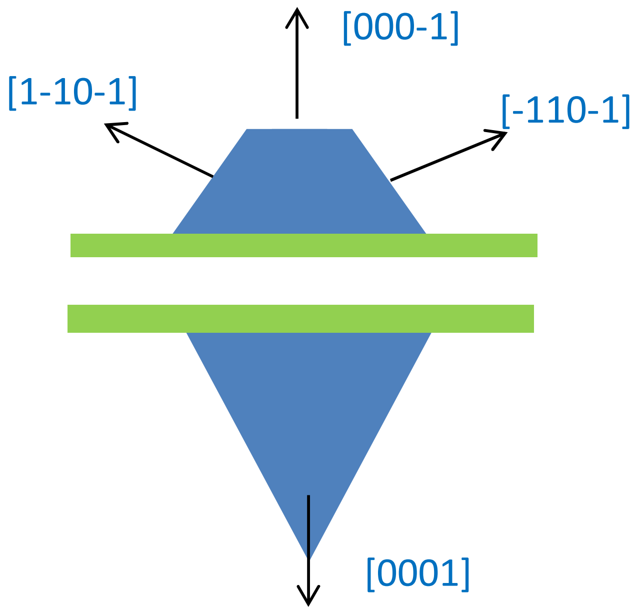

$$\frac{V_{(1-10-1)} - V_{(1-101)}}{2\cos\theta} \le V_{(000-1)} \le \frac{V_{(1-10-1)}}{\cos\theta} \text{ and}$$

$$\frac{V_{(1-10-1)}}{2\sin\theta} - \frac{V_{(000-1)}}{\tan\theta} \le V_{(1-100)} \le \frac{V_{(1-10-1)} + V_{(1-101)}}{2\sin\theta}$$

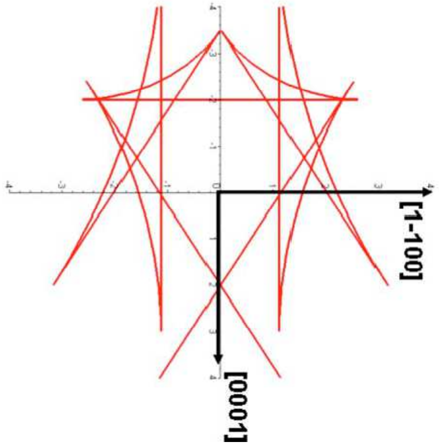

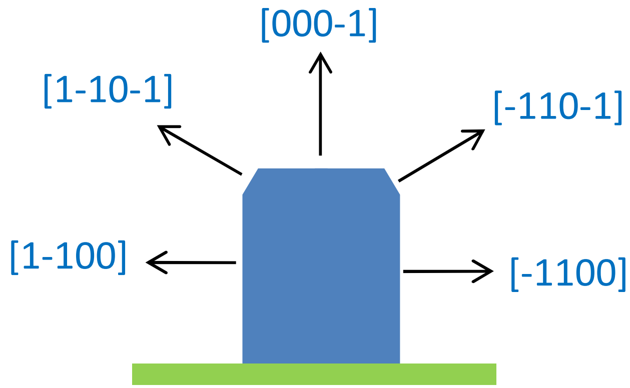

Experimental results in SAG

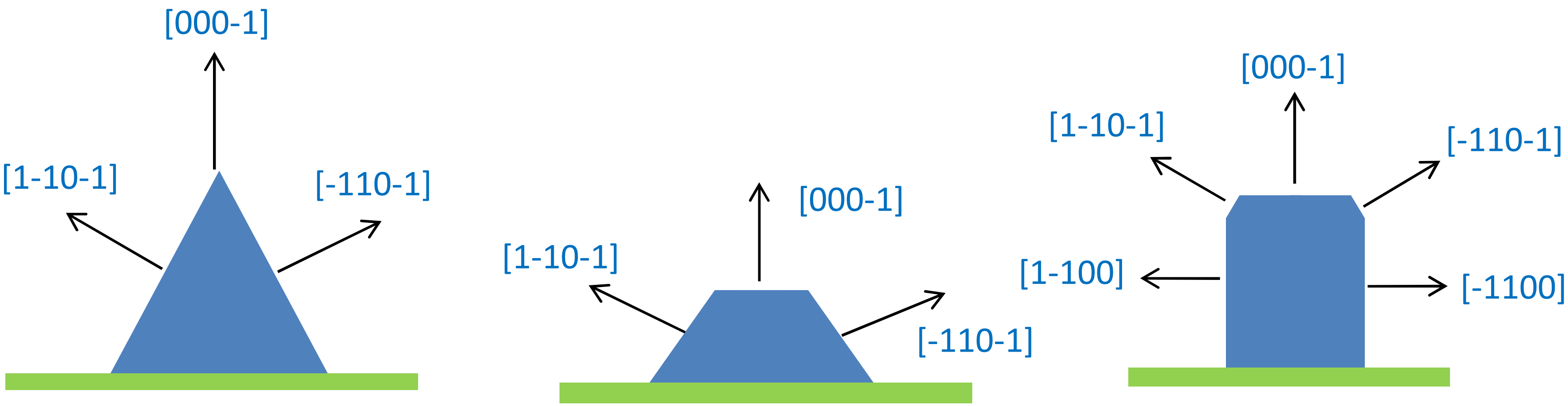

MOCVD SAG growth on SiO_2 masked substrates: N-polar GaN

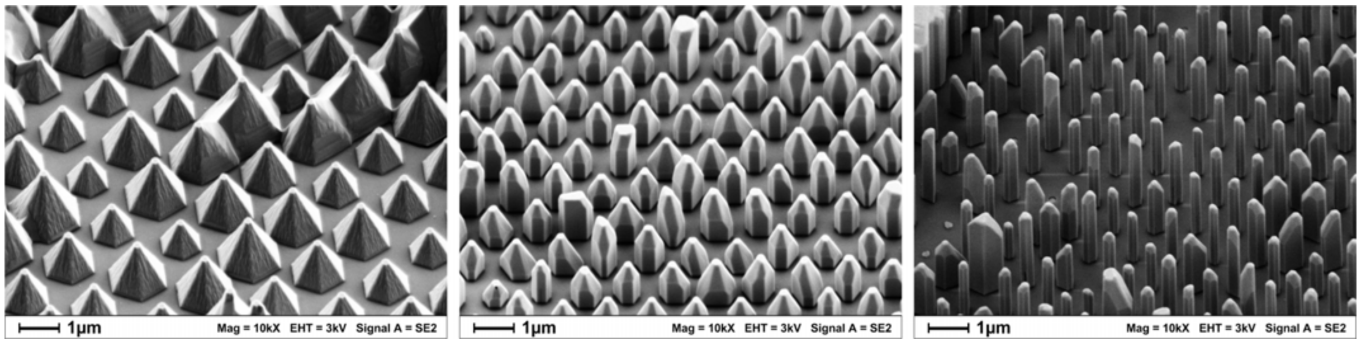

N_2 carrier gas | H_2/N_2 carrier gas 1:2 | H_2/N_2 carrier gas 2:1

Bergbauer et al, Nanotechnol. 21, 305201 (2010)
Osram Opto Semiconductors, Regensburg

Experimental results in SAG

MOCVD SAG growth on SiO_2 masked substrates: Ga-polar GaN

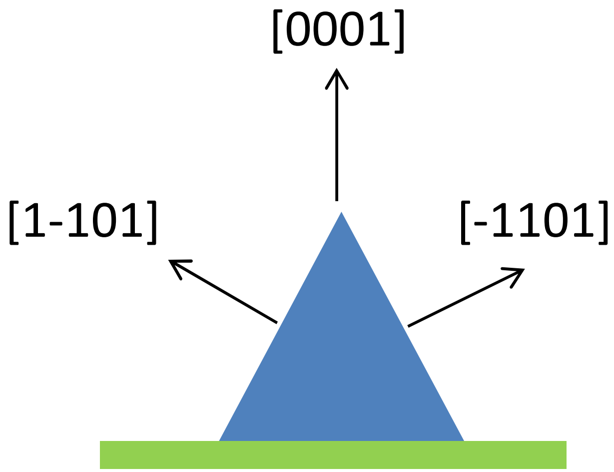

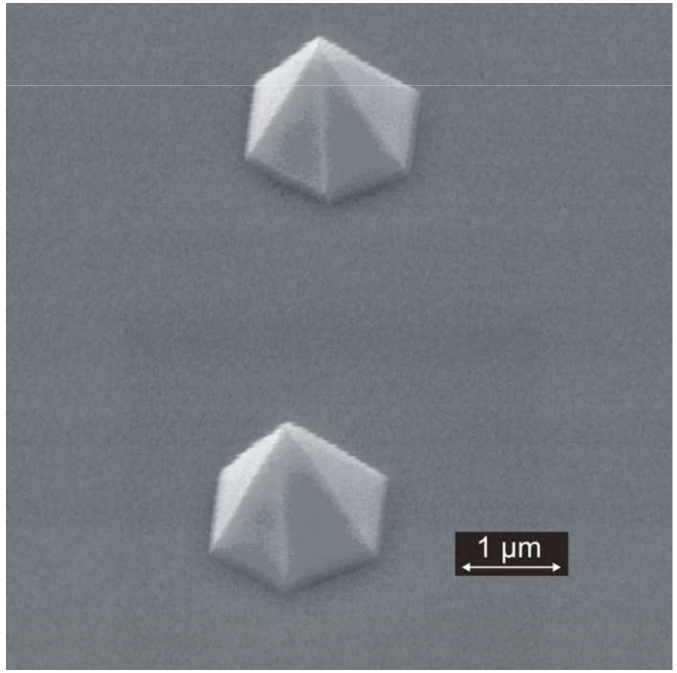

Pérez-Solórzano, Appl. Phys. Lett. 87, 163121 (2005)

2-step growth to form NWs

X.J. Chen et al. , J. Cryst. Growth 322, 15 (2011)
CEA-CNRS-UJF, Grenoble

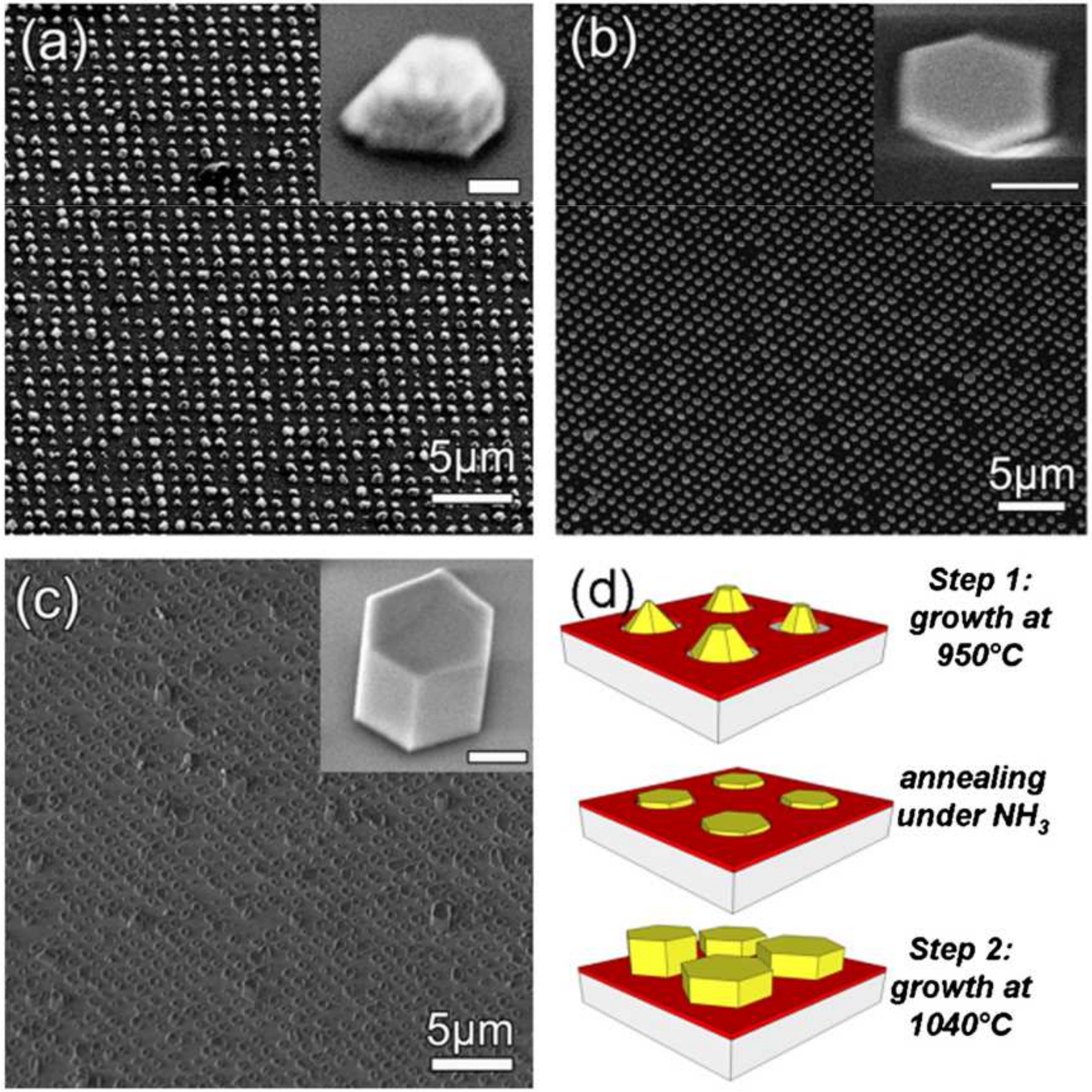

MOCVD GaN SAG on masked c-sapphire

Shape of the nanostructures can be changed by playing with the growth parameters:

Here, the NW shape is stabilized by a 2-step growth at different temperatures.

A more appropriate denomination here:
Microwire

Pulsed growth mode

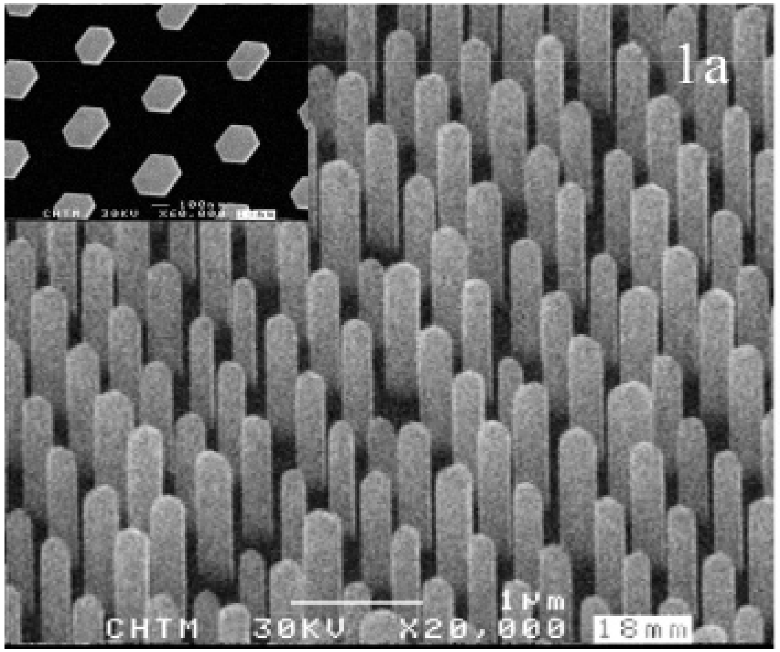

Hersee et al. , Nano Lett . 6, 1808 (2006)
UniVersity of New Mexico, Albuquerque

GaN MOCVD SAG, pulsed growth mode

Initial step to fill the openings:
100 Torr
H_2/N_2 carrier gas
V/III=1500
Ts=1050°C

Pulsed mode after 10 nm
TMGa, 10 sccm, 20 s
NH3, 500 sccm, 30 s

Summary of SAG experiments

Various strategies can be implemented to form NWs in small mask openings:

- Carrier gas mixture
- Multi-step growth at different temperatures
- Pulsed growth

MOCVD is the most popular technique for SAG

Typical wire diameters: 100 nm - 1µm (microwires)

Catalyst-assisted growth

- Method
  - catalyst deposition + dewetting to produce nanoparticles
  - direct deposition of colloidal particles on the substrate

- Advantages:
  - successful for growing NWs of many III-V compounds
  - can promote NW growth in various crystallographic directions
  - very high aspect ratio
  - catalyst size defines the NW diameter

- Drawbacks:
  - possible contamination of the NW by catalyst atoms
  - can generate a lot of stacking faults

Catalyst-assisted growth: change of surface energies

RF plasma MBE
Sapphire substrate
730 ◦C
Ni catalyst

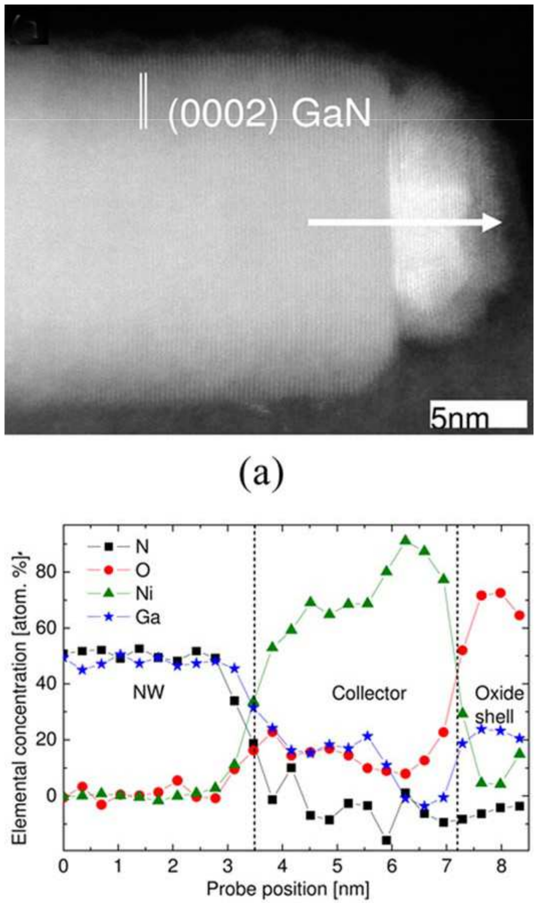

(a)

(b)

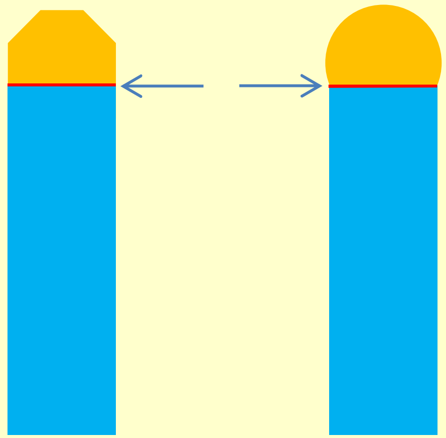

The foreign catalyst (solid or liquid) forms an interface with one crystalline facet of the SC

→ The hierarchy of surface energies is changed

L. Geelhaar, IEEE J. Select. Topics Quantum Electron. 17, 878 (2011)
Paul-Drude-Institut für Festkörperelektronik, Berlin

Catalyst-assisted growth: change of kinetic barriers

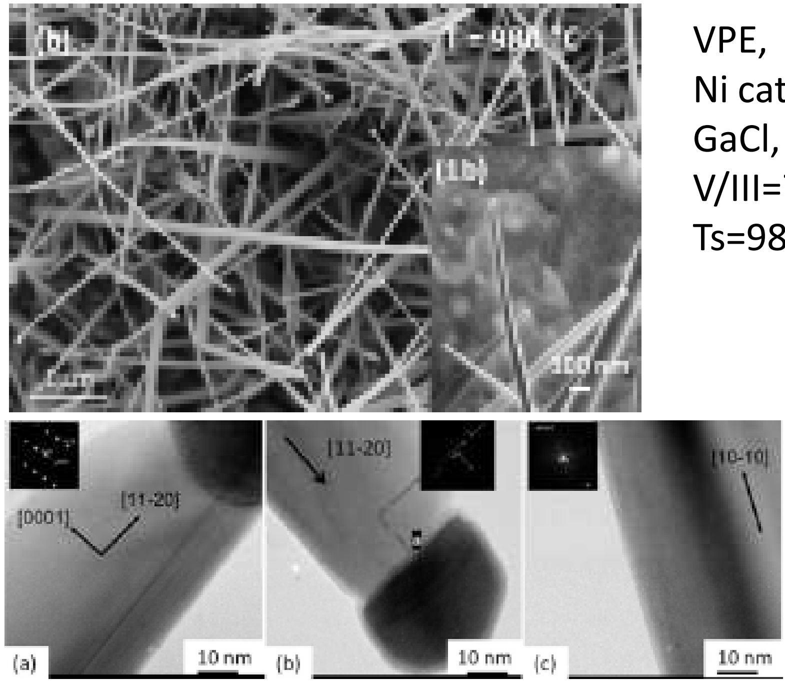

VPE,
Ni catalyst
GaCl, NH_3
V/III=7,
Ts=980°C

Lekhal et al, Nanotechnol . 23, 405601 (2012)
Institut Pascal, Clermont-Ferrand

The catalyst particle can accelerate the decomposition of the precursors

Chemical catalyst

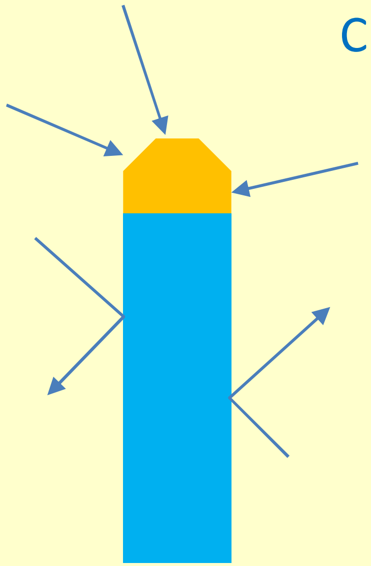

The catalyst particle can accelerate the nucleation of the solid phase

Physical effect

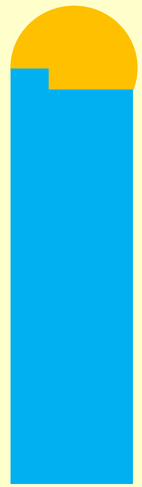

→ The hierarchy of kinetics barriers is changed

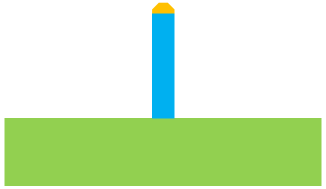

Catalyst-assisted growth: elongation along other growth axis

$LiAlO_2$ substrate

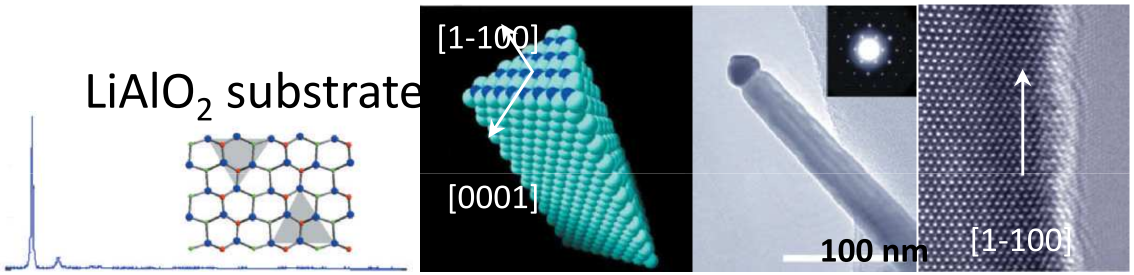

Kuykendall et al, Nature Mat. 3, 524 (2004)
Univ. California, Berkeley, USA

Au-assisted CVD (TMGa+NH_3)

MgO substrate

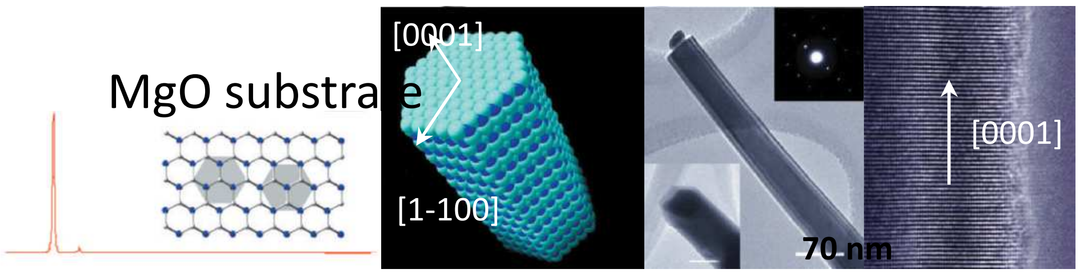

r-plane sapphire

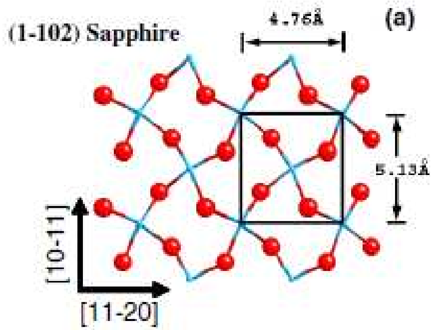

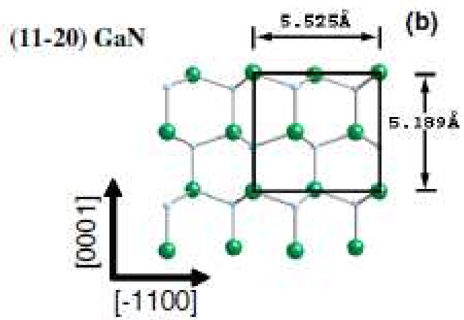

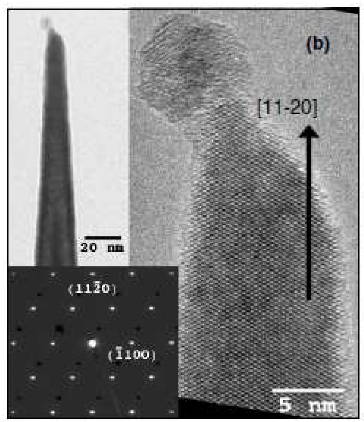

Wang et al, Nanotechnol. 17, 5773 (2006)
Sandia National Labs, USA

Ni-assisted CVD (TMGa+NH_3)

Drawbacks of catalyst-assisted growth

Ni-catalyzed GaN NWs:
Many basal stacking faults

PL spectra of Ni-catalyzed GaN NWs compared to catalyst-free GaN NWs:
D^0X peak 25 times less intense for catalyzed NWs

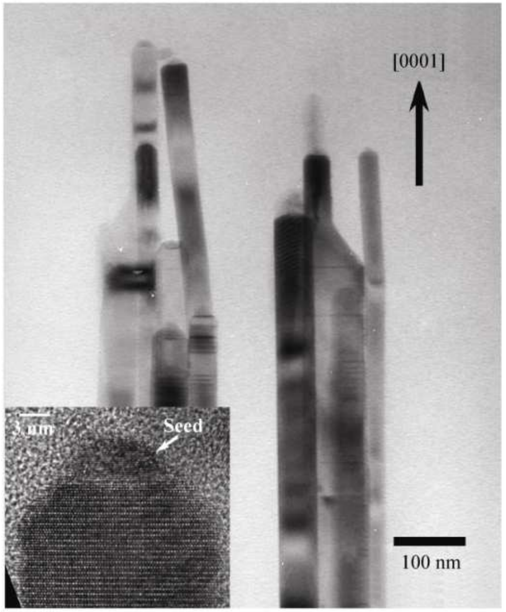

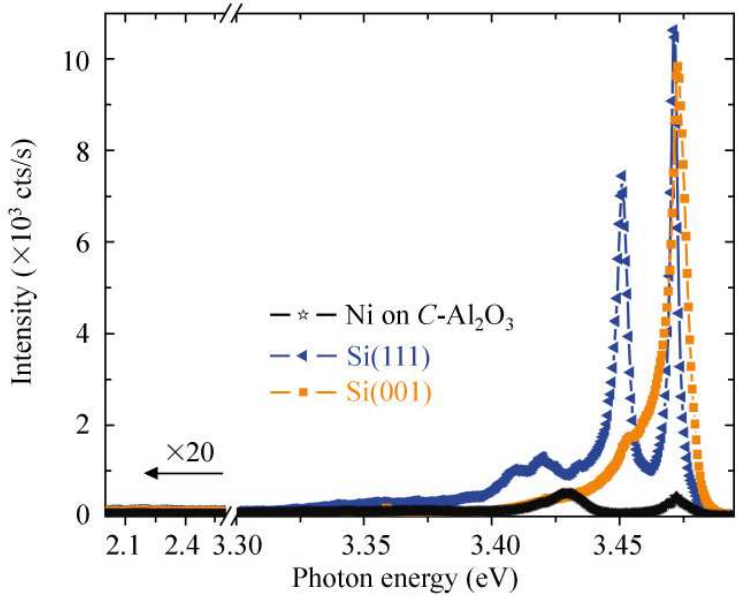

C. Chèze et al, Nano Res. 3, 528 (2010)
Paul-Drude-Institut für Festkörperelektronik, Berlin

Catalyst-free growth: self-formation of NW

Growth diagram of PA-MBE

S. Fernandez-Garrido, J. Appl. Phys. 106, 126102 (2009)
Universidad Politécnica de Madrid

Ga-rich conditions
2D layer
Threading dislocations

As-rich conditions
Vertically elongated grains
No coalescence
Defect-free

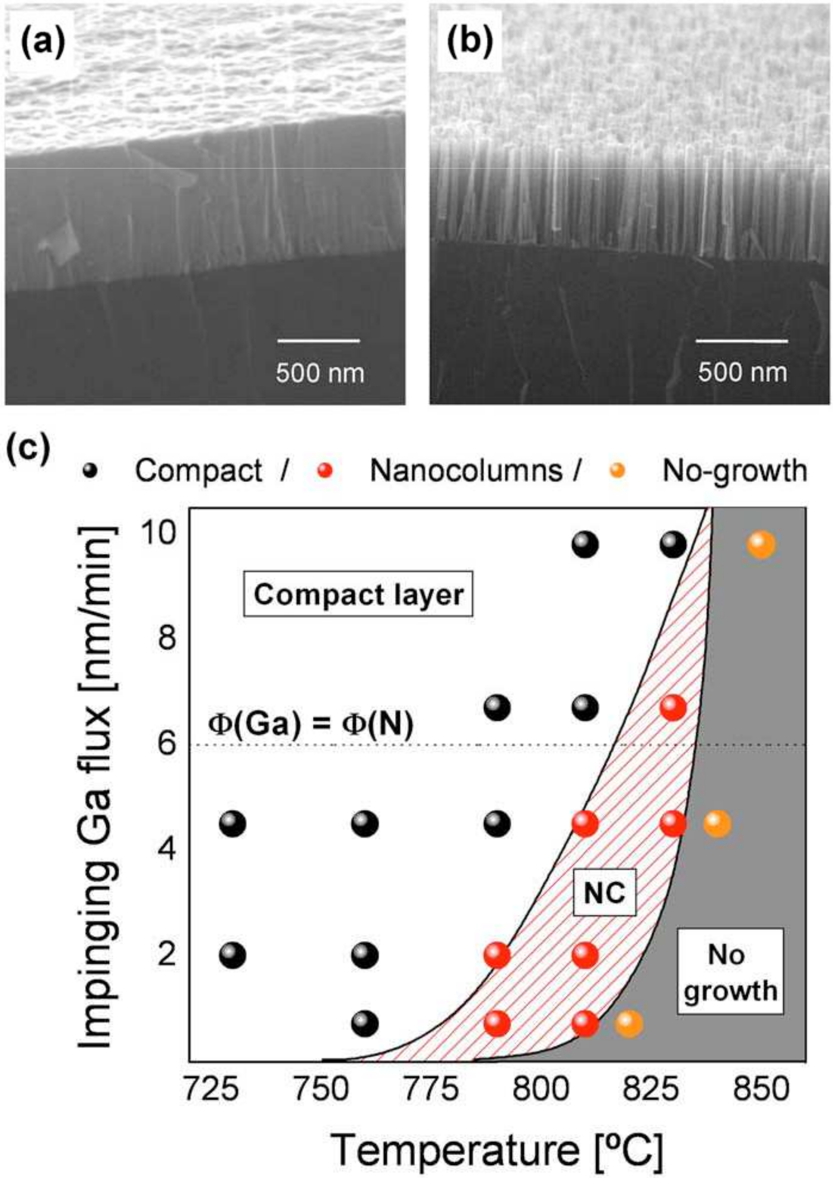

MBE
Ga effusion source
N plasma source
Si (111) substrate

In MBE, NWs form for
- effective N/Ga ratio >1
- 760°C < Ts < 830°C

The impact of evaporation geometry

E. Galopin et al, Nanotechnology 22, 245606 (2011)
LPN, Marcoussis

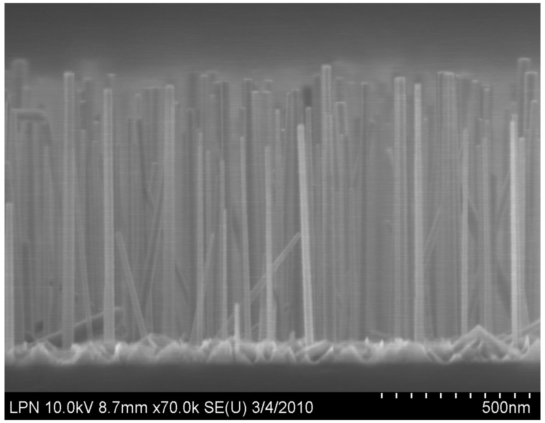

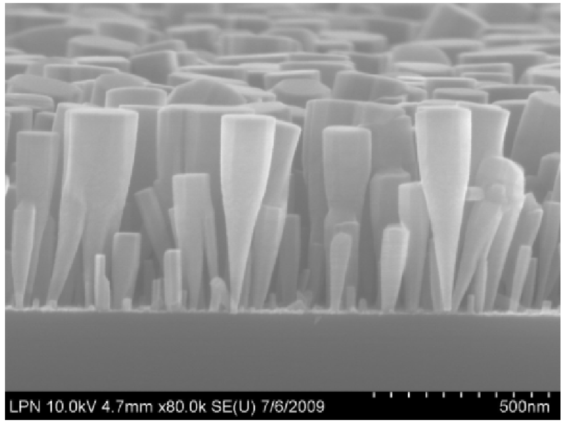

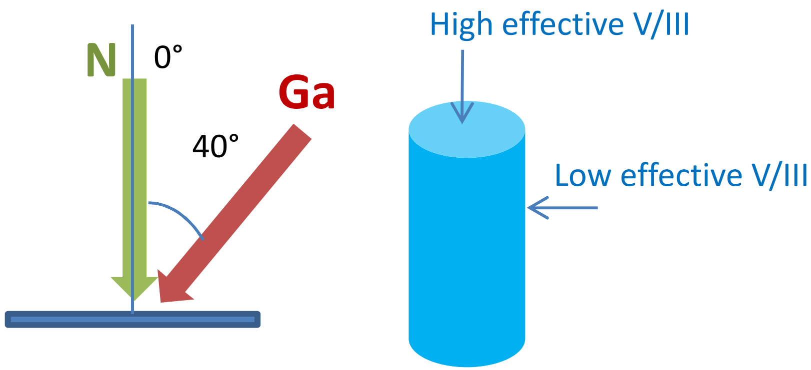

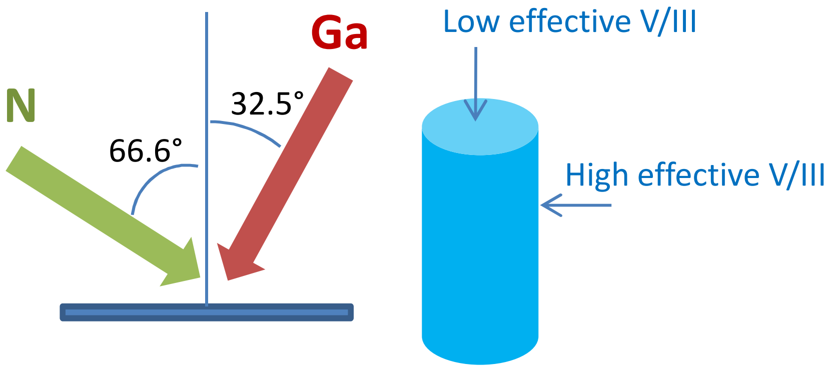

In MBE, the N flux incidence angle has an impact on the shape of the GaN NWs:
lateral growth is reduced at normal incidence / favoured at grazing angles

Kinetics of nanowire growth

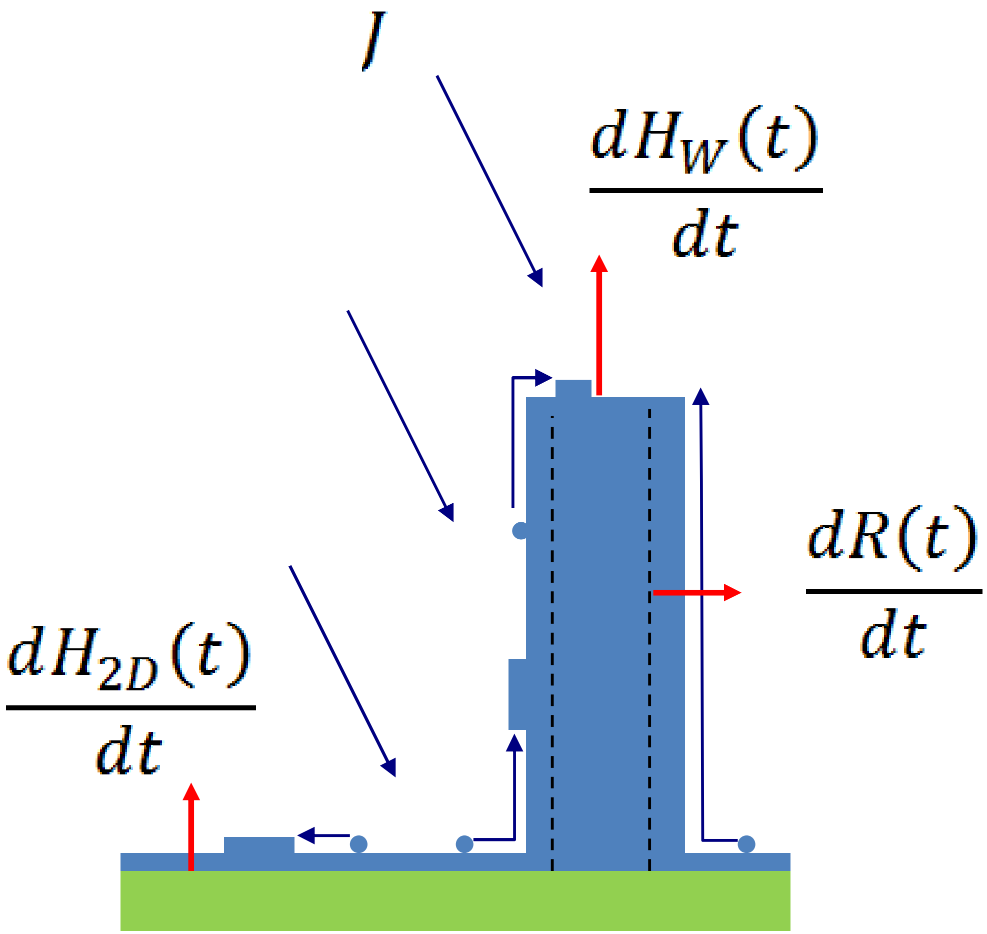

3 competing growth rates:

- Axial growth
- Lateral growth
- Growth on the planar surface

These growth rates are governed by different nucleation rates.

Adatoms can be exchanged between droplet, sidewalls, and substrate via surface diffusion.

Nucleation barrier

Supersaturated phase (gas, liquid, adatoms) $\Delta\mu > 0$

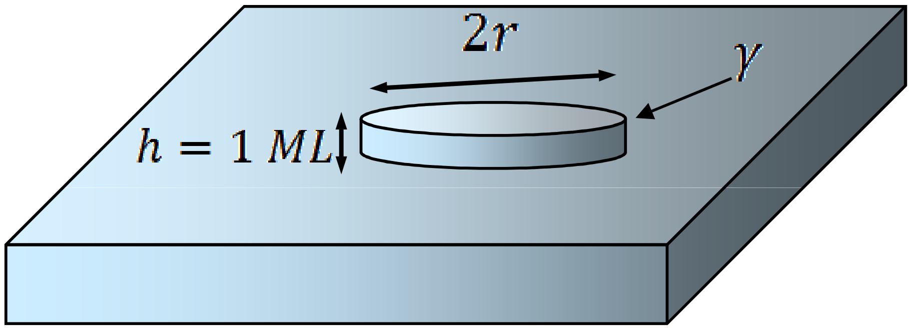

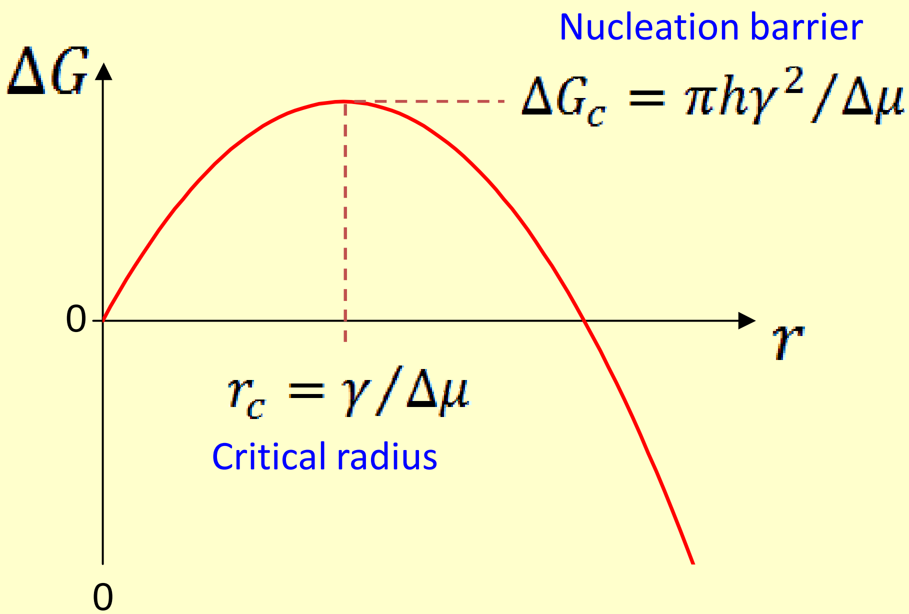

Beyond r_c, nuclei can extend by step flow

Classical nucleation theory

Venables et al, Rep. Prog. Phys. 47, 399 (1984)

Gibbs free energy of nucleus formation

$$\Delta G = -\pi r^2 h \Delta\mu + 2\pi r h \gamma$$

Nucleation rate

$$J \propto \Delta G_c^{-1/2} \exp\left(-\frac{\Delta G_c}{k_B T}\right)$$

Diffusion flows of adatoms

MBE case, adapted from
Dubrovskii 's model, Phys. Rev. B 80, 205305 (2009)

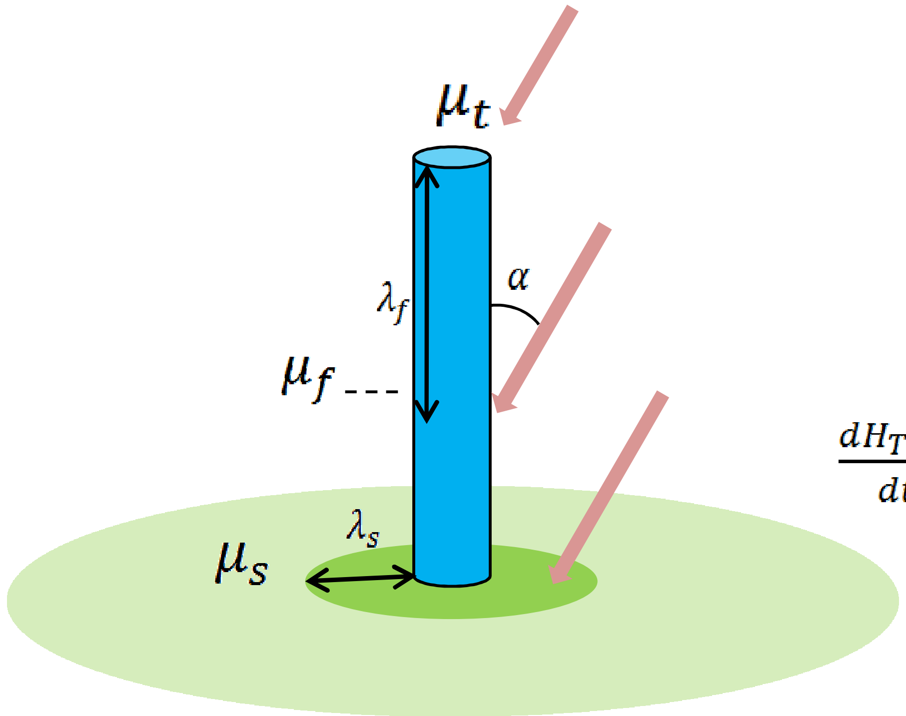

Diffusion equations and balance equation

3 contributions to NW elongation

$$\frac{dH_T(t)}{dt} = J\Omega\left[a + \frac{\left\{\frac{2\lambda_f}{\pi R}(1-\varepsilon_f)\sin(\alpha)\right\}U\left(\frac{H_W(t)}{\lambda_f}\right)+\left\{\frac{2\lambda_s}{R}(1-\varepsilon_s)\cos(\alpha)\delta\right\}}{U'\left(\frac{H_W(t)}{\lambda_f}\right)}\right]$$

$$\varepsilon_f = exp\left(\frac{(\mu_l-\mu_f)}{kT}\right) \qquad \varepsilon_s = exp\left(\frac{(\mu_l-\mu_s)}{kT}\right)$$

$$U(x) = \sinh x + \nu\delta(\cosh x - 1)$$

AlN markers to investigate growth kinetics

E. Galopin et al, Nanotechnology 22, 245606 (2011)
LPN, Marcoussis

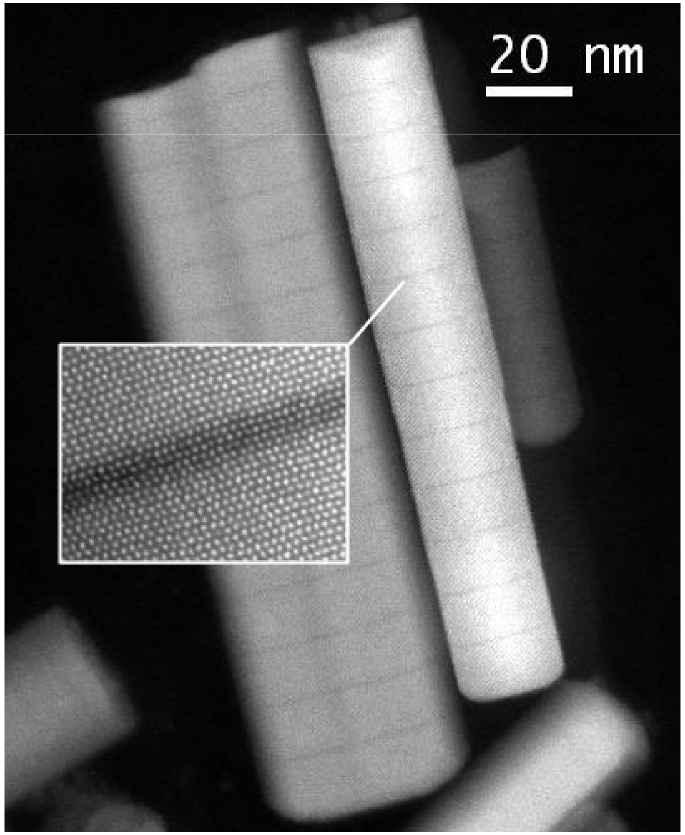

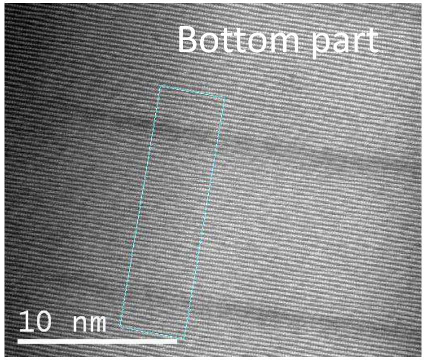

35 ml

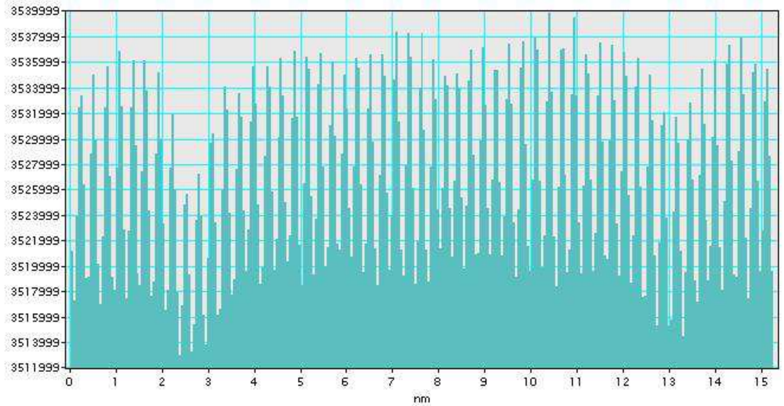

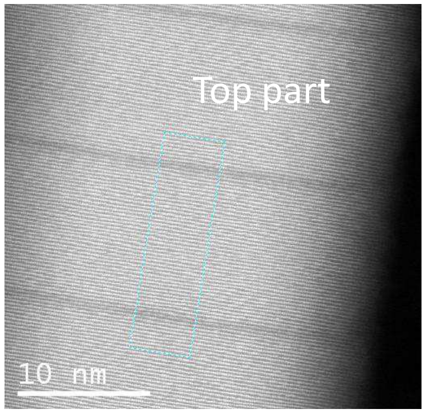

39 ml

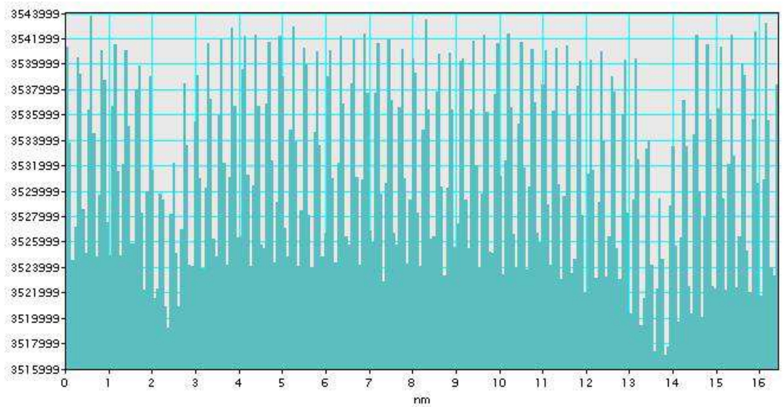

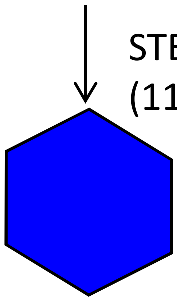

STEM-HAADF
(11-20) zone axis

Evidence Ga adatoms diffusion

E. Galopin et al, Nanotechnology 22, 245606 (2011)
LPN, Marcoussis

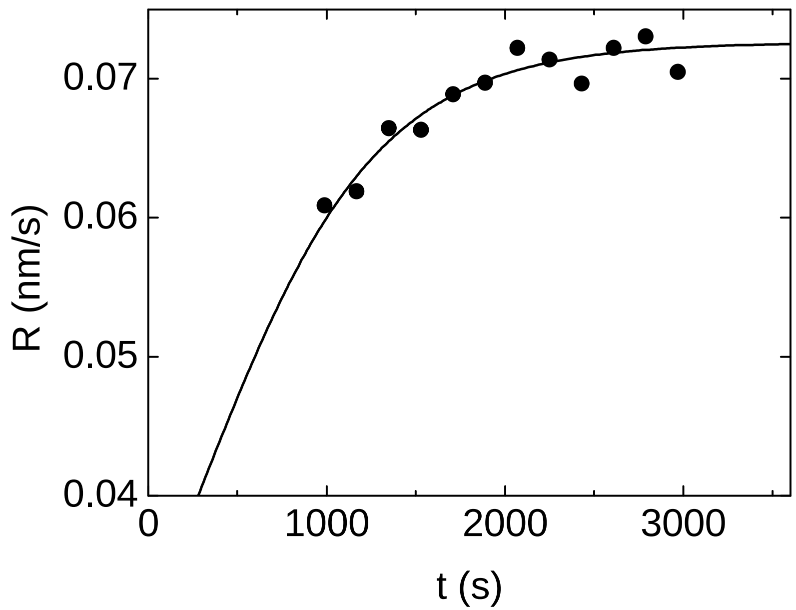

Direct Ga flux equivalent to 0.04 nm/s
V/III>1

→ Surface diffusion of Ga is necessary to explain the elongation rate

→ Collection of Ga by the NW sidewalls

The fit gives
- Ga adatom diffusion length on the sidewalls ≈ 40 nm
- Difference of chemical potentials between the sidewall facets and the top facet : 39 meV/atom
- Incubation time : 280 s

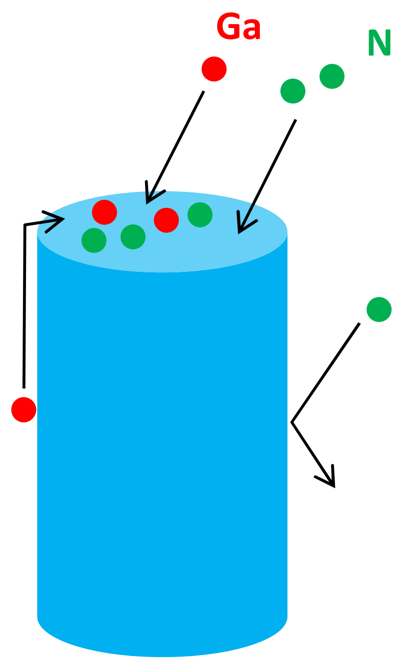

NW growth pursued at V/III <1

Fernandez-Garrido et al, to appear in Nano Lett. 2013
ISOM, Madrid

PAMBE, 2 step growth
1st step, V/III=2
2nd step, variable Ga flux

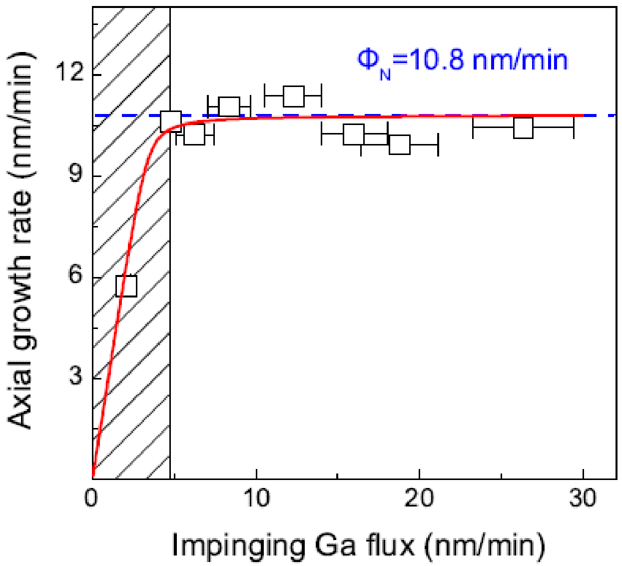

Whatever the V/III is, the axial growth rate is limited by N flux

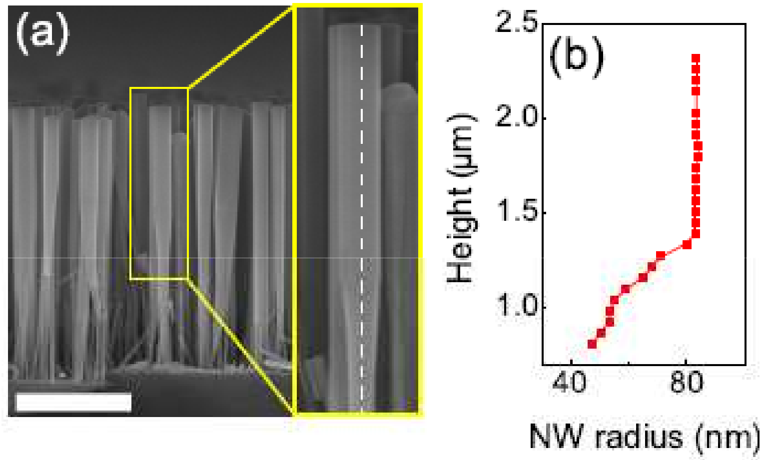

For the second step growth under Ga-rich condition, lateral growth is observed

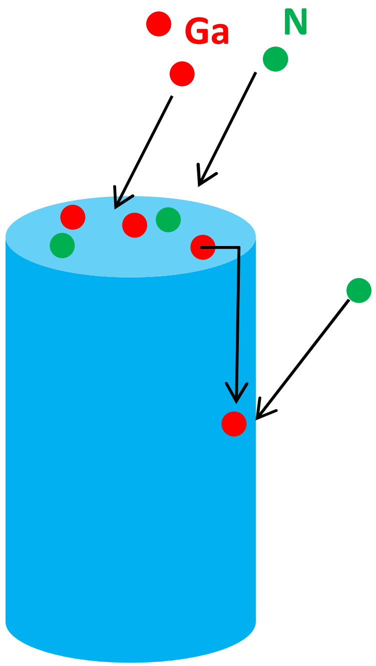

How does lateral growth proceed

E. Galopin et al, Nanotechnology 22, 245606 (2011)
LPN, Marcoussis

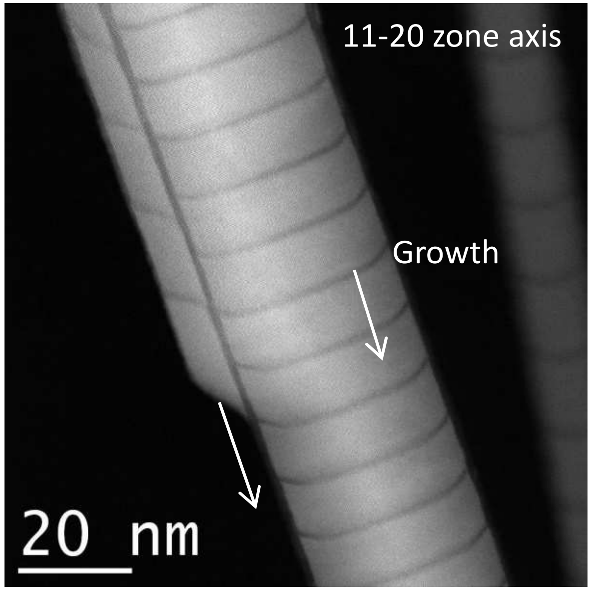

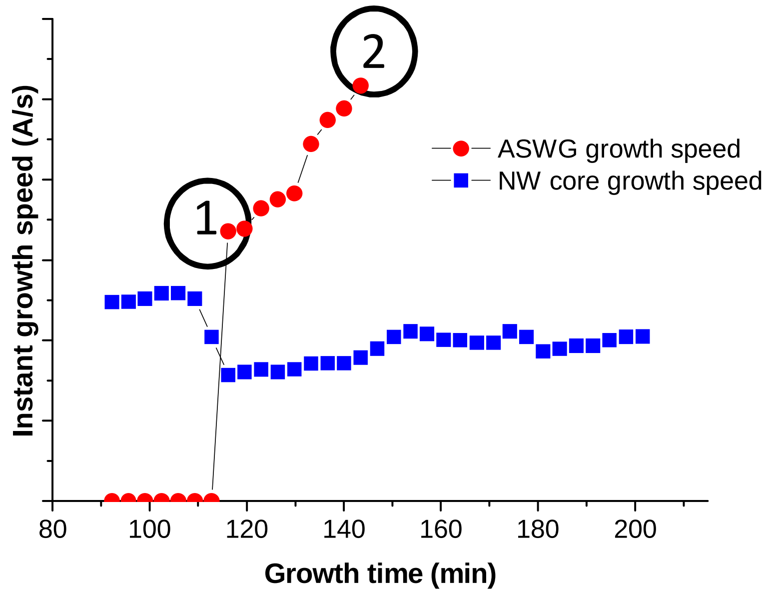

In parallel with the growth of the NW core, stacks of atomic layers progress on the sidewalls, from bottom to top, and eventually catch up the top.

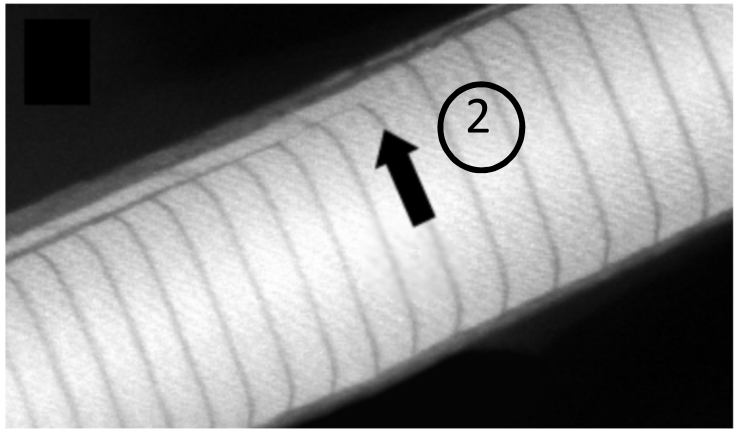

1. Correlations are evidenced: growth rate of the core reduces when a layer starts growing longitudinally on a facet. Ga collection by the sidewalls is shared between the shell and the core

2. Core and shell merge

How does lateral growth proceed

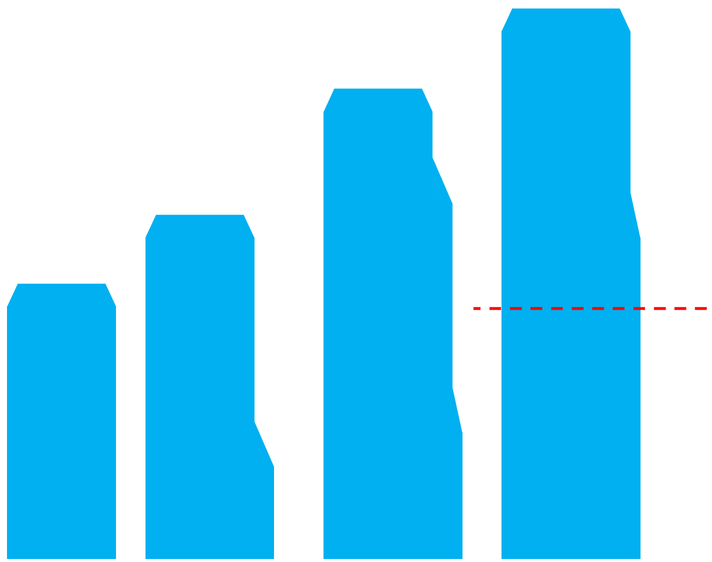

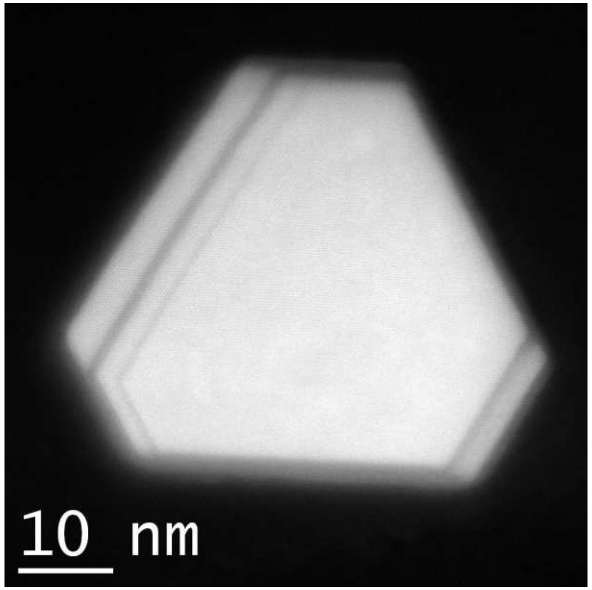

Cross-section

Catalyst-free growth: the initial stage of NW formation

O. Landré, Nanotechnol. 20, 415602 (2009)
CEA-CNRS, Grenoble

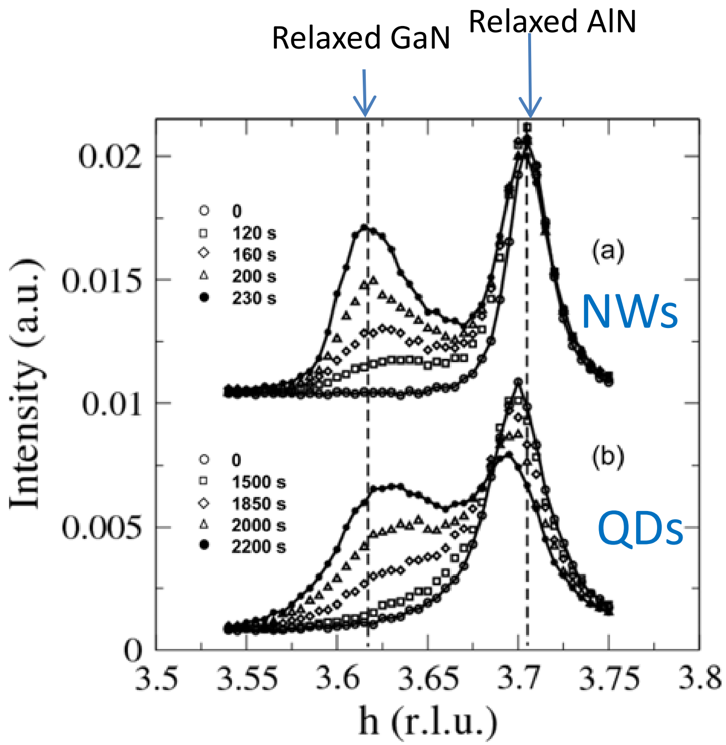

In situ GIXRD measurements
(3030) Diffraction
(the in plane parameter is probed)

Experiment at ESFR

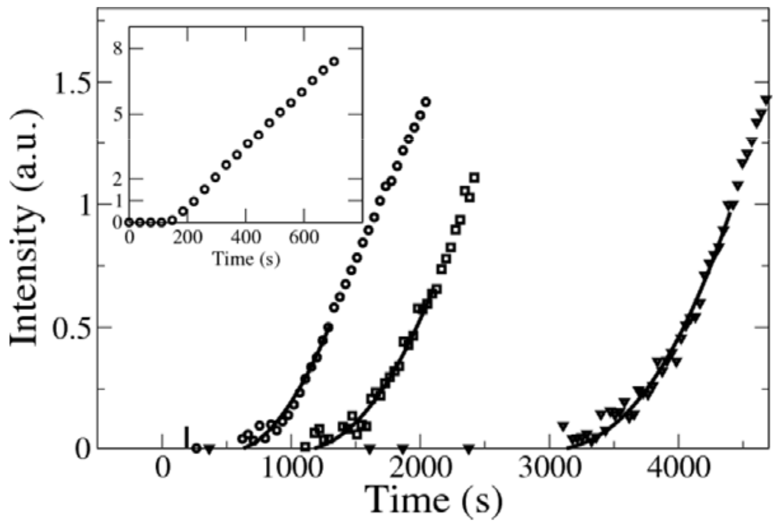

GIXRD intensity of the (30-30) GaN diffraction peak during GaN NW growth

3 stages:

- wetting layer deposition
  → coherent growth: relaxed GaN peak absent
- GaN islands growing laterally (super-linear regime)
  → linear increase of the island diameter ($I_d \propto S \propto R^2 \propto t^2$)
- elongation of fully relaxed GaN NWs
  → linear increase of the NW height ($I_d \propto H \propto t$)

Shape transitions

Consonni et al, Phys Rev B 81, 085310 (2010),
Paul Drude Institute, Berlin

GaN NW formation driven by strain relaxation at the interface

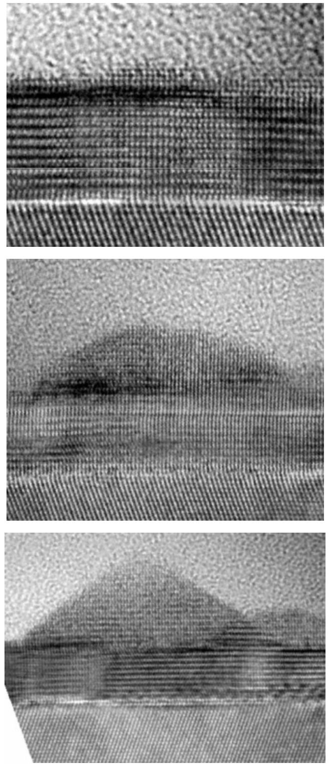

Spherical cap

Truncated pyramid

Full pyramid

1^{st} dislocation

Coherent islands:
They adopt a shape favorable to relief the strain elastically

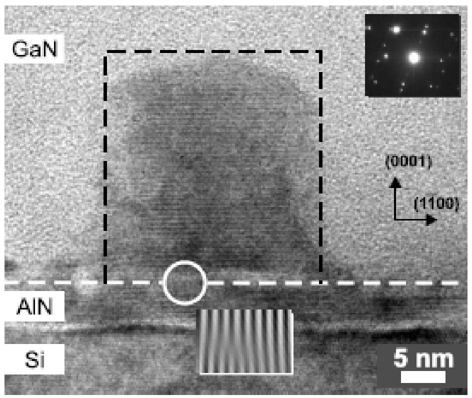

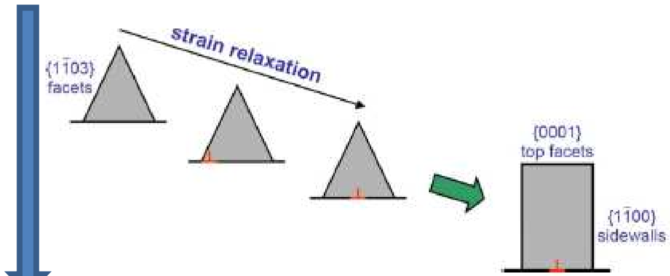

Transition to NW shape
(surface energy of the NW facets
< surface energy of the pyramid facets)

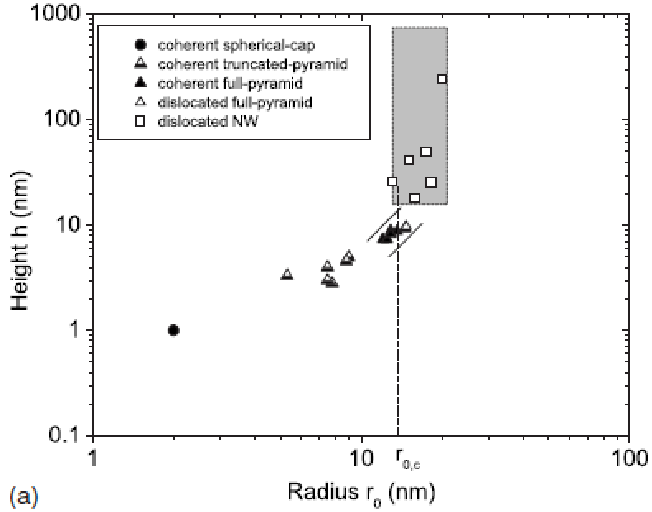

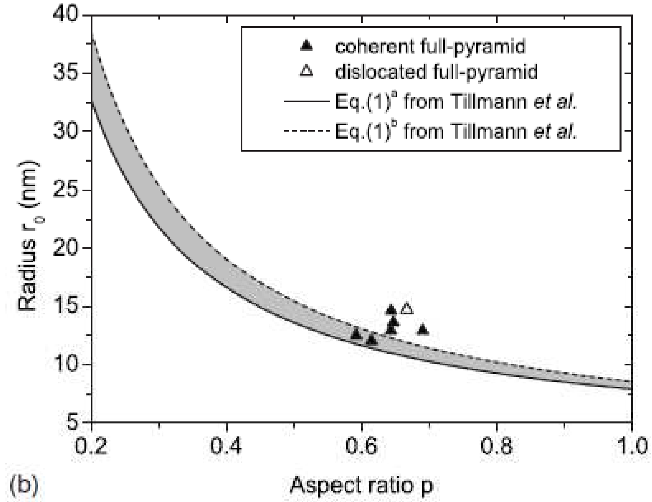

According to this study, all the GaN NWs should contain at least 1 dislocation at their interface with the substrate

Another scenario of NW formation

Largeau et al, Cryst. Growth Des. 12, 2724 (2012)
LPN-CNRS, Marcoussis

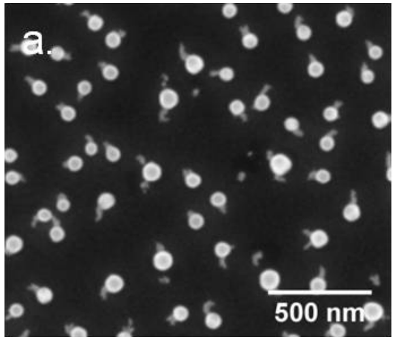

Deposition of Al on Si substrate
Formation of Al-Si liquid droplets

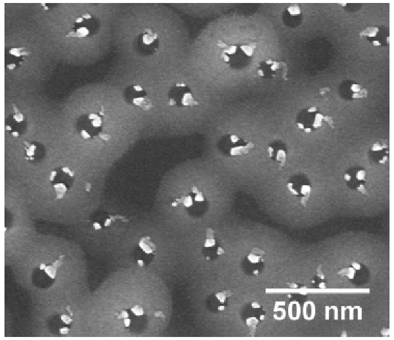

Exposure to N flux
Formation of AlN pedestals

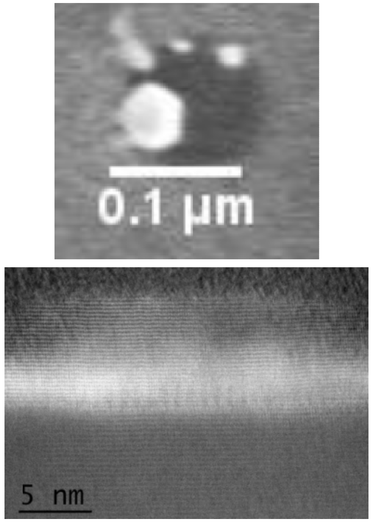

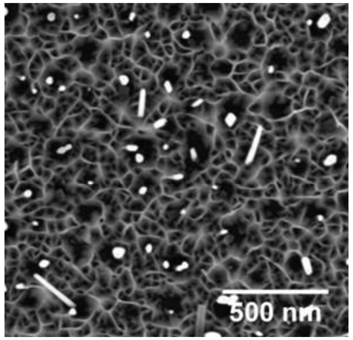

GaN growth at 800 °C
Formation of GaN NWs

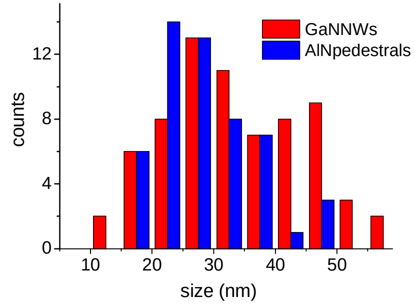

N-polar AlN pedestals

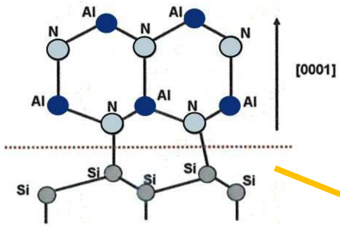

Al-polar AlN layer

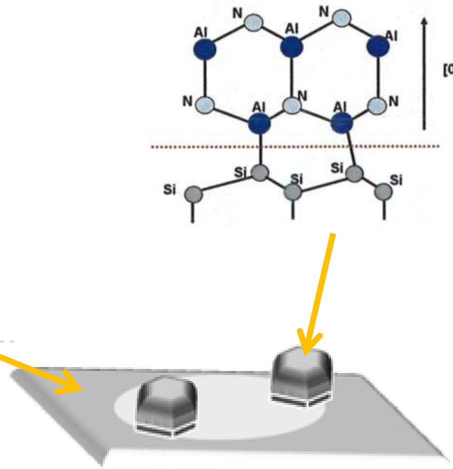

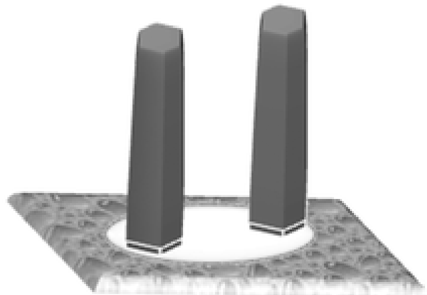

N-polar GaN nanowires

Tuning the NW composition: $Al_xGa_{1-x}N$ and $In_xGa_{1-x}N$ alloys

Elaboration of $Al_xGa_{1-x}N$ NWs over a wide range of composition

Pierret et al, Nanotechnol. 24, 115704 (2013)
CEA/INAC , Grenoble

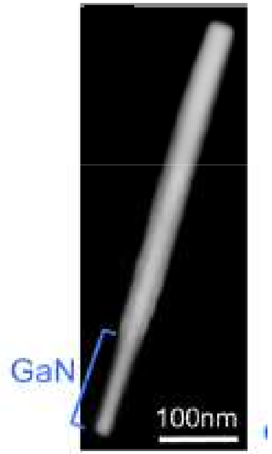

PAMBE growth
AlGaN rods on top of GaN stems

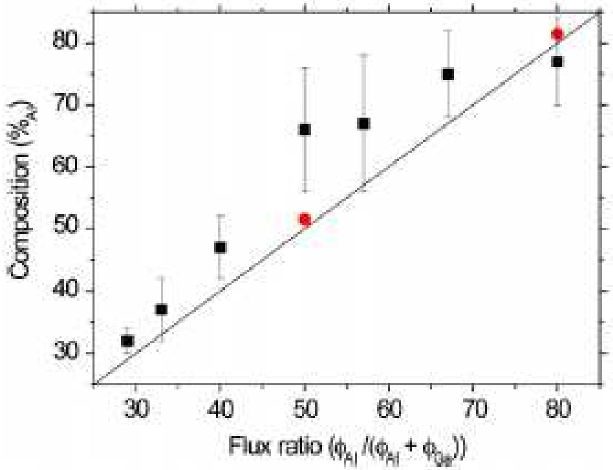

Squares: Raman spect., circles: XRD
Whole range of composition

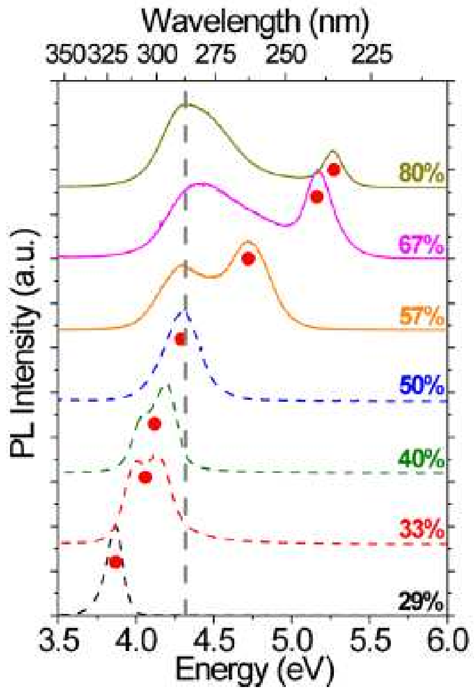

5K PL spectra
Emission in the UV range

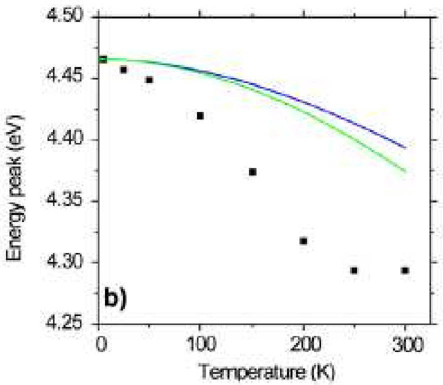

Temperature dependence of the PL peak

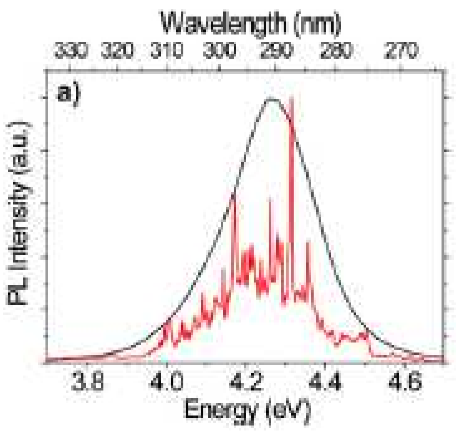

µ-PL on a few NWs

Existence of localized centers probably related to composition fluctuations (Ga-rich clusters)

Elaboration of $In_xGa_{1-x}N$ NWs over a wide range of composition

Kuykendal et al, Nature Mat. (2007)
Univ. California, Berkeley

~10 % variation of c parameter

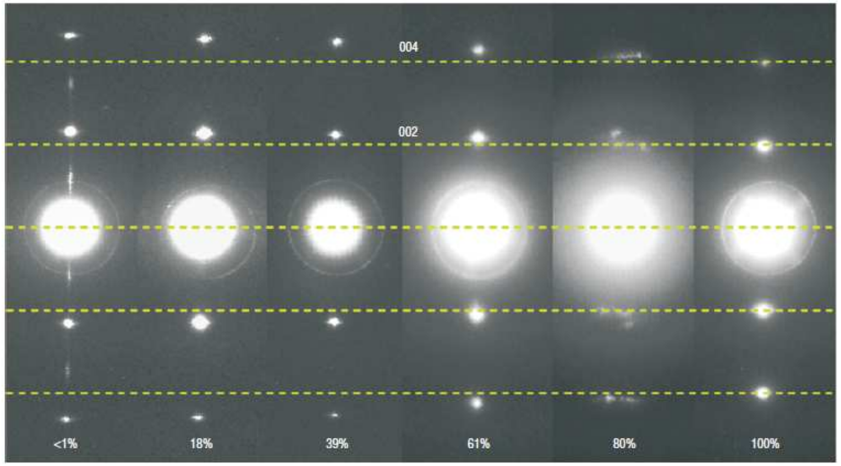

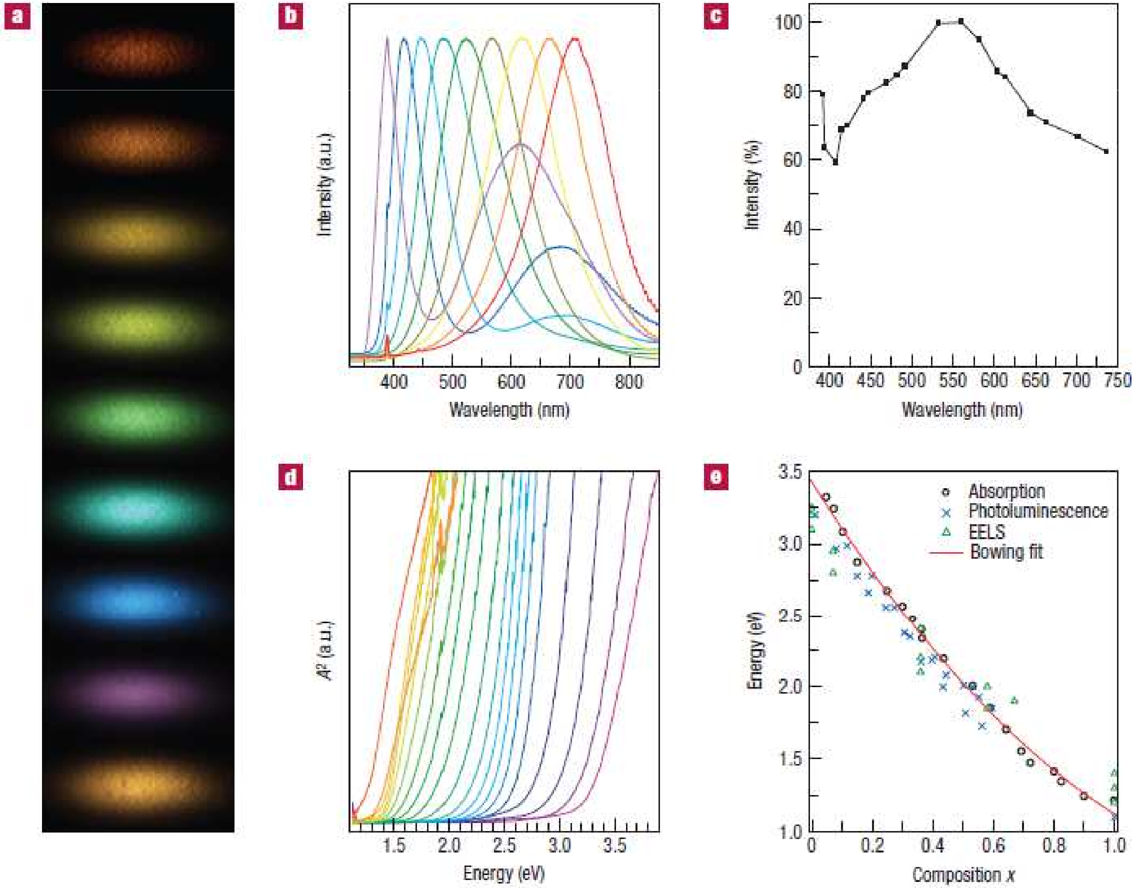

CVD,
$InCl_3$, $GaCl_3$, NH_3
525°C< Ts <575°C

NW morphology → strain-relaxed growth → less phase separation

NW growth

Complex

- various mechanisms
- method-dependent
- growth condition-dependent

Flexible

- large choice of substrates
- original heterostructures
- many parameters to obtain the desired shape

Solves a major issue of III-nitrides growth :

Lattice mismatch and difference of thermal expansion with the substrates are much less critical

Free sidewalls $\rightarrow$ Elastic relaxation of strain

No threading dislocations, no cracks $\rightarrow$ High crystalline quality on any substrate

- Introduction
- GaN nanowire growth mechanisms
- Critical dimensions of nanowire heterostructures
- Nanowire characterization
- Nanowire applications

Hetero-epitaxial systems in general

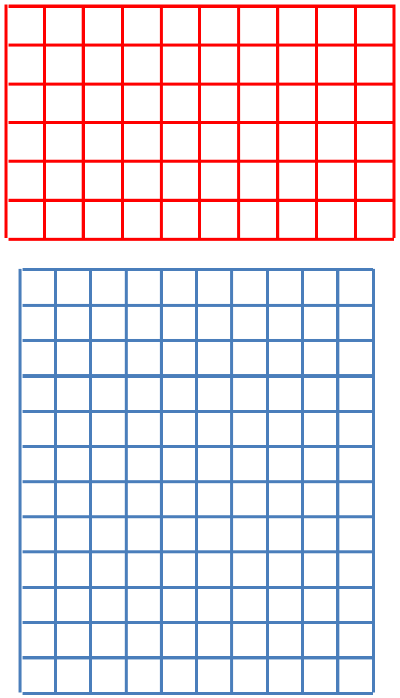

material B on material A
$a_B \neq a_A$

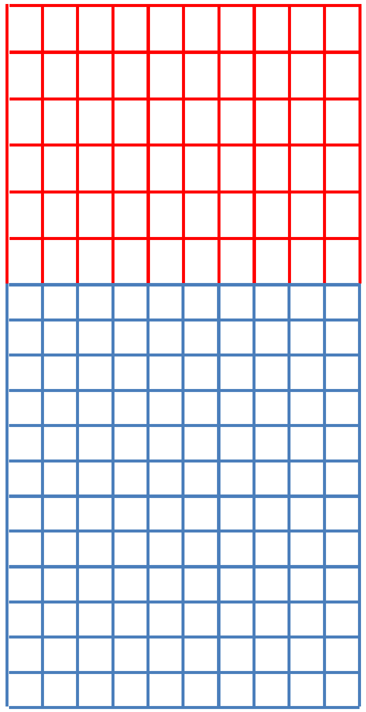

The lattice is strained to accomodate the misfit

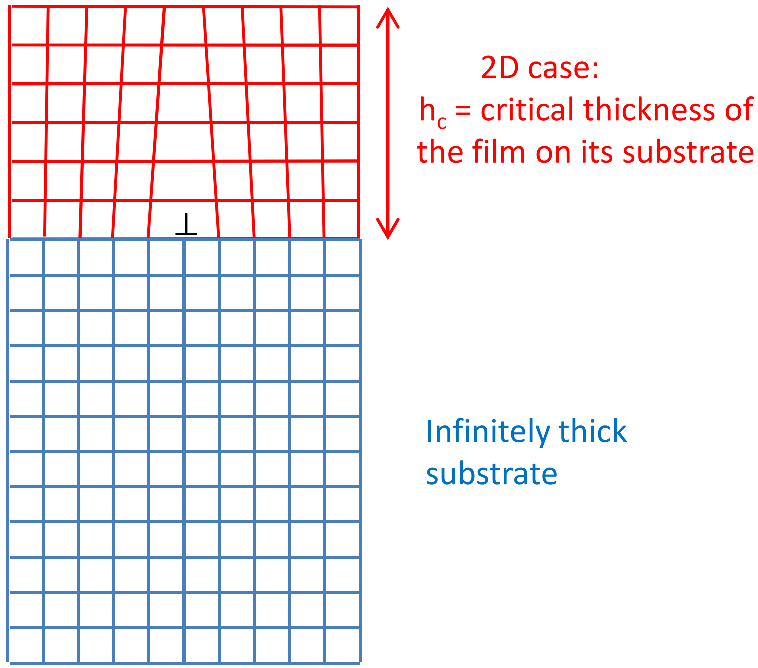

Lost of coherence of the crystalline lattices
Strain energy > dislocation energy
Strain relaxation via formation of dislocations

Due to the presence of free surfaces, the NW morphology allows accommodating larger lattice-mismatches as compared to 2D films

(the forces on any free surface cancel)

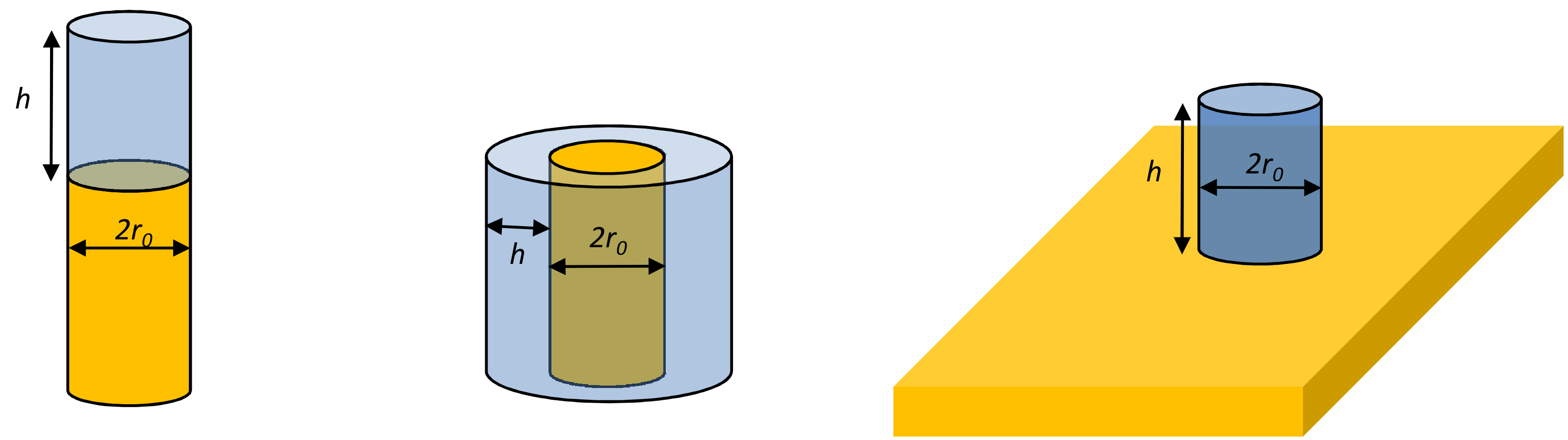

3 cases to be considered

The case of axial heterostructures

F. Glas, Phys. Rev. B 74, 121302 (2006)
LPN-CNRS, Marcoussis

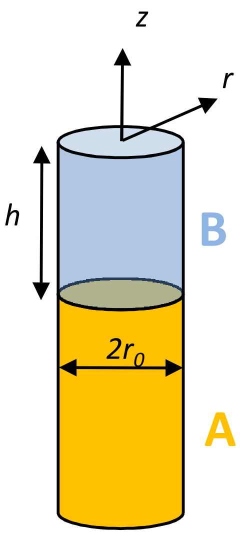

Axial heterostructure

Assumptions:
- elastic stiffness tensor is isotropic
- infinite nanowire length (material A)
- ε_0: misfit of material B
- Circular cross-section

$$W_e = \frac{E}{1-\nu} f_\nu(\rho)\pi r_0^2 h \epsilon_0^2 \simeq \frac{E}{1-\nu}\frac{\pi r_0^2 h \epsilon_0^2}{1+A_\nu \rho}$$

Method:
Calculate the total strain energy of the system, W_e, as a function of h (finite-element calculations and approximate analytical expression)

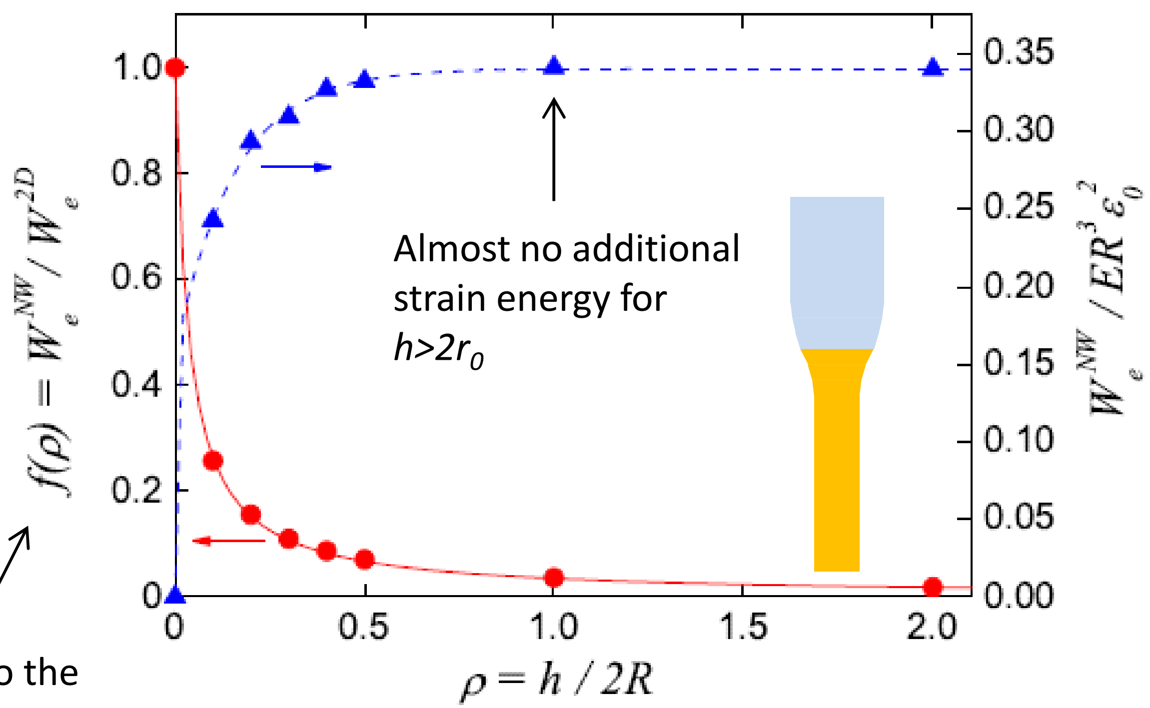

Normalized to the case of 2D layers

Introduction of dislocations

F. Glas,Phys. Rev. B 74, 121302 (2006)
LPN-CNRS, Marcoussis

Dislocation formation:

A single pair of orthogonal dislocations is considered

The total energy is modified :

- W_e is reduced (partial relaxation)
-Additionnal energy W_d (dislocation energy)

$$w_d = \frac{E(1-\nu\cos^2\theta)b^2}{8\pi(1-\nu^2)}\left(1+\ln\frac{\bar{h}}{b}\right)$$

$\bar{h}$ distance between the dislocation line and the free surface
b Burger vector
θ Angle between the dislocation line and the Burger vector
E Young modulus
ν Poisson ratio

Pure edge (θ=π/2, b_{eff}=b)
or 60° type (θ=π/3, b_{eff}=b/2)

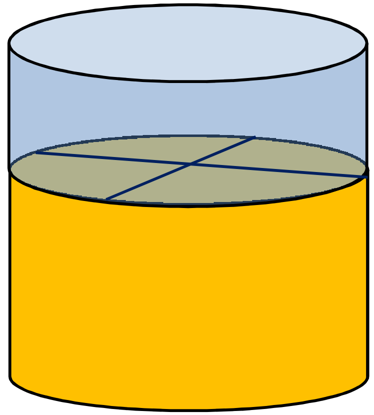

Excess of energy of the state with the dislocation pair with respect to the coherently strained case

$$\Delta W(r_0,h) = \frac{Er_0}{1-\nu}\left[f_\nu\left(\frac{h}{2r_0}\right)\pi r_0 h\left(\frac{\alpha^2 b_{\mathrm{eff}}^2}{4r_0^2} - \frac{\alpha b_{\mathrm{eff}}}{r_0}\epsilon_0\right) + C\left(1+\ln\frac{\bar{h}(r_0,h)}{b}\right)\right]$$

with $C=(1-\nu\cos^2\theta)b^2/[2\pi(1+\nu)]$

$\Delta W(r_0,h)=0$ → critical dimensions

Critical dimensions of axial heterostructures

F. Glas,Phys. Rev. B 74, 121302 (2006)
LPN-CNRS, Marcoussis

Existence of a critical radius below which the critical height is infinite

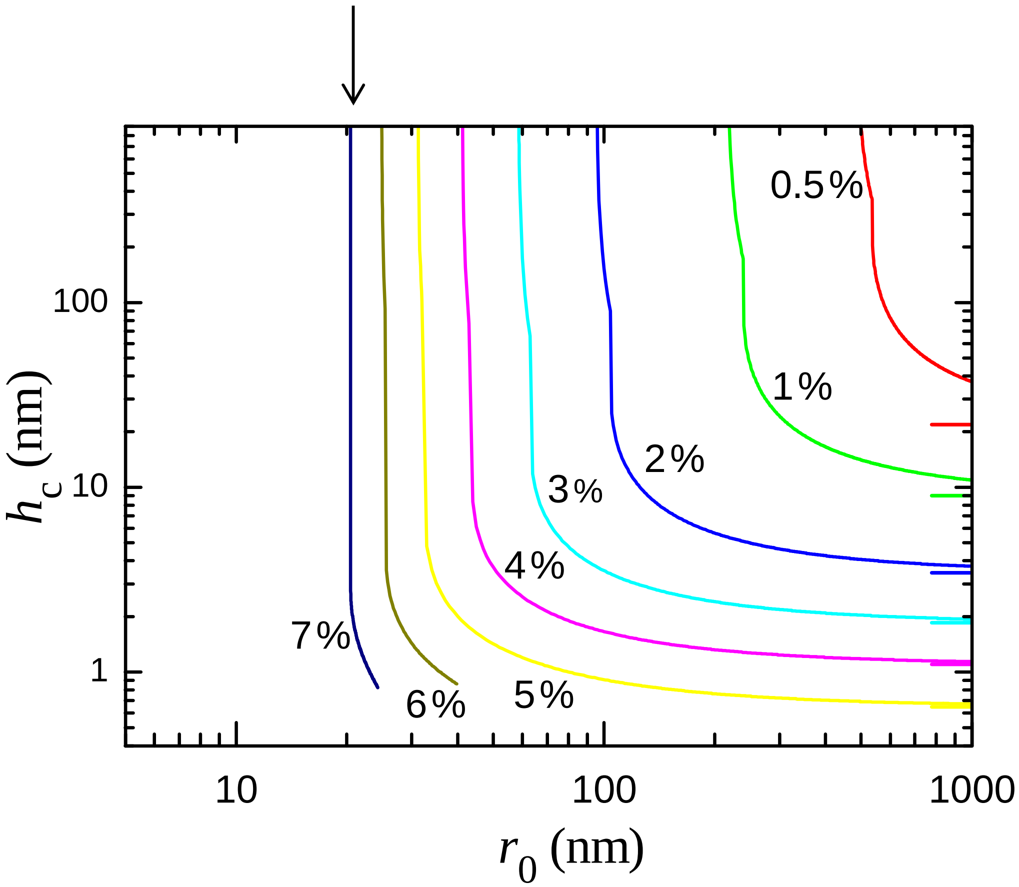

Critical dimensions as function of the misfit
Calculation based on GaAs parameters

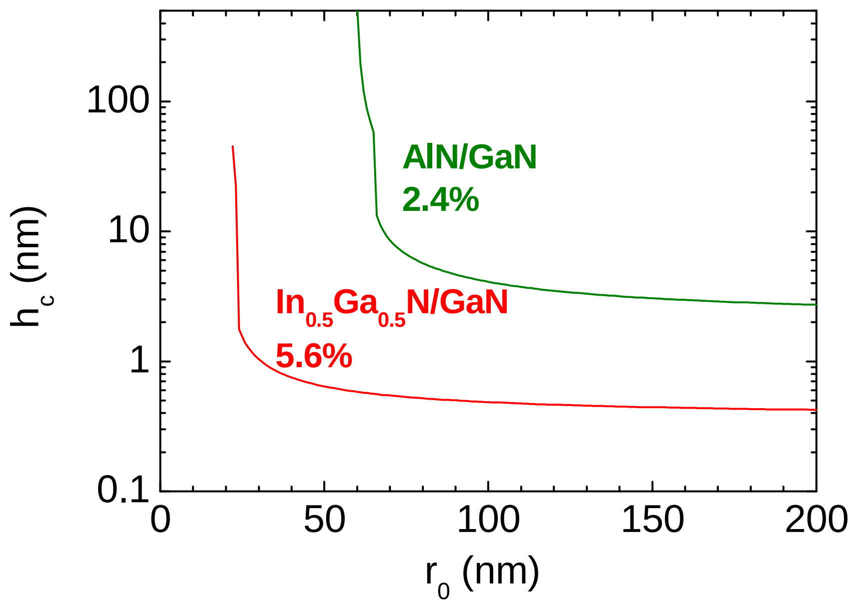

Calculation for III-N systems

The critical radius of axial III-N heterostructures

$$\frac{2\pi}{A_v}\left(\frac{\alpha^2 b_{\mathrm{eff}}^2}{4} - \alpha b_{\mathrm{eff}}\epsilon_0 r_0^c\right) + C\left(1 + \ln\frac{\beta r_0^c}{b}\right) = 0$$

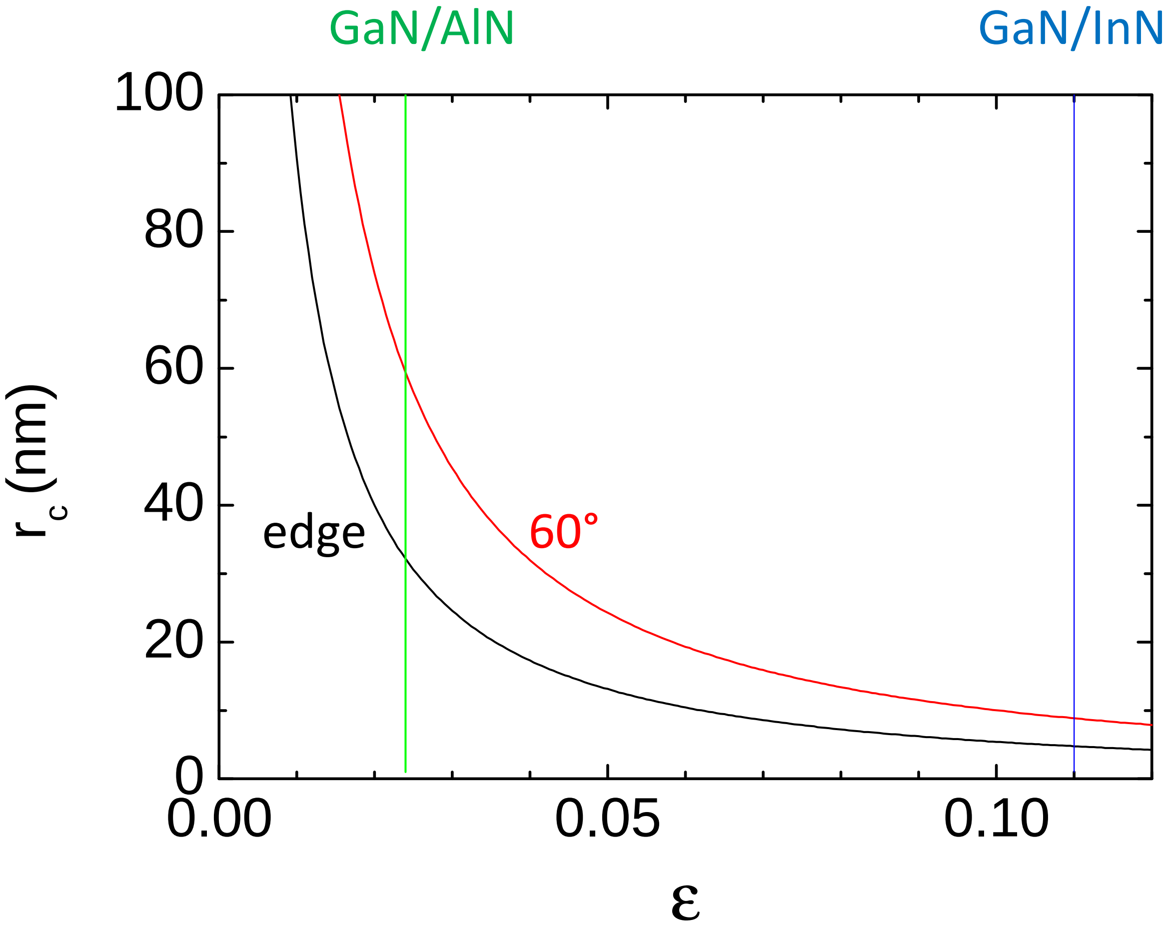

The case of radial heterostructures

Raychaudhuri and Yu, J. Appl. Phys. 99, 114308 (2006)
University of California, San Diego

The core-shell structure

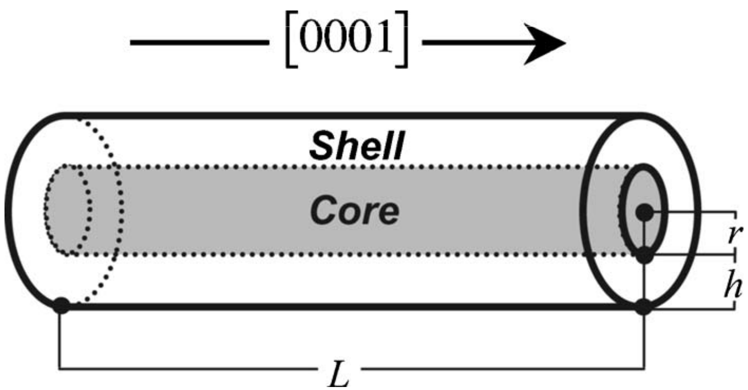

Longitudinal (c) and tangential strain (a)
at the interface
for the core (i) and for the shell (ii)

$$f_c^{(i)} = \frac{c - c^{(i)}}{c^{(i)}} \qquad f_c^{(ii)} = \frac{c - c^{(ii)}}{c^{(ii)}}$$

$$f_a^{(i)} = \frac{a - a^{(i)}}{a^{(i)}} \qquad f_a^{(ii)} = \frac{a - a^{(ii)}}{a^{(ii)}}$$

Assumptions:
- elastic stiffness tensor is isotropic in a cross-sectional plane
- infinite nanowire length L
- Circular cross-section

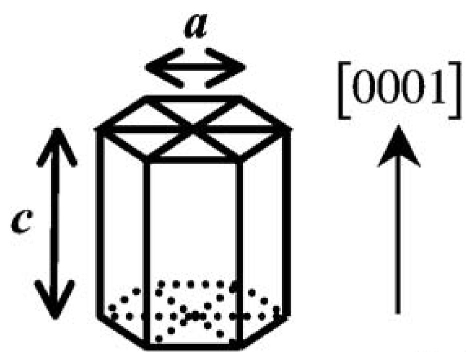

Equilibrium parameters in a radial heterostructure

Raychaudhuri and Yu, J. Appl. Phys. 99, 114308 (2006)

Method:

Express the total strain energy of the system as a function of

- strain components
- elastic stiffness tensor elements

$$U^{(i)} = \frac{[c_{11}^{(i)} f_a^{(i)}]^2 - [c_{12}^{(i)} f_a^{(i)} + c_{13}^{(i)} f_c^{(i)}]^2 + c_{11}^{(i)} f_c^{(i)} [c_{13}^{(i)} f_a^{(i)} + c_{33}^{(i)} f_c^{(i)}]^2}{2 c_{11}^{(i)}} L\pi (r^2),$$

$$U^{(ii)} = \frac{[c_{11}^{(ii)} f_a^{(ii)}]^2 - [c_{12}^{(ii)} f_a^{(ii)} + c_{13}^{(ii)} f_c^{(ii)}]^2 + c_{11}^{(ii)} f_c^{(ii)} [c_{13}^{(ii)} f_a^{(ii)} + c_{33}^{(ii)} f_c^{(ii)}]^2}{2 c_{11}^{(ii)}} L\pi [(r+h)^2 - r^2].$$

Find the equilibrium lattice parameters a and c which minimize this expression

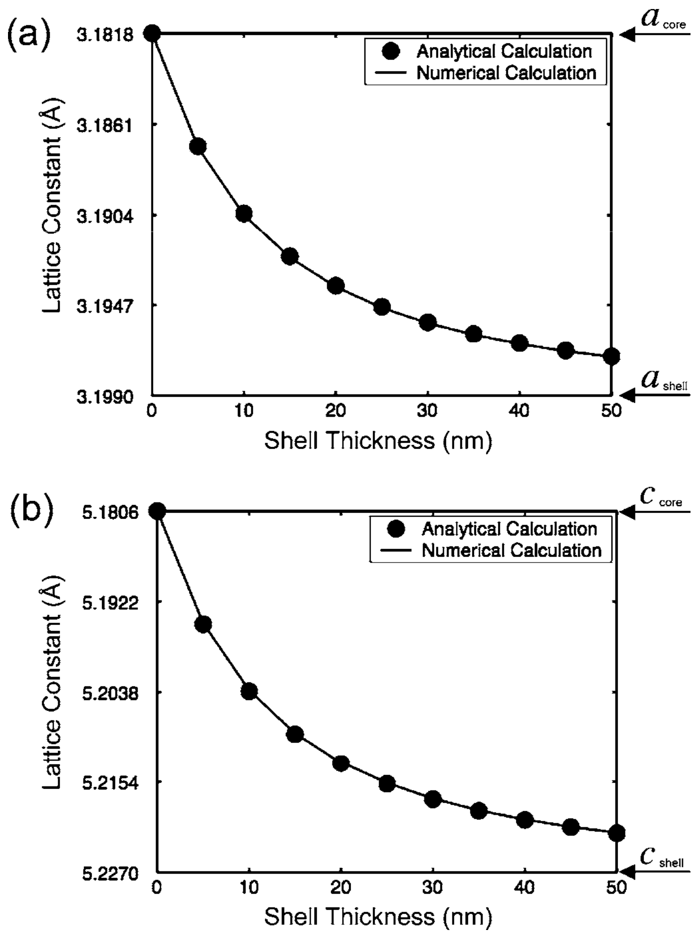

Equilibrium lattice parameters of a coherent core-shell structure:
25 nm GaN core - $Al_{0.2}Ga_{0.8}N$ shell

Strain fields calculated by the VFF model and their experimental observation

Hestroffer, Nanotechnology 21, 415702 (2010)
CEA-CNRS, Grenoble

Valence Force Field (VFF) atomistic model

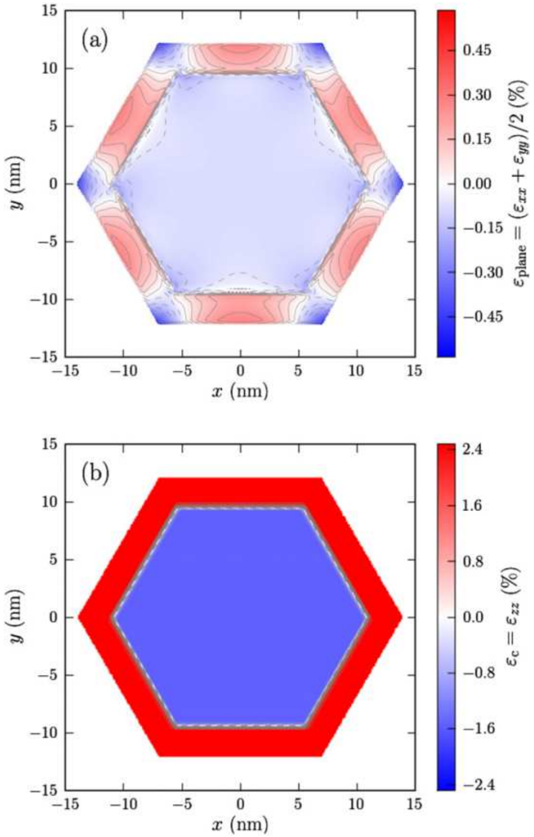

GaN/AlN core-shell

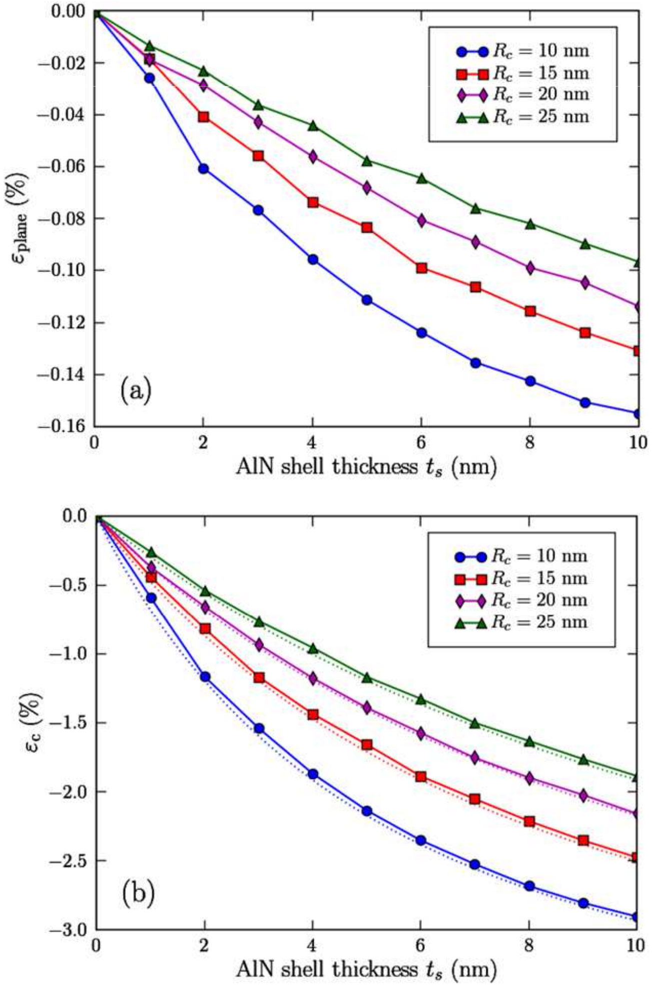

Strain along the axis

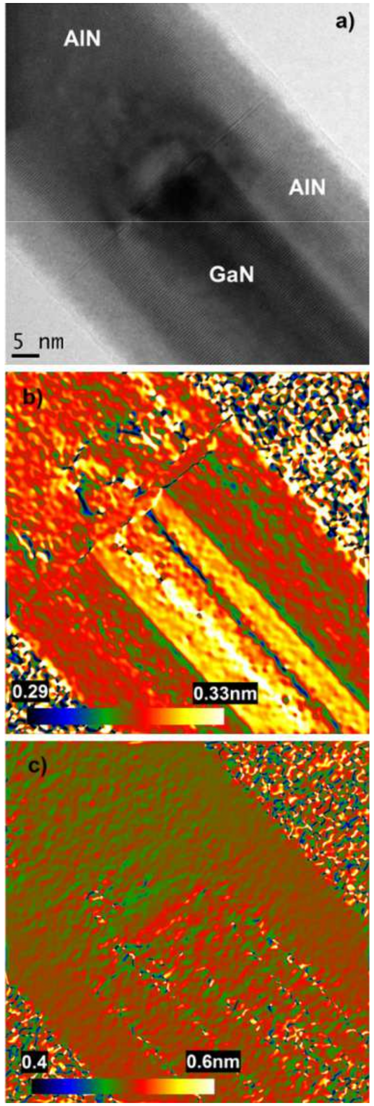

In-plane parameter

AlN shell has the same a as the relaxed AlN

Axial parameter
GaN and AlN have almost the same c in the core-shell region

Geometrical phase analysis (GPA): Maps of the a and c parameters

Introduction of dislocations

Raychaudhuri and Yu, J. Appl. Phys. 99, 114308 (2006)

Dislocation formation (two types)

pure edge dislocation along [0001]
with Burger vector in <11-20>
(relaxes the tangential strain)

edge dislocation loop
with Burger vector in [0001]
(relaxes the longitudinal strain)

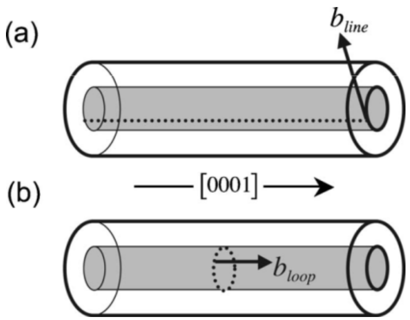

$$U_{\mathrm{line}} = n_{\mathrm{line}} 2\pi r L \left[\frac{c_{11}^{(ii)} - c_{12}^{(ii)}}{2c_{11}^{(ii)}} \right] \frac{b_{\mathrm{line}}^2}{4\pi} \log\left(\frac{4h}{b_{\mathrm{line}}} \right)$$

$$U_{\mathrm{loop}} = n_{\mathrm{loop}} L 2\pi r [c_{13}^{(ii)} + \sqrt{c_{11}^{(ii)} c_{33}^{(ii)}}] \sqrt{\frac{c_{44}^{(ii)}[\sqrt{c_{11}^{(ii)} c_{33}^{(ii)}} - c_{13}^{(ii)}]}{c_{11}^{(ii)}[c_{13}^{(ii)} + 2c_{44}^{(ii)} + \sqrt{c_{11}^{(ii)} c_{33}^{(ii)}}]}} \frac{b_{\mathrm{loop}}^2}{4\pi} \times \log\left(\frac{32r}{b_{\mathrm{loop}}} - 1 \right).$$

$$U_{\mathrm{tot}} = U^{(i)} + U^{(ii)} + U_{\mathrm{line}} + U_{\mathrm{loop}}$$

$$\partial U_{\mathrm{tot}} / \partial n|_{n=0}$$

$$f_a^{(i)} = \frac{a - a^{(i)}}{a^{(i)}} - \left[\frac{a^{(i)} - a}{|a^{(i)} - a^{(ii)}|} \right] n_{\mathrm{line}} b_{\mathrm{line}},$$

$$f_a^{(ii)} = \frac{a - a^{(ii)}}{a^{(ii)}} - \left[\frac{a - a^{(ii)}}{|a^{(i)} - a^{(ii)}|} \right] n_{\mathrm{line}} b_{\mathrm{line}},$$

$$f_c^{(i)} = \frac{c - c^{(i)}}{c^{(i)}} - \left[\frac{c^{(i)} - c}{|c^{(i)} - c^{(ii)}|} \right] n_{\mathrm{loop}} b_{\mathrm{loop}},$$

$$f_c^{(ii)} = \frac{c - c^{(ii)}}{c^{(ii)}} - \left[\frac{c - c^{(ii)}}{|c^{(i)} - c^{(ii)}|} \right] n_{\mathrm{loop}} b_{\mathrm{loop}}.$$

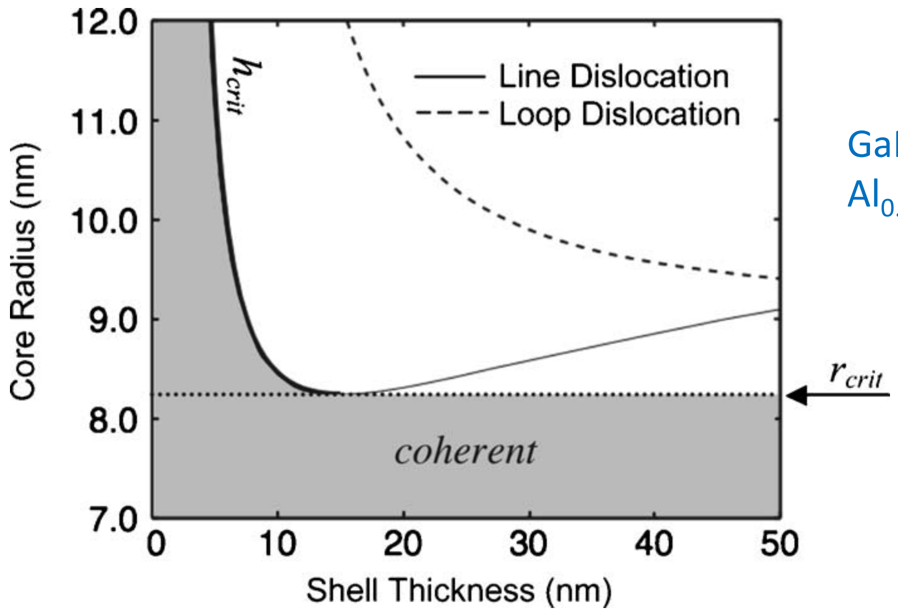

GaN core
$Al_{0.5}Ga_{0.5}N$ shell

Critical dimensions of radial heterostructures

Raychaudhuri and Yu, J. Appl. Phys. 99, 114308 (2006)

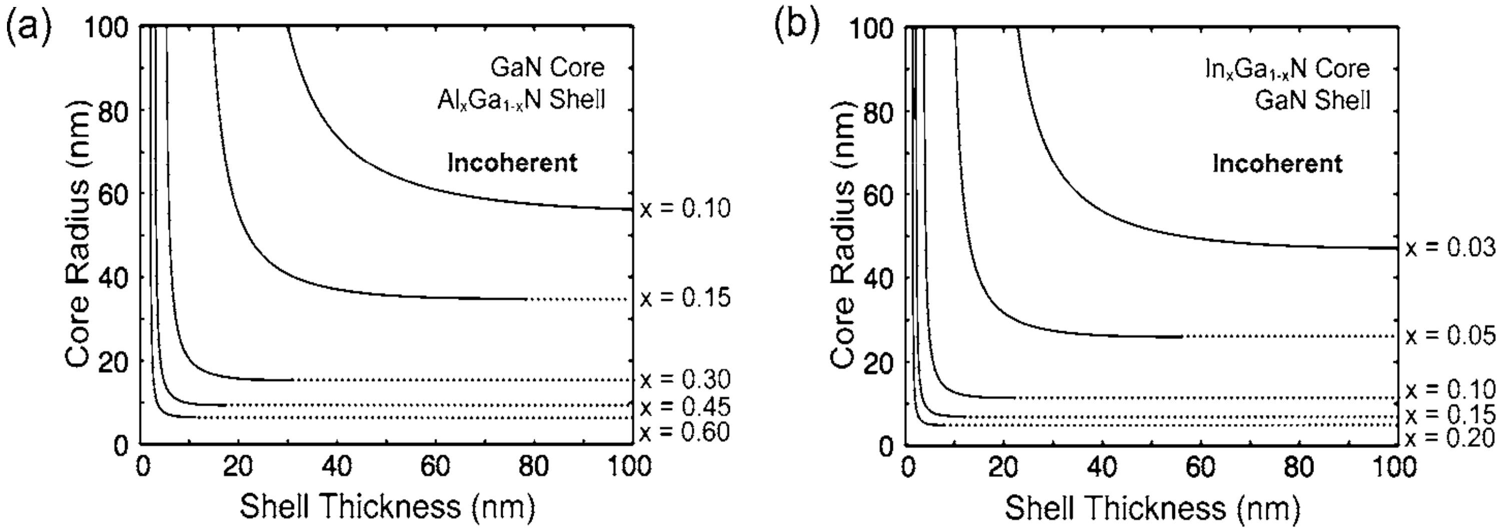

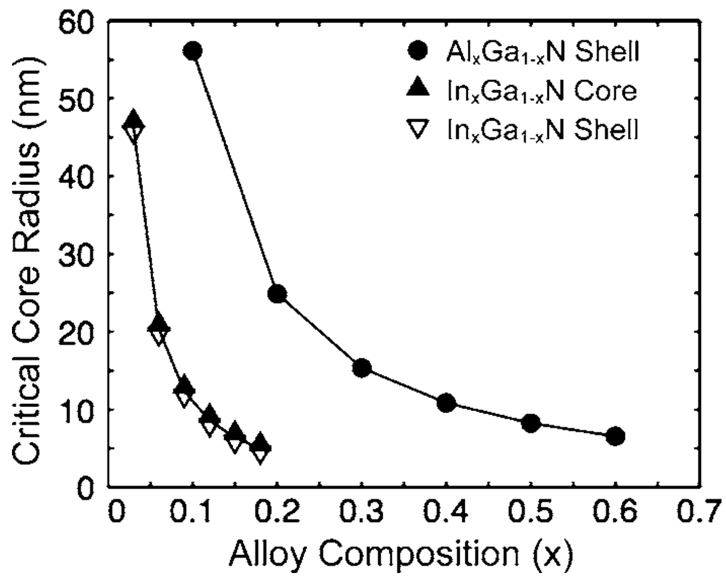

● GaN core/$Al_xGa_{1-x}N$ shell

▲ $In_xGa_{1-x}N$ core/GaN shell

▽ GaN core/$In_xGa_{1-x}N$ shell

The case of a NW on a planar substrate

X. Zhang et al, Cryst. Growth Des. 11, 5441 (2011)
St. Petersburg Academic University

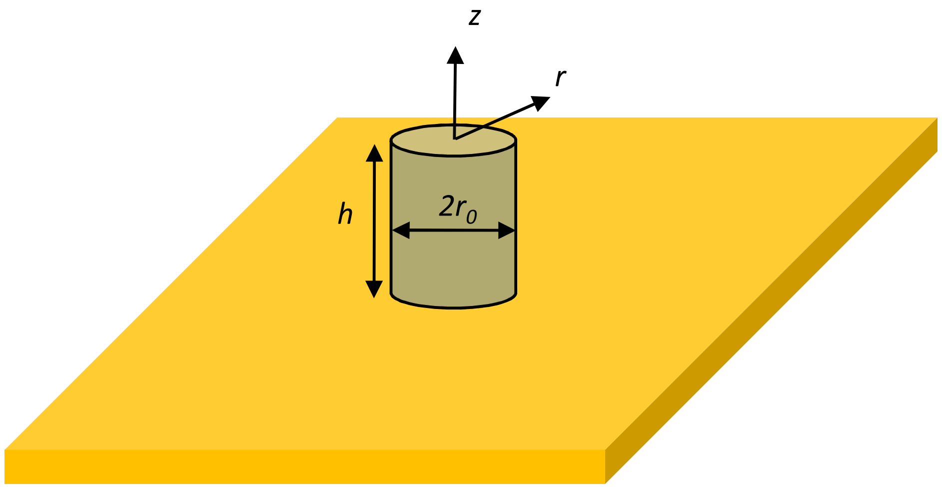

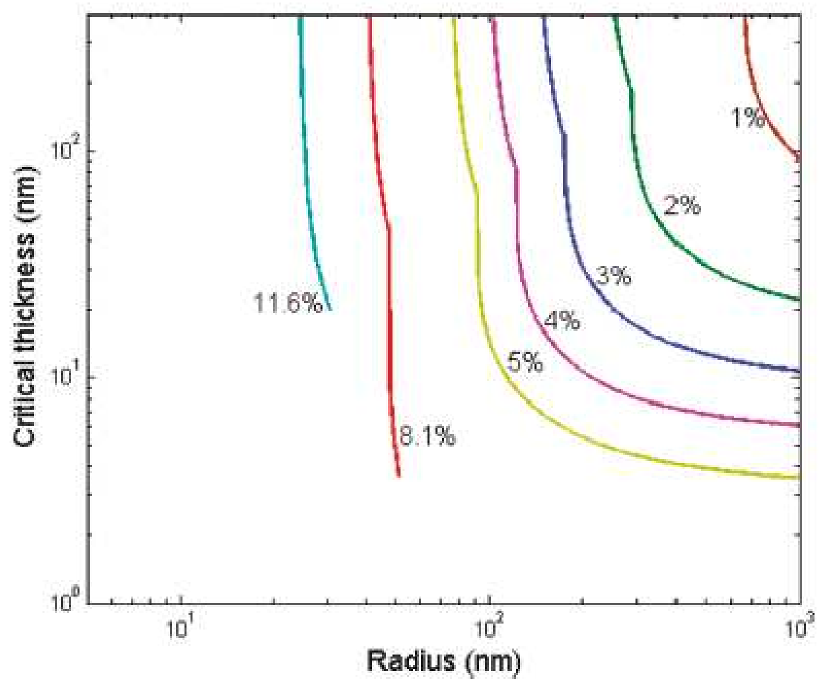

The critical radius of epitaxial GaN nanowires on misfitting substrates

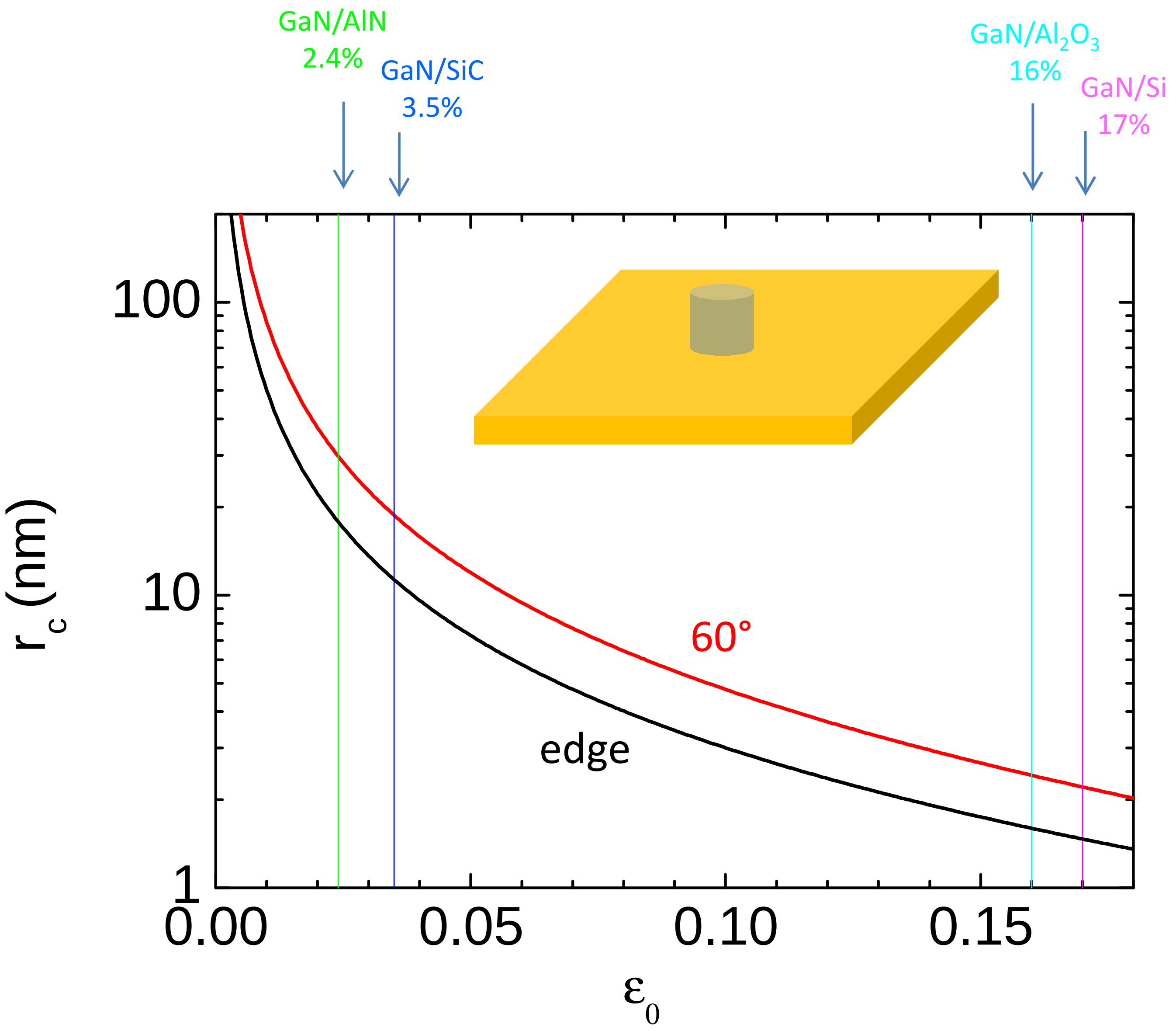

Summary on the critical dimensions of nanowire heterostructures

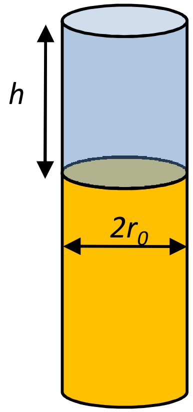

In axial heterostructures, there are practical cases which really benefit from the NW morphology.
Ex: AlN deposited on a GaN stem, r_c= 60 nm

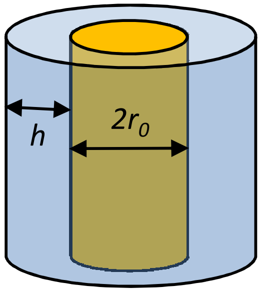

In radial heterostructures, the advantage compared to the 2D case is less obvious.
Ex: GaN shell deposited on a $In_{0.15}Ga_{0.85}N$ core, r_c= 7 nm

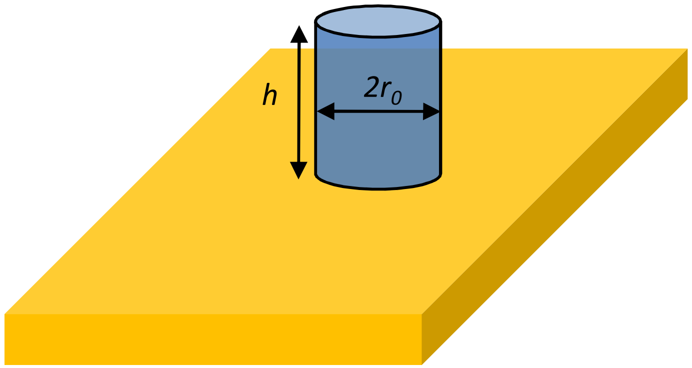

In most practical cases, a few discolations might exist at the GaN NW/substrate interface.
Ex: GaN NW grown on SiC, r_c= 20 nm
Ex: GaN NW grown on Si, r_c= 2 nm

The real benefit here is to avoid threading dislocations.

- Introduction
- GaN nanowire growth mechanisms
- Critical dimensions of nanowire heterostructures
- Nanowire characterization
- Nanowire applications

μ-PL on single GaN NWs

Brandt et al, Phys. Rev. B 81, 045302 (2010)
Paul Drude Institute, Berlin

Chen et al, Appl. Phys. Lett. 99, 251910 (2011)
CEA, Grenoble

MBE grown GaN NWs
Catalyst-free
Si (111) substrate

D^0X_A @ 3.4716 eV (FWHM 0.84 meV)
$(D^0X_A)^s$ @ 3.4749 eV : surface donor bound X (FWHM 0.28 meV)
FX_A @ 3.4789 eV

(a) After growth
(b) 1 month later
(c) 5 months later

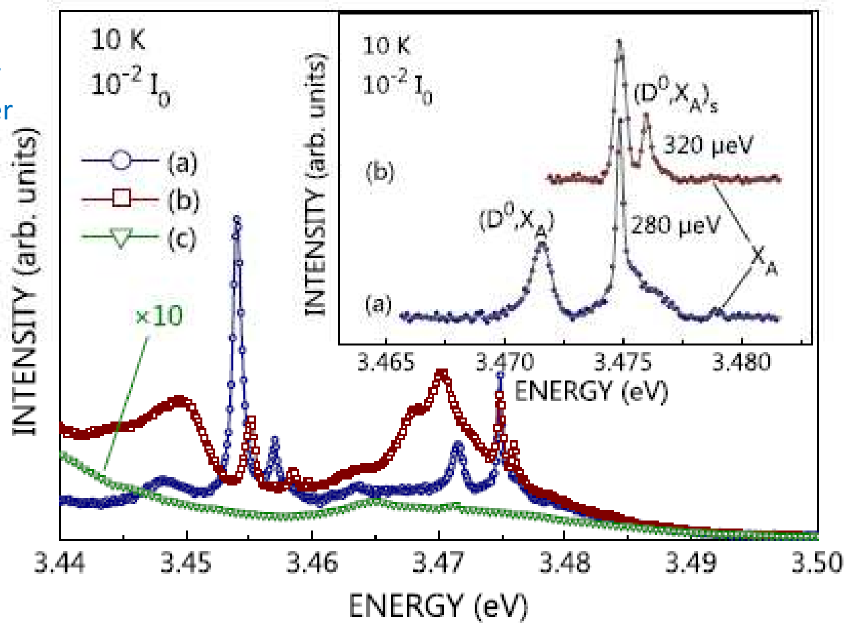

MOVPE grown GaN NWs
Catalyst-free
C-sapphire substrate

D^0X_A @ 3.470 eV (FWHM 0.95 meV)
D^0X_B @ 3.473 eV
FX_A @ 3.477 eV
FX_B @ 3.482 eV

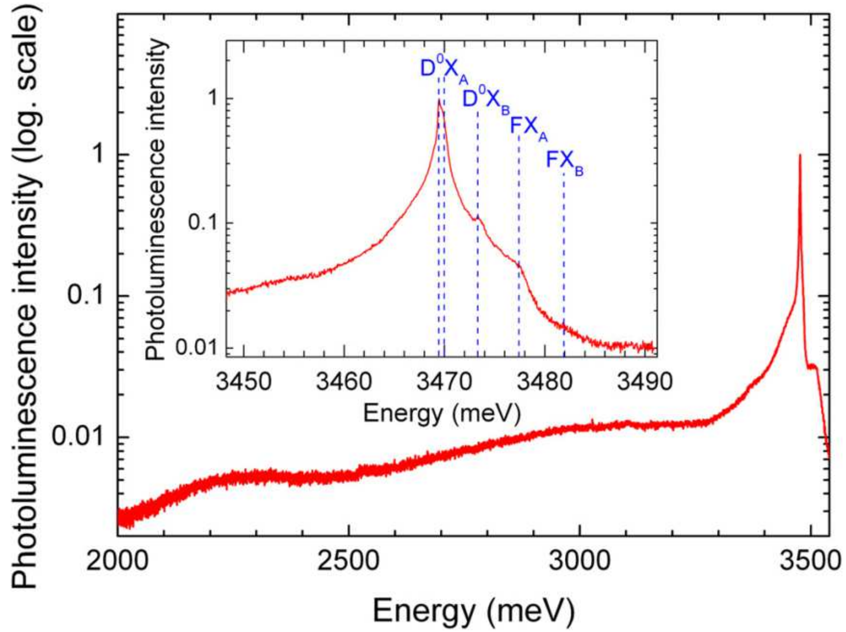

✓Sharp excitonic lines (narrower than for 2D films)
✓No yellow band
✓Degradation with time (sensitive to surface evolution)

Sensitivity to the environment

GaN NWs under illumination (He-Cd laser) and exposed to air → Progressive PL quenching at RT

P. Lefebvre et al., Superlattices and Microstruct. 52, 165 (2012)
Lab. Charles Coulomb, Montpellier

- Intensity ÷ 10
- no spectral change
- reversible

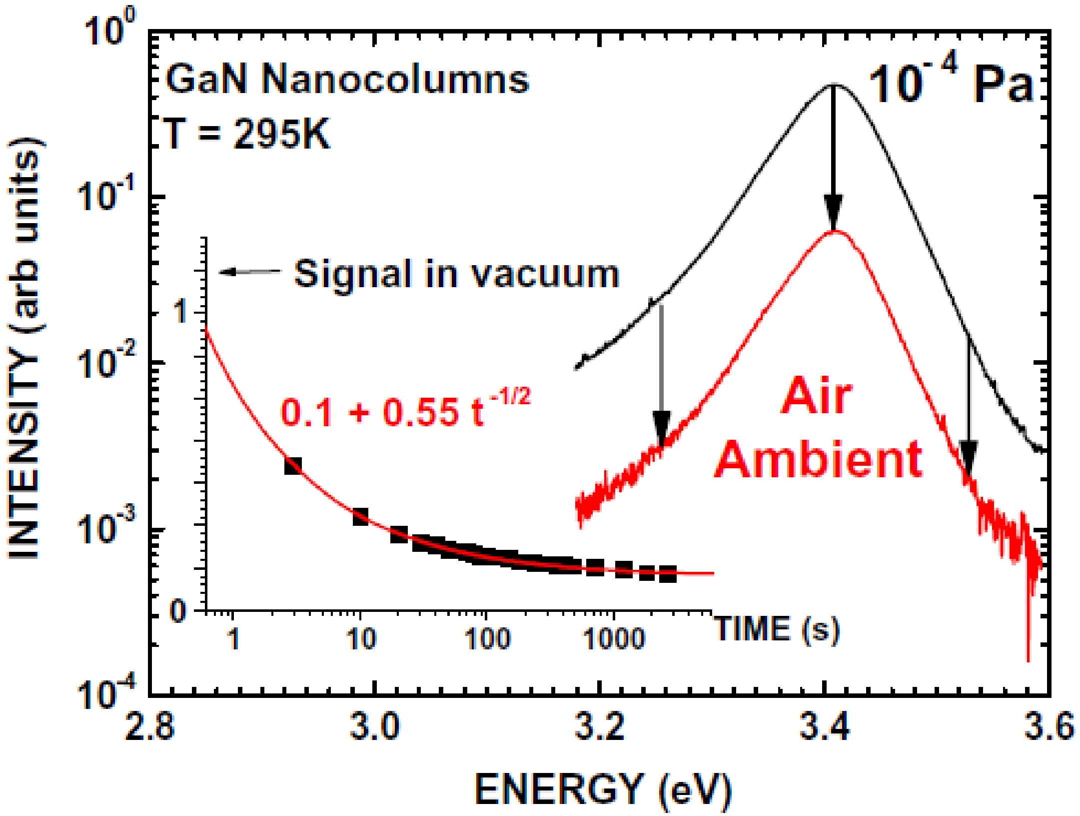

Photoabsorption of oxygen

Absorbed O creates
- non radiative channels at the surface
- or strong band bending in the NW

µPL of a GaN/AlN heterostructure

NW growth: Maria Tchernycheva, LPN, Marcoussis

µPL : Julien Renard, Bruno Gayral, CEA-DRFMC ,Grenoble

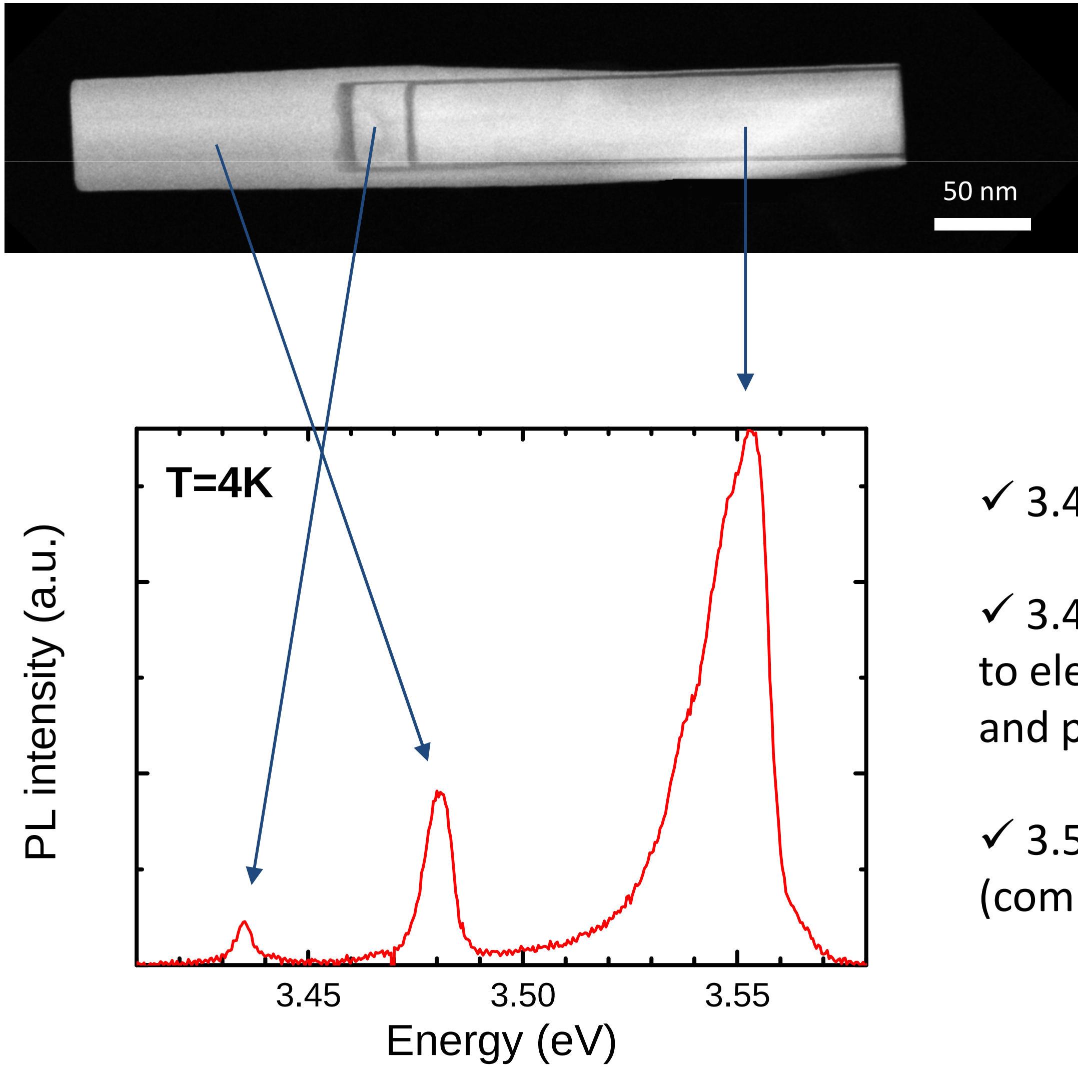

- ✓ 3.48 eV: GaN at the top of the wire
- ✓ 3.43 eV: GaN short segment QCSE due to electric field (spontaneous polarisation and piezoelectric field)
- ✓ 3.55 eV: GaN at the bottom of the wire (compressive strain)

Nano-cathodoluminescence

Zagonel et al, Nanotechnol. 23, 455205 (2012)
Laboratoire de Physique des solides, Orsay

GaN/AlN NW heterostructure

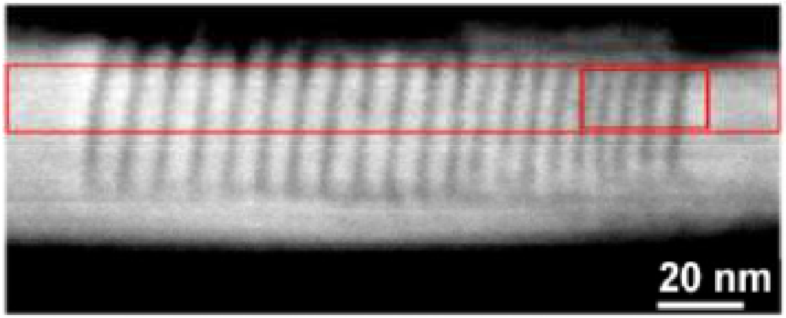

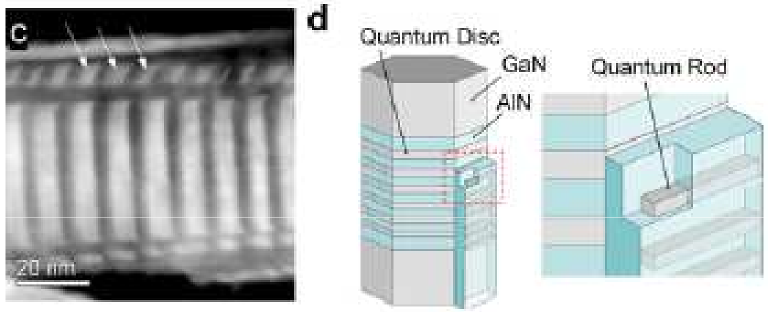

Quantum disc + unintentional quantum rods

- ➢Ideal tool to identify the emission of nano-structures
- ➢High spatial resolution due to strong carrier confinement

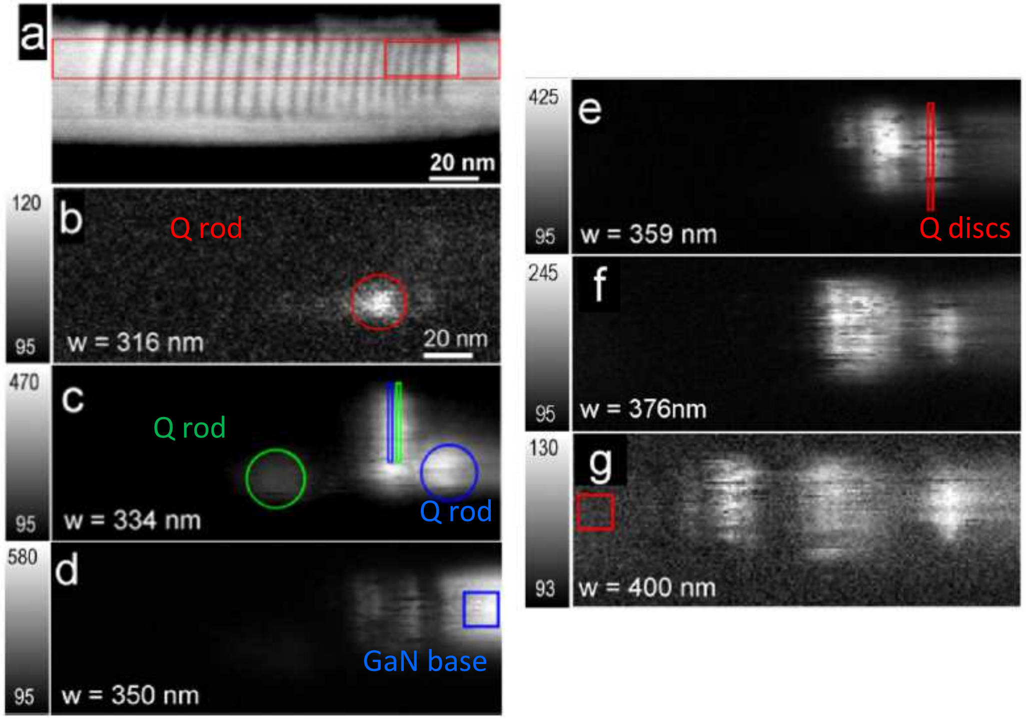

Q disc emission: affected by the disc thickness (confinement and QCSE)

Micro-PL of strained core-shell structures

Rigutti et al, Phys Rev B 83, 155320 (2011)
IEF, Orsay

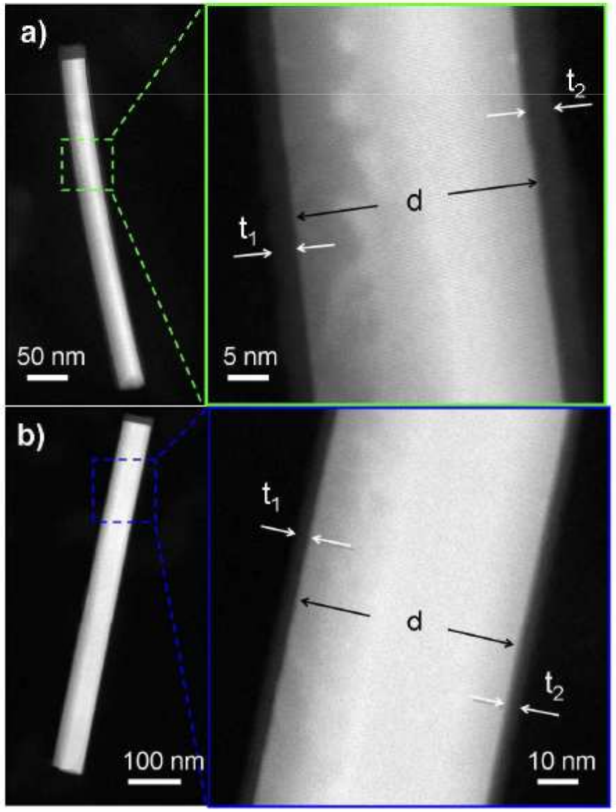

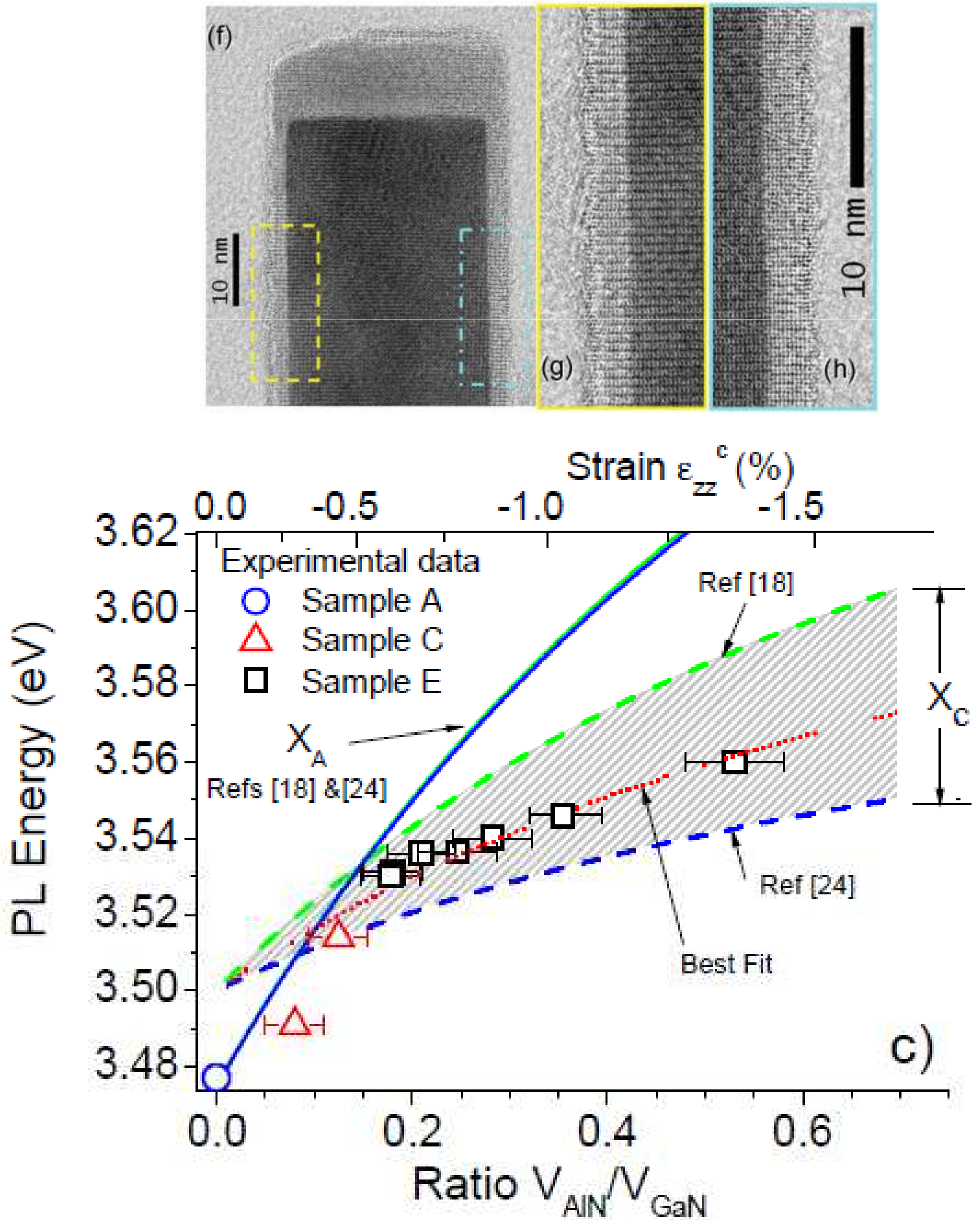

The strain modify the band structure: the optical transition of lower energy changes from X_A type to X_C type

This kind of study necessitates micro-PL + TEM measurements on the very same objects

How to measure the electrical properties of nanowires

- Implementing Hall effect is very challenging
- Field effect is commonly used

Y. Huang et al, Nano Lett. 2, 101 (2002)
Harvard Univ.

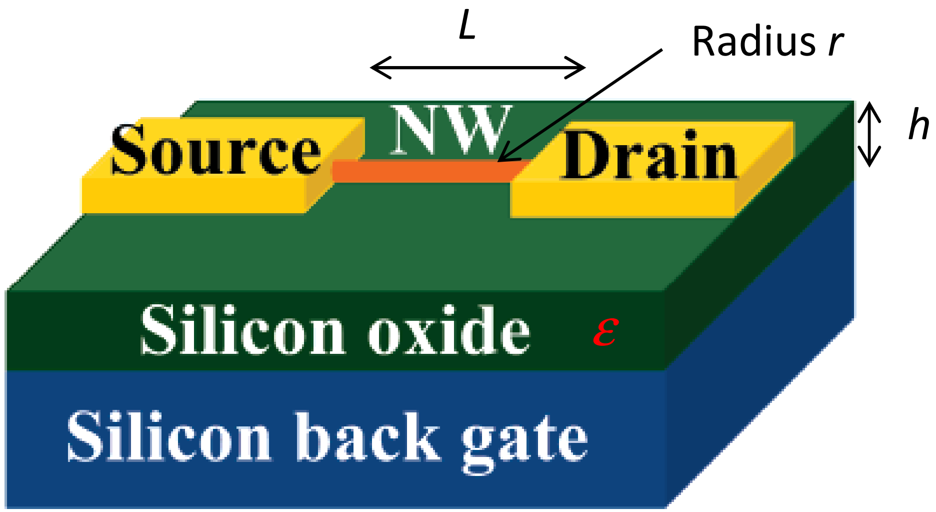

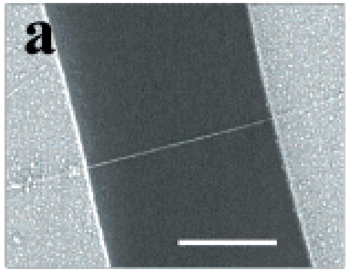

Field effect mobility

L length of NW between the contacts

h gate oxide thickness

r NW radius

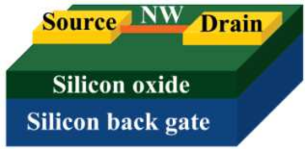

Y. Huang et al, Nano Lett. 2, 101 (2002)
Harvard Univ.

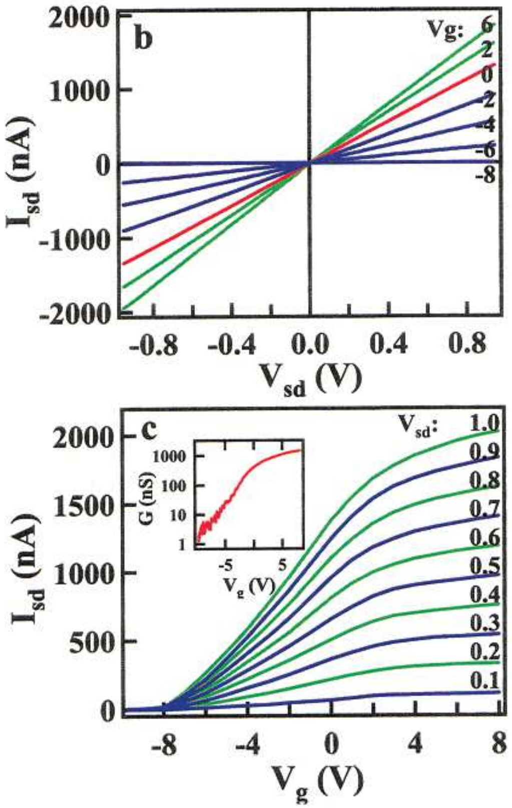

$$Q_{tot} = CV_{th}$$

Depletion voltage

For the back gate configuration:

$$C = \frac{2\pi\varepsilon L}{\cosh^{-1}\left((r+h)/r\right)}$$

$$h >> r \qquad C \approx \frac{2\pi\epsilon L}{\ln(\frac{2h}{r})}$$

$$n = \frac{Q}{e\pi r^2 L}$$

$$\frac{\partial I_{ds}}{\partial V_g} = \mu \frac{C}{L^2} V_{ds}$$

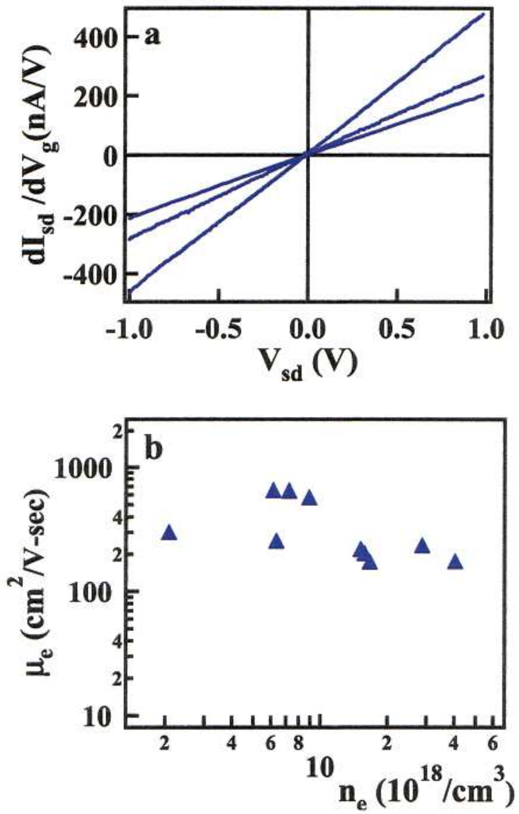

Comparison with Hall effect measurements

(case of InAs NWs)

Problems:

• In actual situations, the assumptions to derive the previous C formula are not verified

• C is very sensitive to interface charges!
If the interface charges are neglected,
μ_{FE} is underestimated
n is overestimated

See
- Khanal and Wu, Nano Lett 7, 2778 (2007)
- Dayeh et al, Small, 3, 326 (2007)

Ch. Blömers et al, Appl. Phys. Lett. 101, 152106 (2012)
Peter Grünberg Institute, Jülich

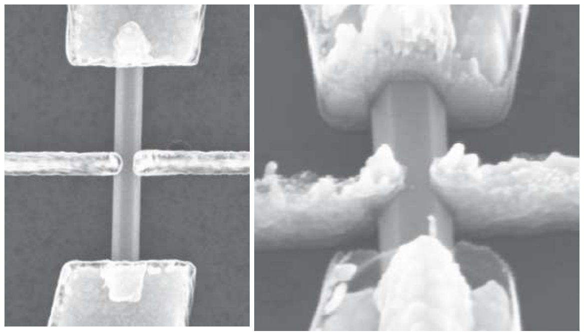

"Hall bar" fabricated by e-beam lithography on InAs NWs

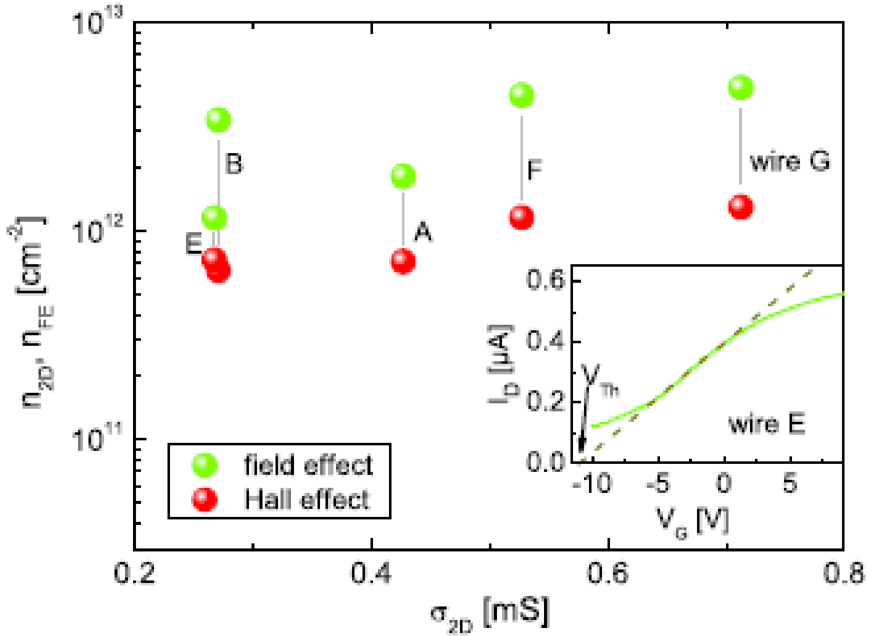

Measuring the minority carrier diffusion length by EBIC

Gutsche et al, Nano Lett. 12, 1453 (2012)
Univ. Duisburg Essen

Also possible with a Schottky contact

Allen et al, Nature Nanotechnol. 3, 168 (2008)
Northwestern University, Evanston

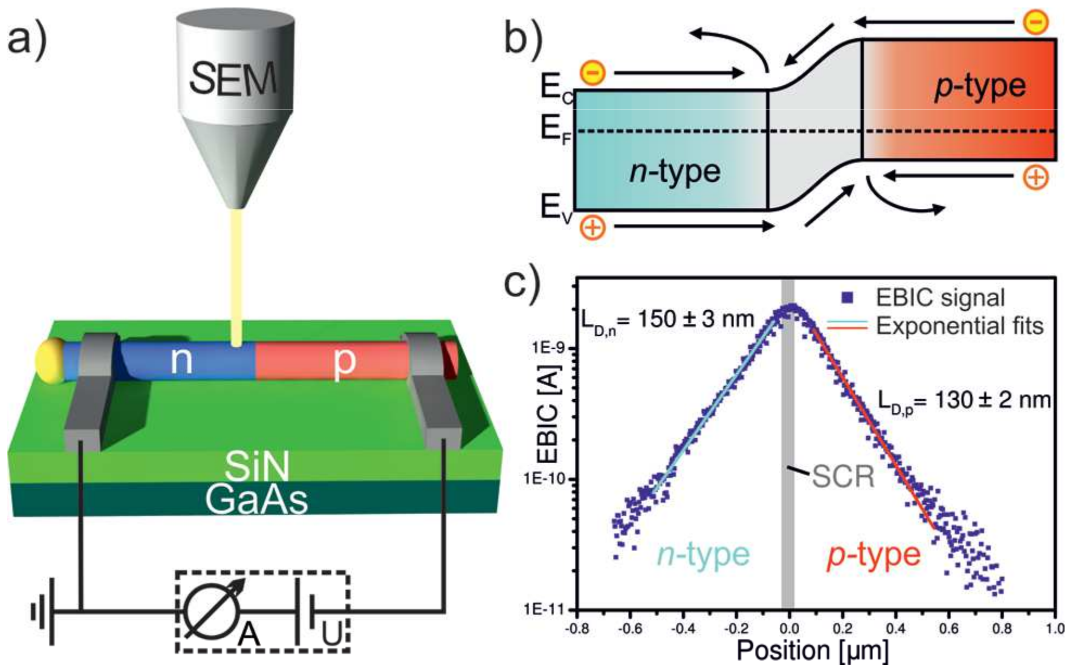

$$I = I_0 e^{-x/L}$$

GaAs NWs

x distance to the junction
L minority carrier diffusion length

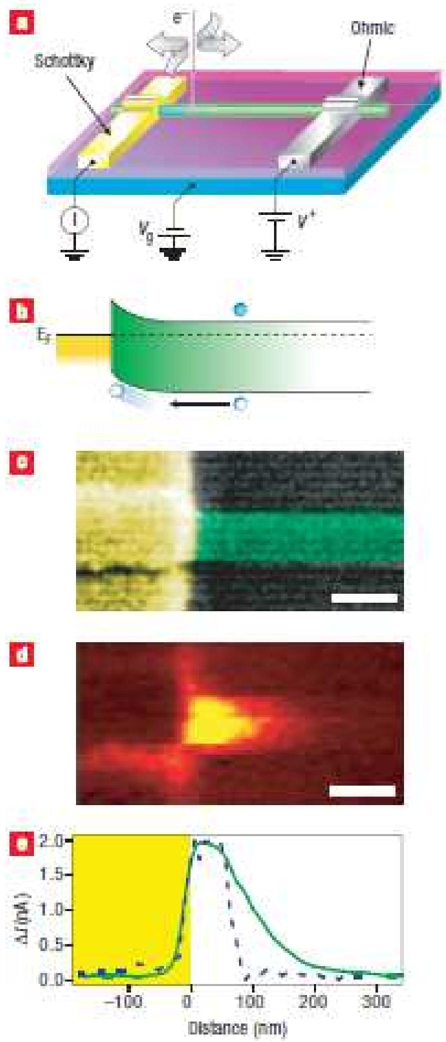

Si NWs

Not yet applied to III-N nanowires

Alternative (but more questionable) technique applied to III-N heterostructures

Baird et al,Physica B 404, 4933 (2009).
Baird et al,Appl. Phys. Lett. 98, 132104 (2011)

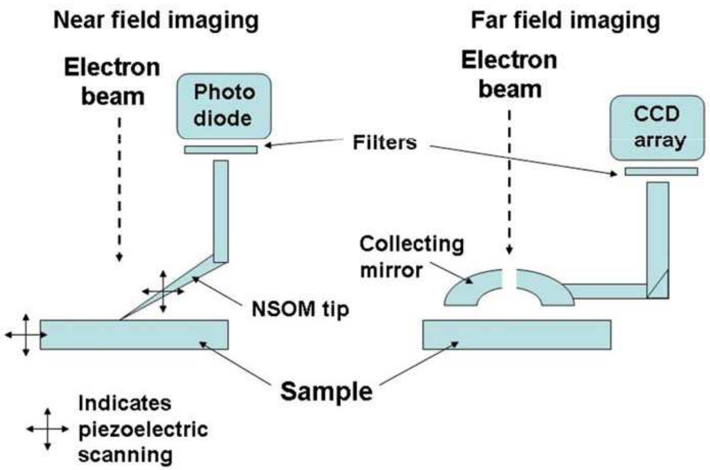

Near field scanning optical microscopy is used to visualize the radiative recombinations of e^-/h pairs created by and incident e^- beam.

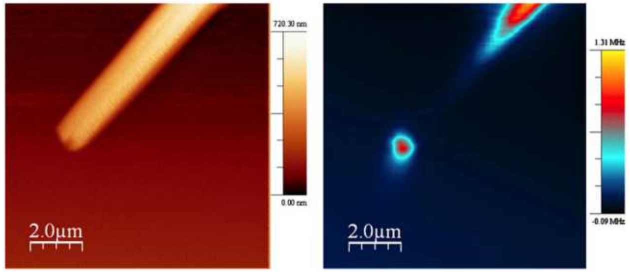

Wire	Diameter (nm)	Diffusion length (nm)
AlGaN/GaN-n-type	200	1100
	500	1200
	700	1100
GaN-n-type	300	130
	500	660
	700	830
InGaN/GaN-n-type	500	350
	700	430
	1000	470

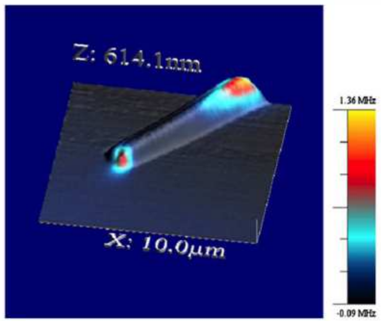

Higher and radius-independent values are obtained with an AlGaN shell.

Structural properties and composition (2 lectures today)

TEM/STEM

X-ray diffraction

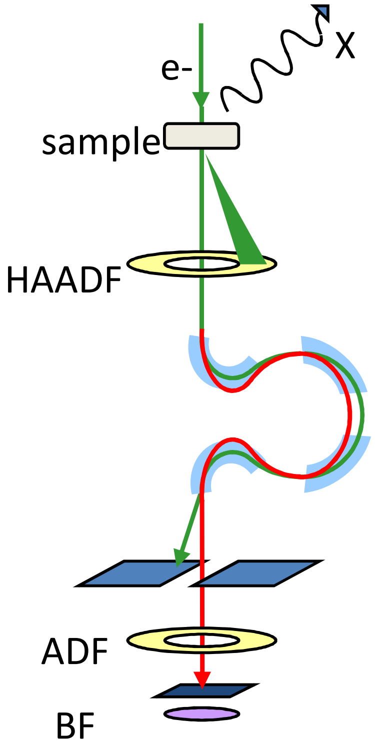

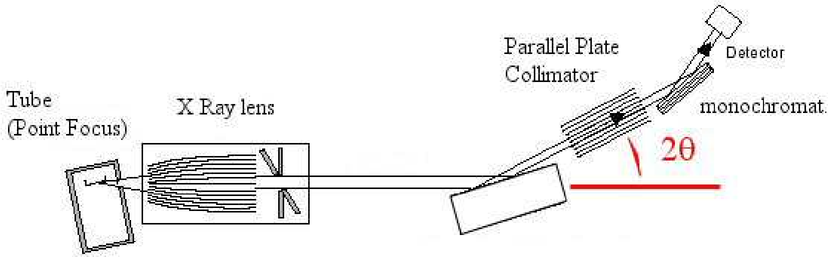

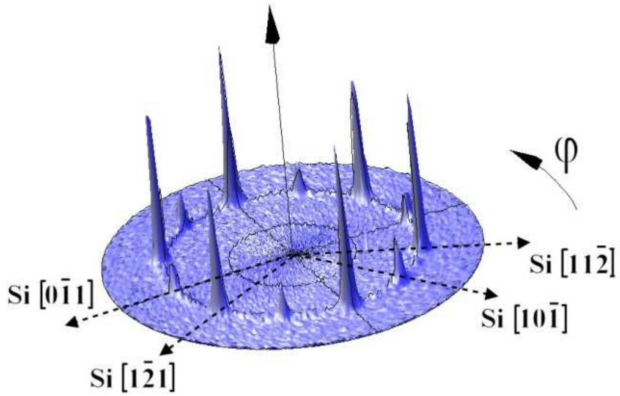

- Introduction
- GaN nanowire growth
- Critical dimensions of nanowire heterostructures
- Nanowire characterization mechanisms
- Nanowire applications

Potential benefits of III-N NWs for LEDs

(NWs ensembles compared to 2D layers)

- Less crystal defects (dislocations and cracks)
  Operation at lower carrier density, reduced Auger effect
- Large choice of substrates (thermal management and cost issues)
- More efficient light extraction
- Reduced quantum confined Stark effect in QW structures
  axial QWs: reduced strain → reduced piezoelectric fields
  Lateral QWs: non-polar facets
- Good tuning of the InGaN or AlGaN composition
  (wavelength tuning, colorimetry)
- Lower material consumption

NW structures for LEDs

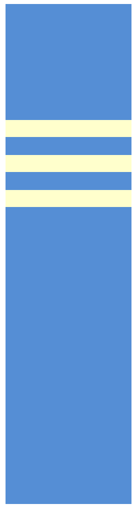

More strain accommodation
Easier wavelength tuning

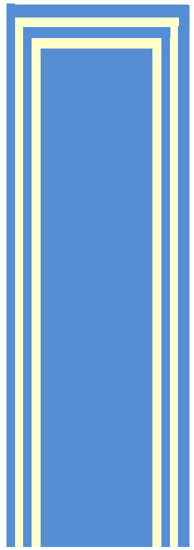

Large emitting area
Non-polar lateral QWs

Strategies to tune the emission wavelength

- GaInN discs or radial QWs of various composition
- GaInN discs radial QWs of various thicknesses
- NWs of different diameters

To get white emission

- GaInN segment with a gradual composition
- Stack different discs – QWs

LED efficiency

$$\eta_{LED} = \overbrace{\eta_{inj} \cdot IQE \cdot \eta_{extr}}^{EQE} \cdot \eta_{volt}$$

Leakage currents

Internal light reflection

Serial resistances

Non radiative recombination

Auger effect

Crystalline defects

Surface

Losses

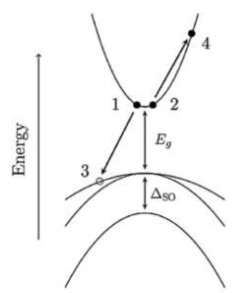

Auger recombination

$In_xGa_{1-x}N$ discs of various thicknesses

PAMBE, self organized NWs,

Lin et al, Appl. Phys. Lett. 97, 073101 (2010)
National Tsing-Hua University, Taiwan

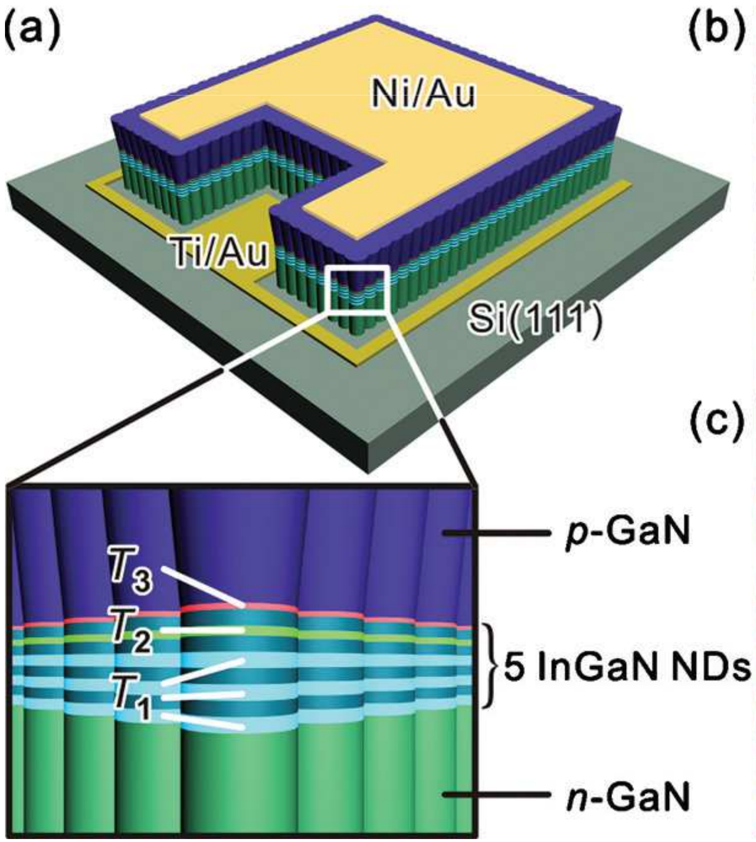

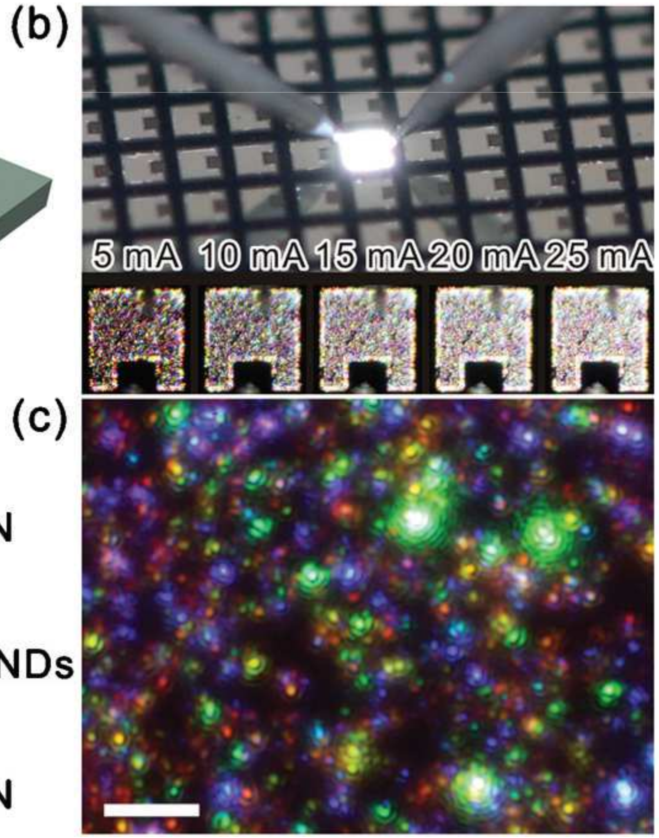

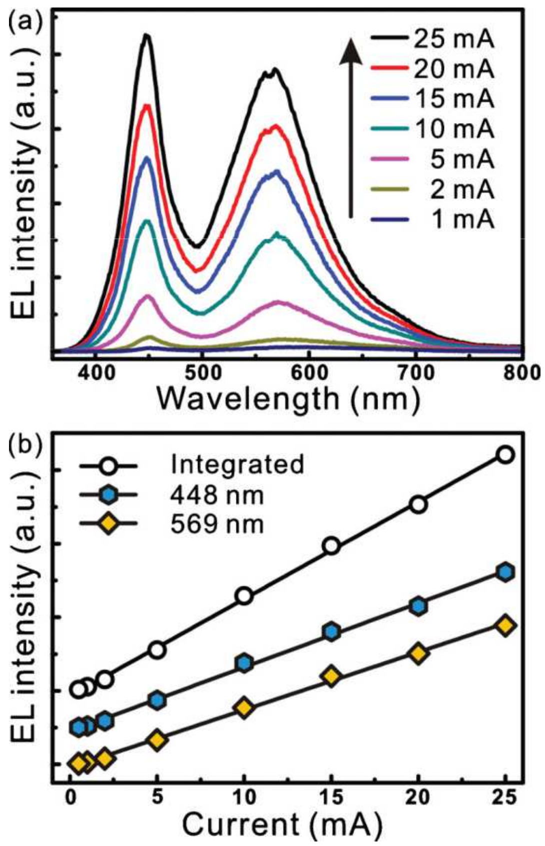

blue-band @ 448 nm
yellow-band @ 569 nm

InGaN discs of different thicknesses (10-25 nm)

White emission is obtained

Only a small part of the NWs are contacted

Almost no spectral shift with increasing electrical injection (reduced QCSE)

No current density values

$In_xGa_{1-x}N$ segments of various composition

Guo et al, Appl. Phys. Lett. 98, 193102 (2011)
Univ. Michigan, Ann Arbor

PAMBE, self organized NWs, GaInN/GaN discs

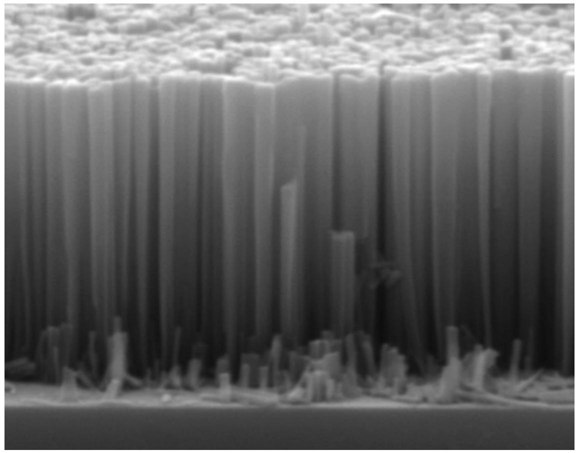

Straight NWs on Si (100)

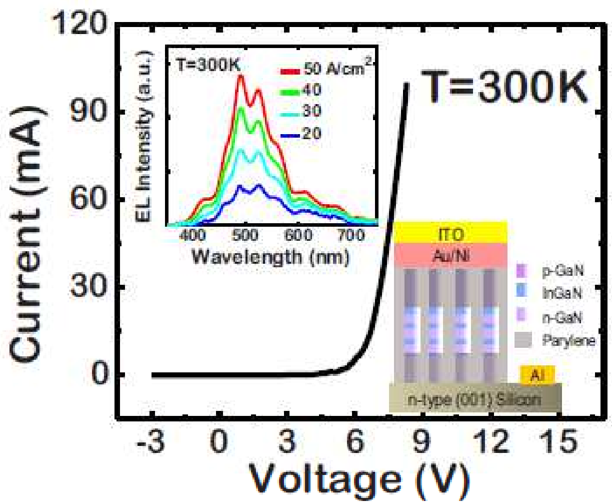

Almost no spectral shift
(reduced QCSE)

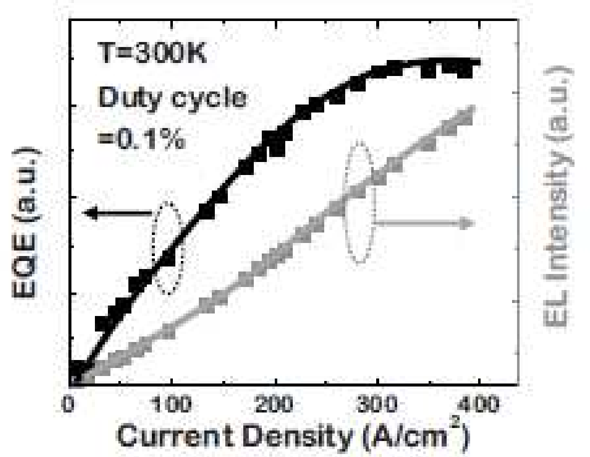

No efficiency droop up to 400A/cm^2
(reduced Auger effect)

$In_xGa_{1-x}N$ dots in GaN NWs

Chang et al, Appl. Phys. Lett. 96, 013106 (2010)
Nguyen et al, Nano Lett. 11, 1919 (2011)
McGill Univ., Montreal

PAMBE, self organized NWs,

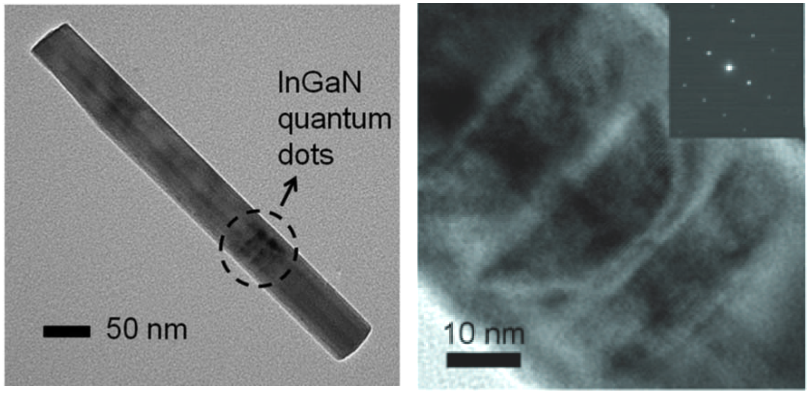

InGaN/GaN dots-in-a-wire heterostructures

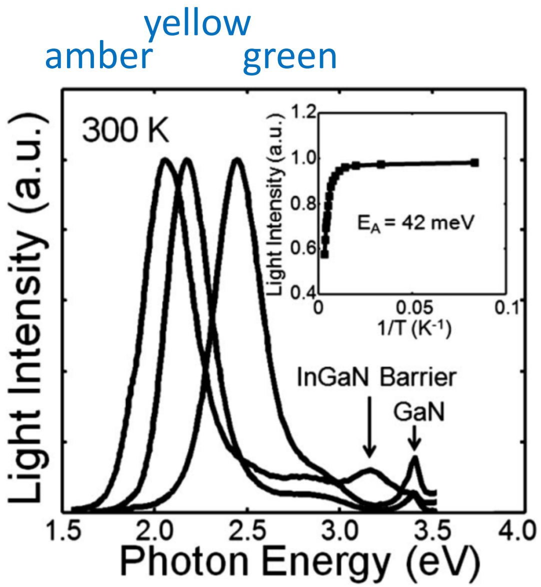

Good IQE
in the « green gap »
45% @ 564 nm

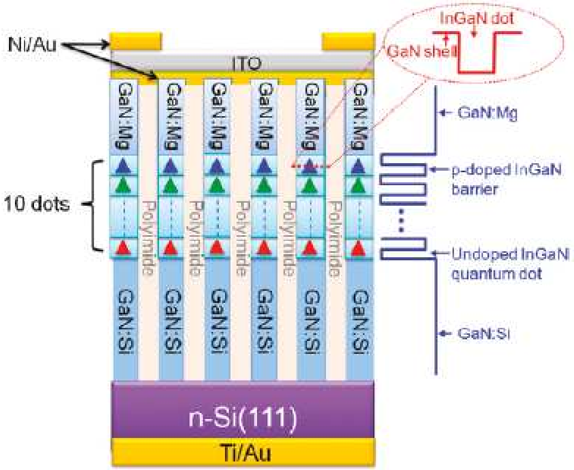

P doped InGaN/GaN dots

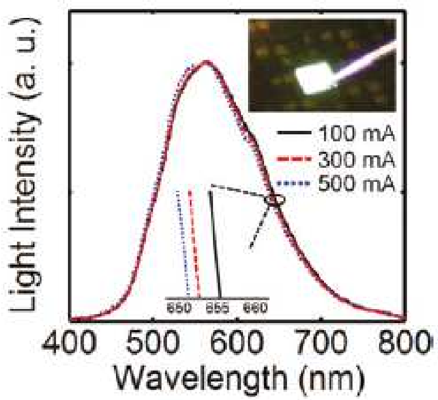

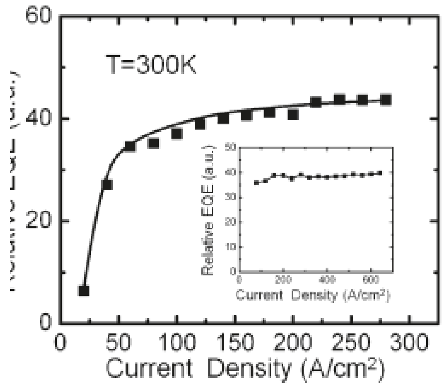

White emission
no efficiency droop
@ 300 A/cm²

Estimated IQE at 300 K:
57%

Regular NW arrays of different diameters

PAMBE, regular NW arrays, Ti mask

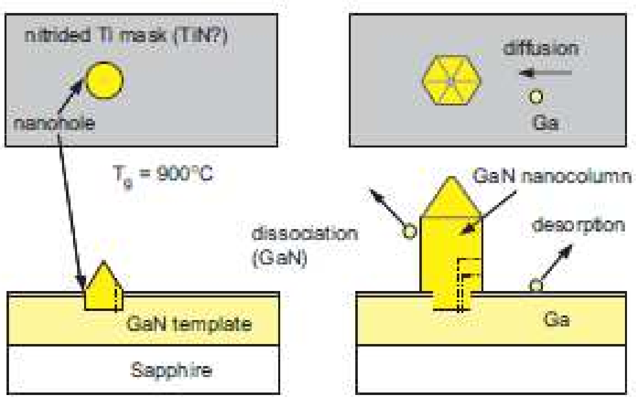

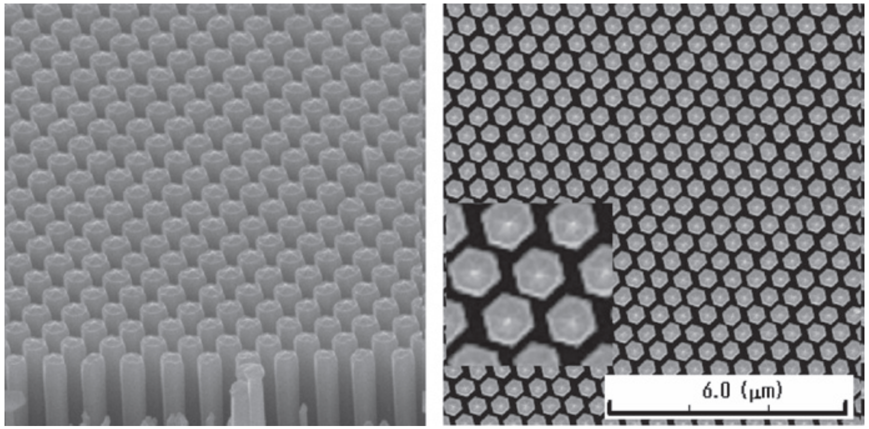

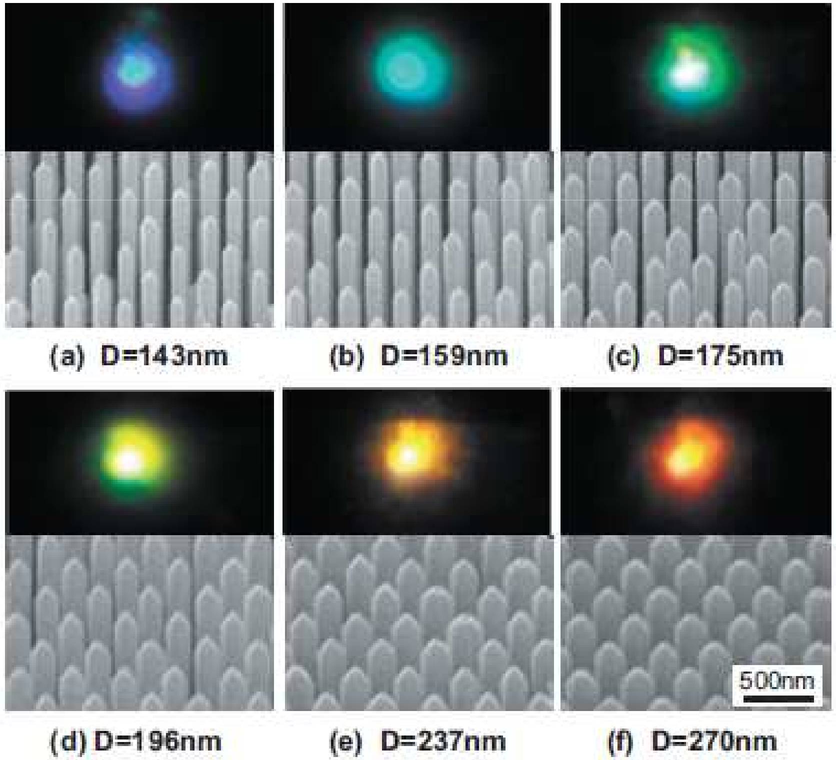

77% IQE @ λ=487 nm

K. Kishino et al, J. Cryst. Growth 311, 2063 (2009)
Sophia Univ. Tokyo

Sekiguchi et al, Appl. Phys. Lett. 231104 (2010)
Sekiguchi , Kishino et al, Appl. Phys. Express 124002 (2008)
K. Kishino et al, Appl. Phys. Express 6, 012101 (2013)

Sophia Univ. Tokyo

Radial InGaN/GaN heterostructures for LEDs

Koester et al, Nano Lett. 2011, 4839
CEA Grenoble (France)

Non-polar radial QWs
Lateral growth on {1$\bar{1}$00} *m*-plane sidewalls
MOCVD

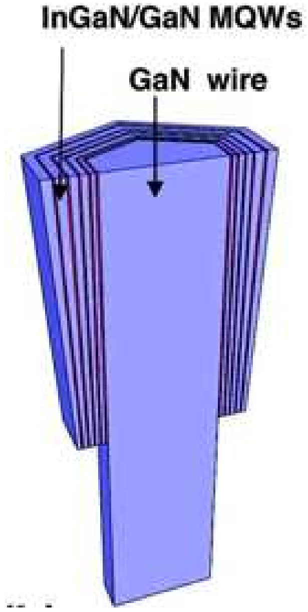

Difficulty to get uniform thicknesses

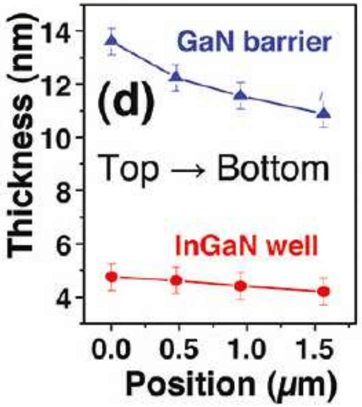

InGaN well-GaN barrier thicknesses
1.0 nm / 7.5 nm

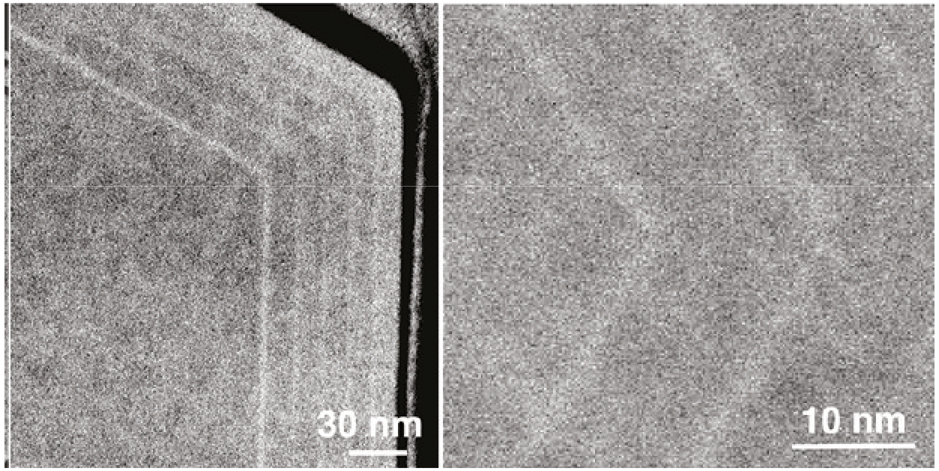

5.2 nm / 11.6 nm

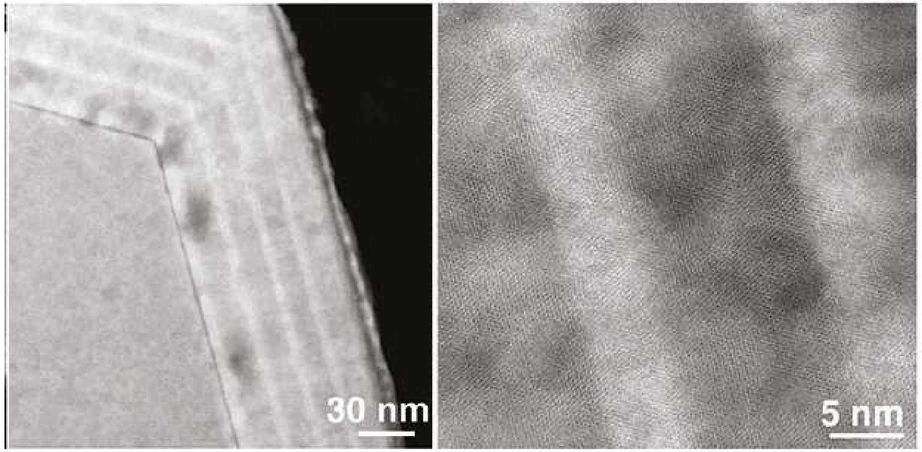

Too thick radial InGaN QWs generate dislocations

Radial InGaN/GaN heterostructures for LEDs

Yong-Ho et al, Nano Lett. ASAP , 2013
Chonbuk National University, Korea

Au-catalyzed MOCVD

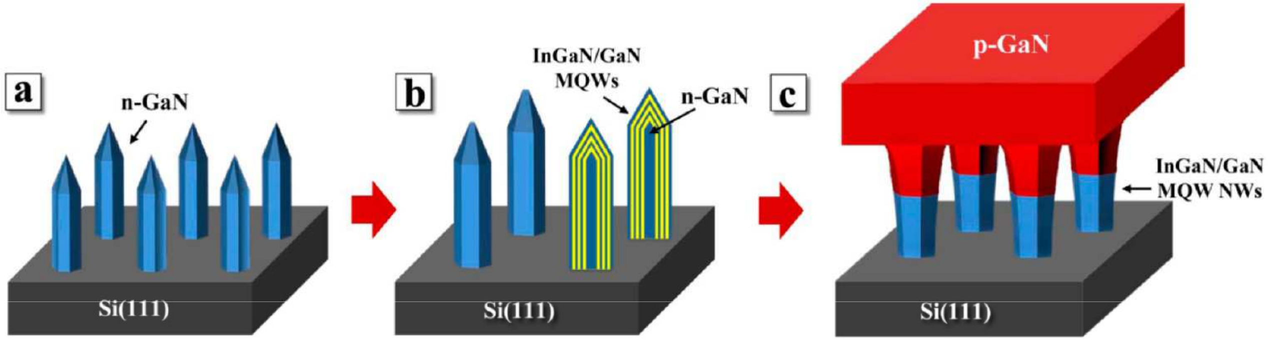

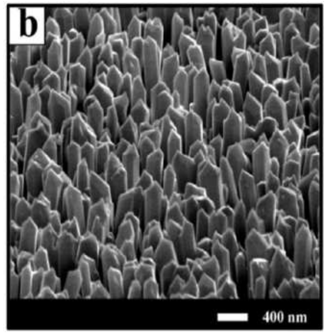

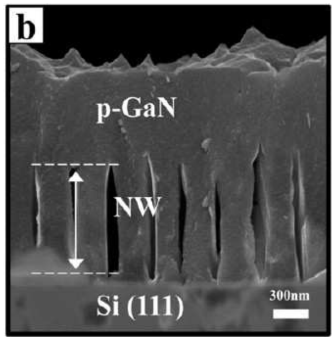

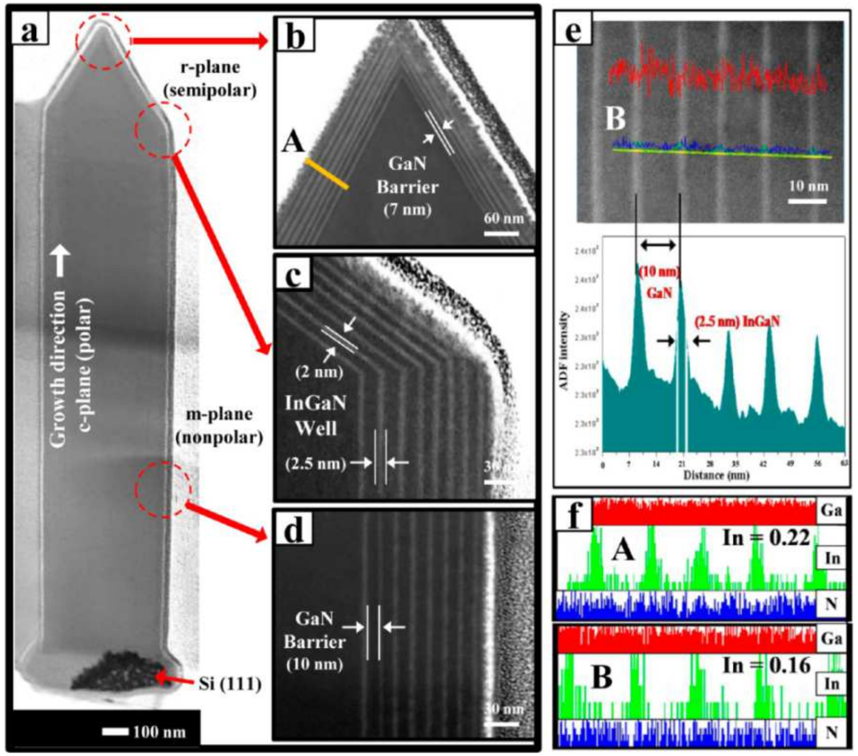

InGaN QWs on m planes and r planes
No dislocations

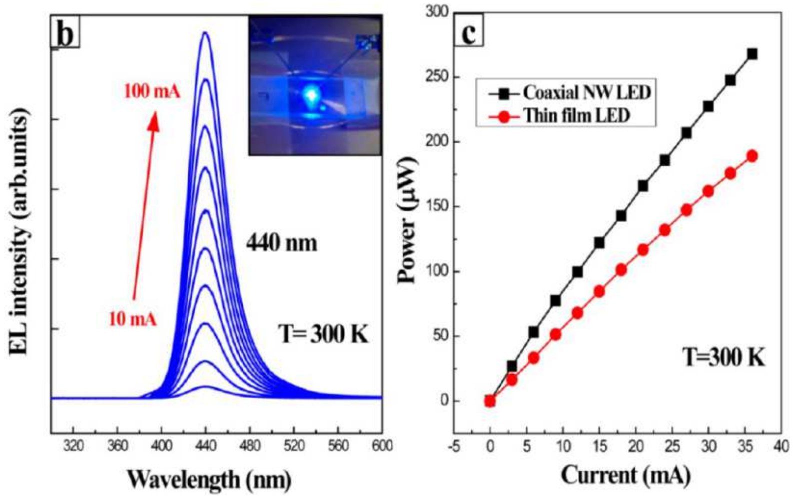

Blue emission @ 440 nm
EQE ≈ 28%

Ga(In)N nanowires for LEDs

LEDs based on GaN microwires on 200-mm Si substrates

http://www.aledia.com/en/
LETI, Grenoble (France)

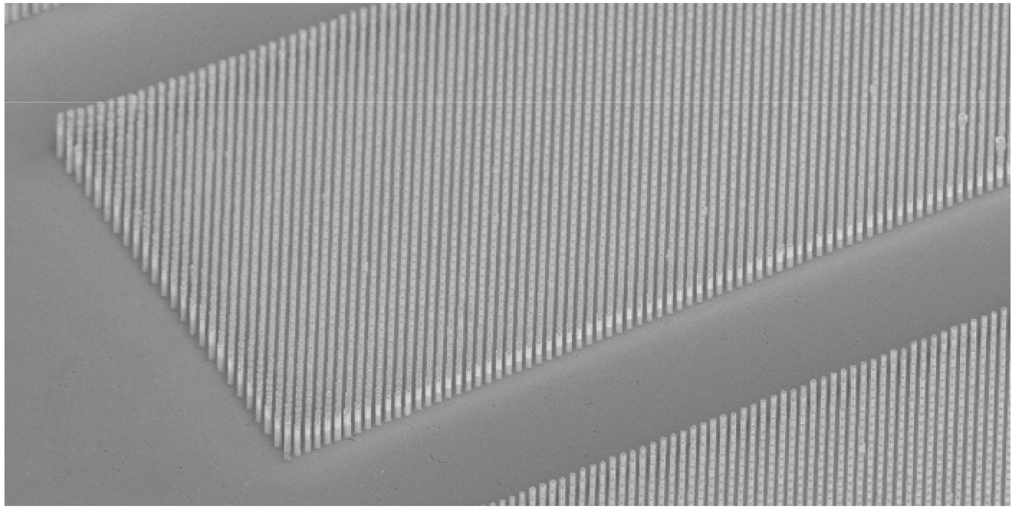

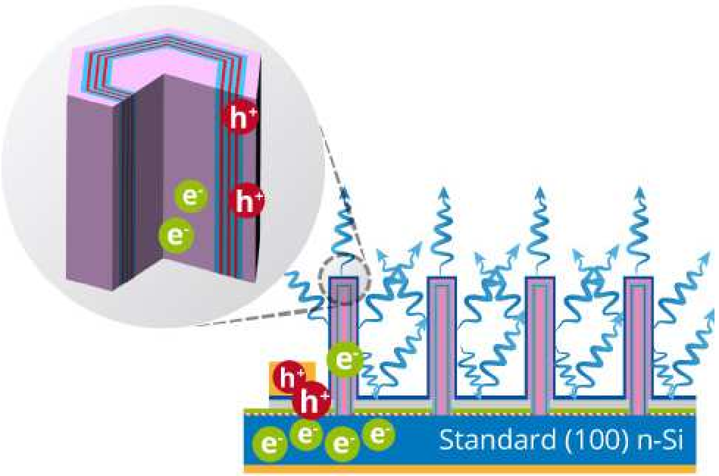

Objective : $/lumen divided by 10

3D (Microwire) LEDs:
- Large, economical substrate
- Fast MOCVD growth process (low capital expenditure)
- Low materials consumption
- Existing high-volume silicon wafer fabs
- Light emission area = up to 3X the 2D area = more light/mm^2 or less current density, less efficiency droop
- Multiple colors on one wafer or even on one chip

Potential benefits of III-N NWs for Photovoltaics

(NWs ensembles compared to 2D layers)

- Less crystal defects (dislocations and cracks)
  less carrier recombination
- Large choice of substrates (cost issue)
- Lower material consumption (cost issue, exhaustible elements)
- Good tuning of the InGaN composition
- More flexibility in designing heterostructures
- Reduced reflection of light and light trapping effect (improves absorption)
- Charge separation over short distances in radial junctions

Three possible junction designs

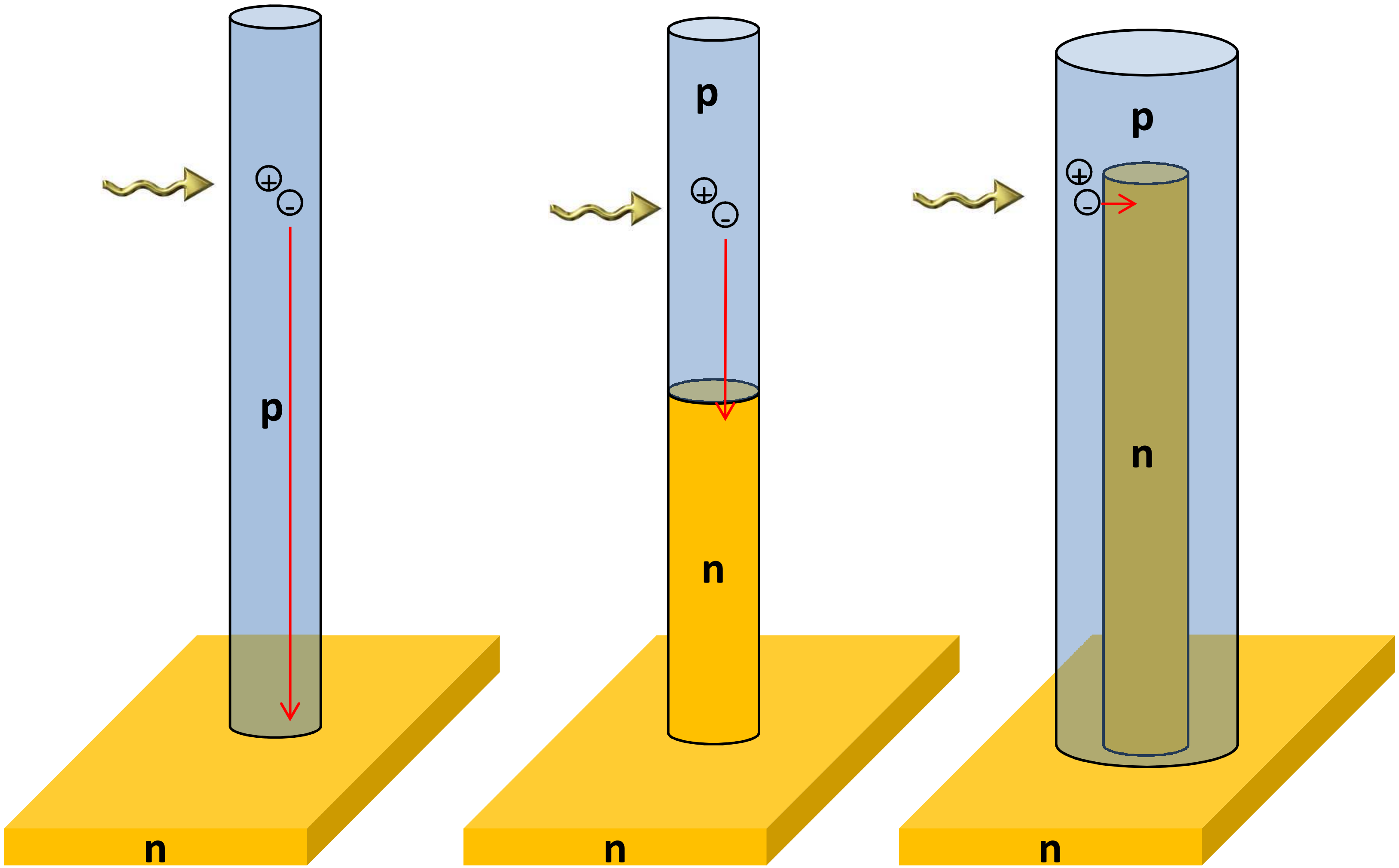

Best design:

Large junction area
Short distance for minority carrier transport
Large contact area possible on the p-shell

Surface recombination

Optimal shape for absorption

B. Wang et al, Nanotechnology 2012, 194003
University of Pittsburgh, USA

Array of small diameter NWs
→ low reflection but high transmission

Array of large diameter NWs
→ low transmission but high reflection

Array of nanocones: good trade-off

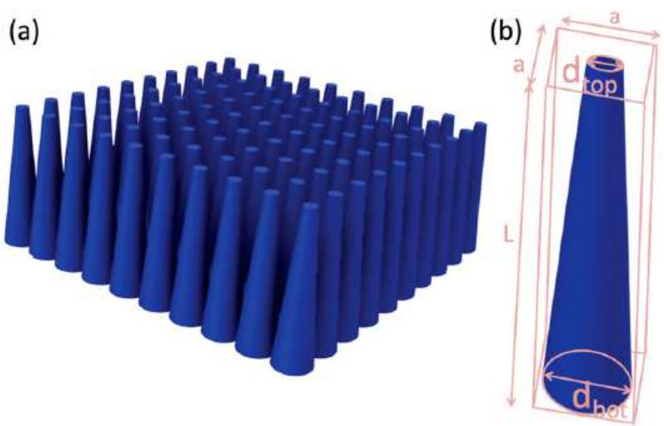

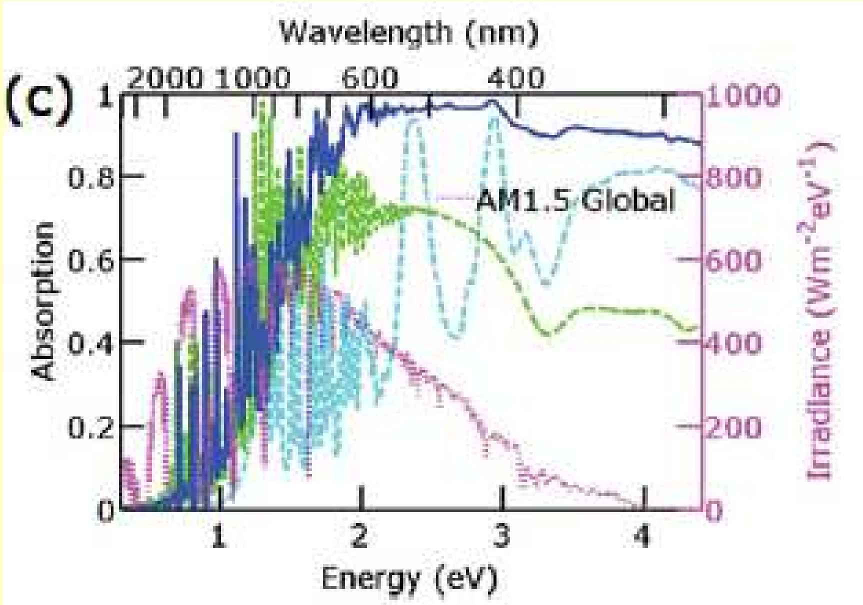

Cones : d_{top} = 200 nm, d_{bottom} = 600 nm

Cylinders: d = 200 nm

Cylinders: d= 560 nm

AM 1.5 solar spectrum

Enhanced absorption in silicon nanocone arrays

Light trapping and enhanced absorption

Y. Lu et al, Nano Lett. 2010, 4651
Cornell University, USA

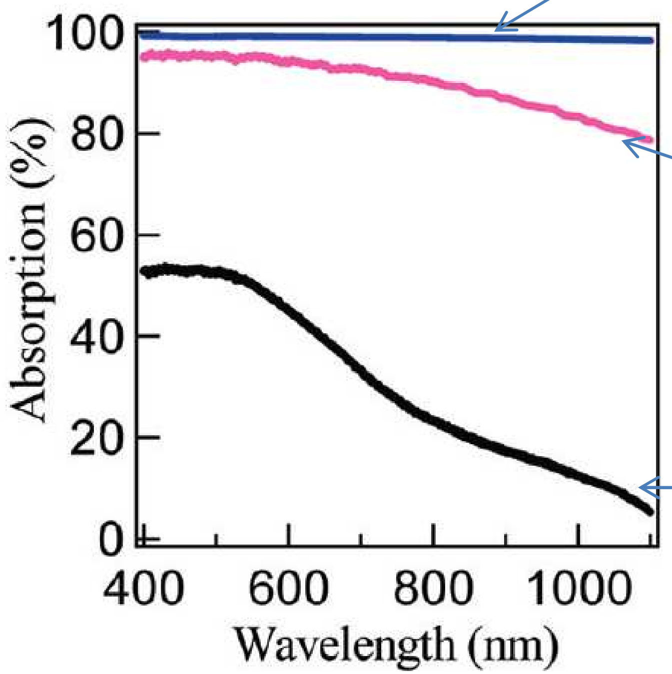

Si nanocones
Top radius: 170 nm
Bottom radius: 400 nm
Height: 3.5 µm
Slant angle: 3.8 °
+ planar Si (2 µm thick)

Si nanowires
Constant radius: 170 nm
Height: 3.5 µm
+ planar Si (2 µm thick)

Bare Si
(5 µm thick)

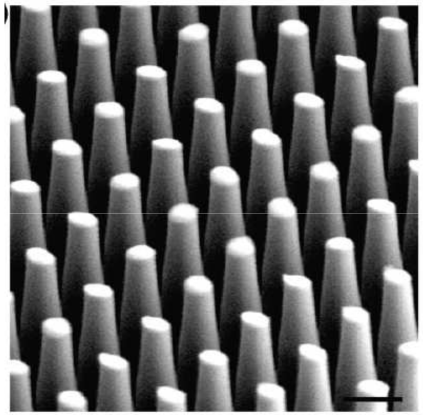

Process:
Electron lithography
RIE etching

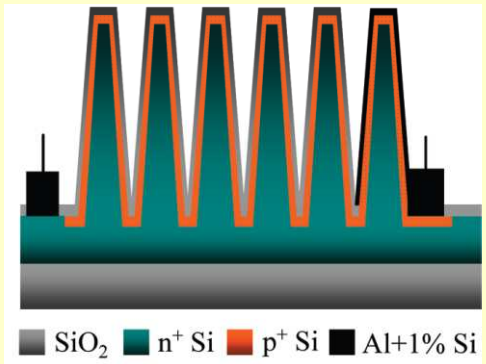

Solar cell efficiency : 10.8%
Less than bulk Si
limited by surface recombination losses

GaN(p) NWs on Si(n) substrate

Tang et al, Nano Lett. 8, 4191 (2008)
City UniVersity of Hong Kong,

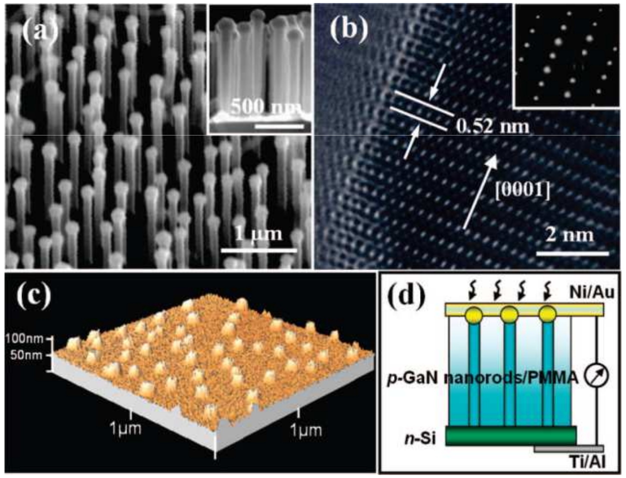

Mg doped GaN NWs
CVD catalyzed by Au particles
PMMA encapsulation
Ni/Au top contact

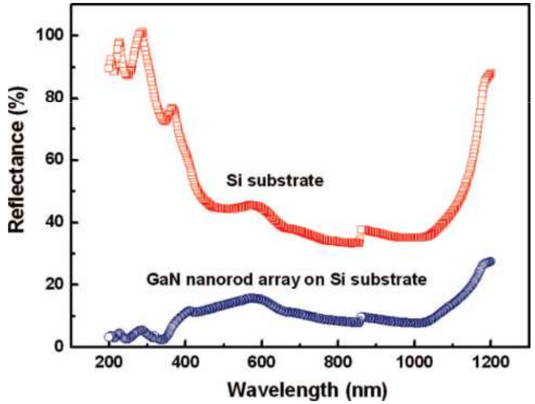

Reflectivity improved as compared to bare Si, but far from optimal (contact layer reflectivity)

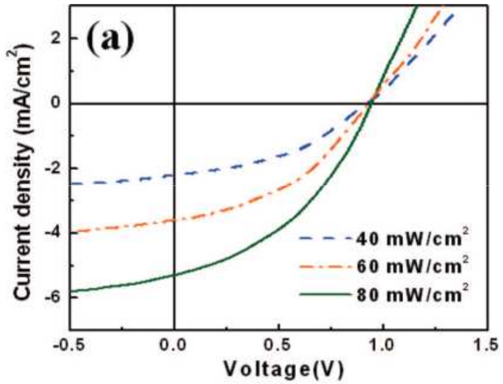

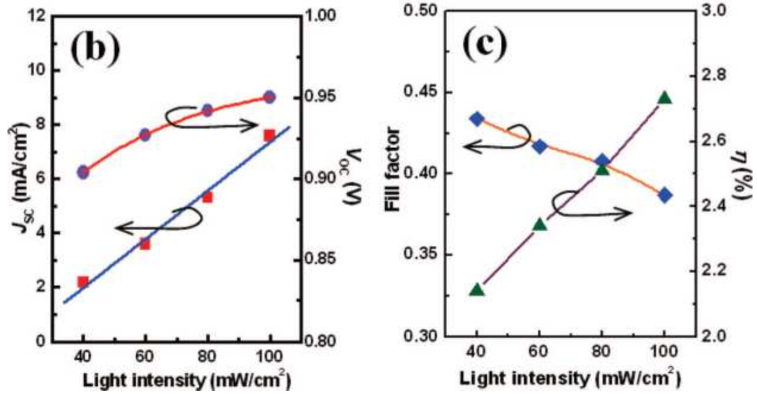

J_{SC} increases linearly with light intensity
Fill factor degrades (resistive losses)
Conversion efficiency 2-3 %

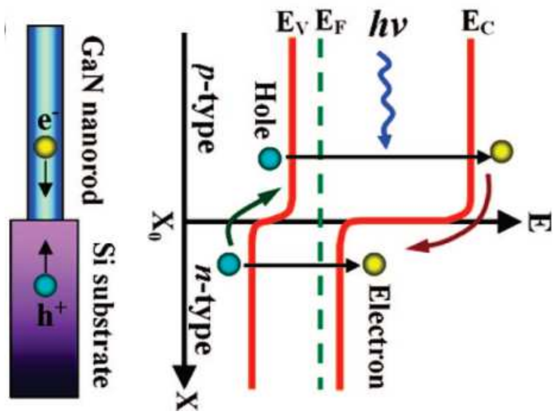

Today, the best efficiency of InGaN solar cells is obtained with 2D layers cell (6%)

Some comparative references

Today, the best efficiency of InGaN solar cells is obtained with 2D layers cell: η ≈ 6%

B. W. Liou, Thin Solid Films 520, 1084 (2011)
WuFeng University, Taiwan

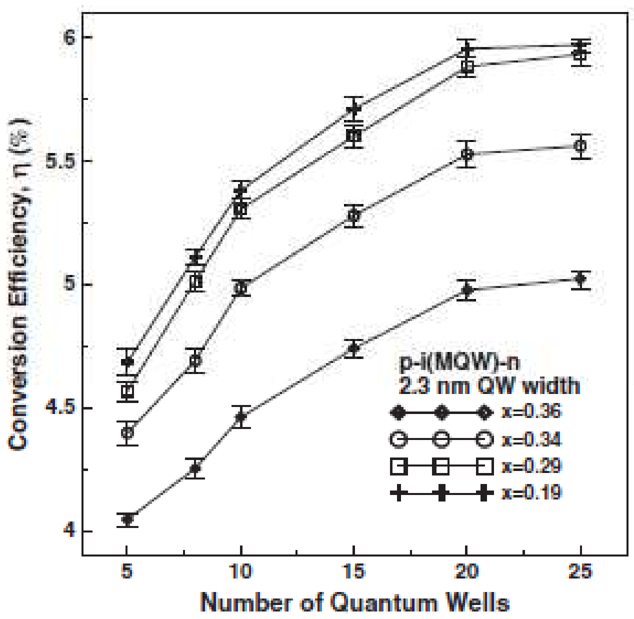

Today, the best NW solar cell is based on InP NWs (pin axial structure): η=13.8%

Wallentin et al, Science 339, 1057 (2013)
Univ. Lund

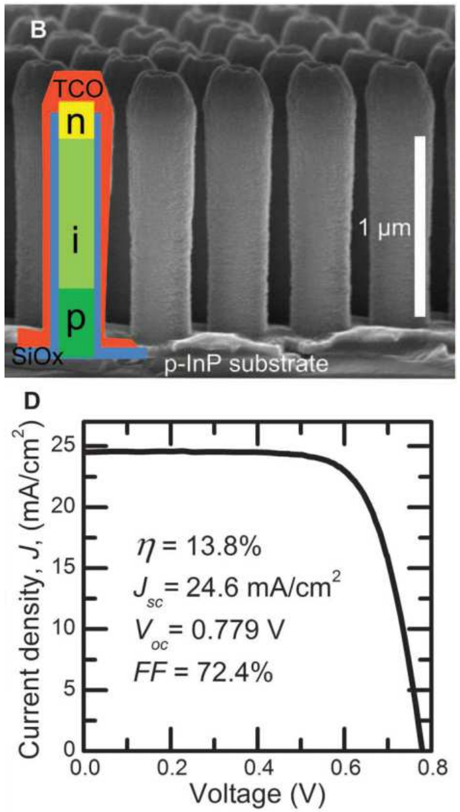

Single NW photovoltaic device
core-shell n-p junction

Dong et al, Nano Lett. 9 (5), 2183 (2009)
Harvard Univ.

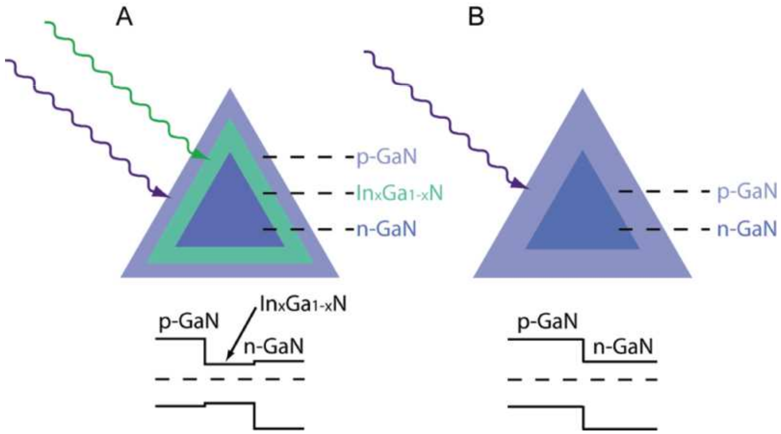

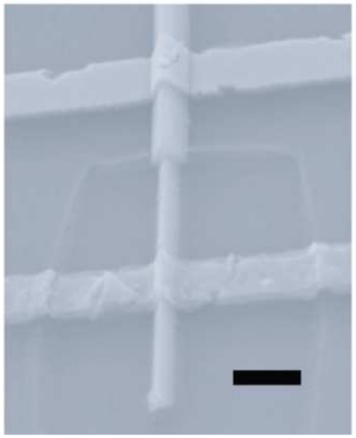

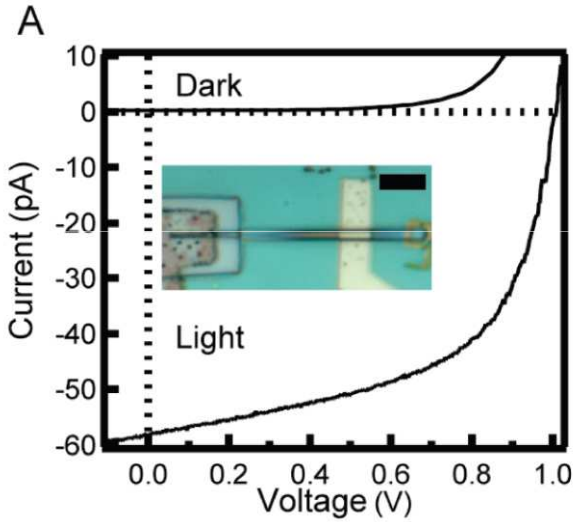

Green cell (EL peak at 556 nm)
1-sun illumination
J_{SC}=58pA
V_{OC}=1V
Conversion efficiency =0.2%
(very weak absorption)

→ nano-photodetector

Nanolasers and nano-photodetectors

J.C. Johnson et al, Nature Mat. 1, 106 (2002)
Univ. California, Berkeley

Single GaN NW

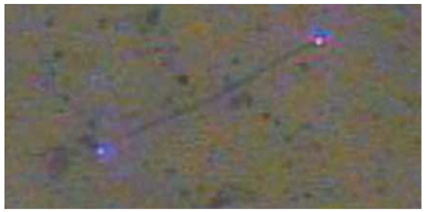

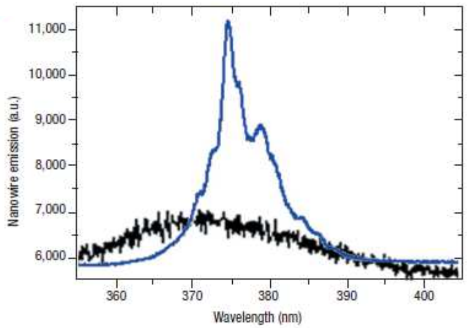

PL under CW optical excitation (1mW)
Lasing under pulsed excitation (1µJ.cm^{-2})

Application→ nanodevices on bio-chips / nano-sensors

Rigutti et al, Nano Lett. 10, 2939 (2010)
IEF, Orsay

GaN n-i-n device

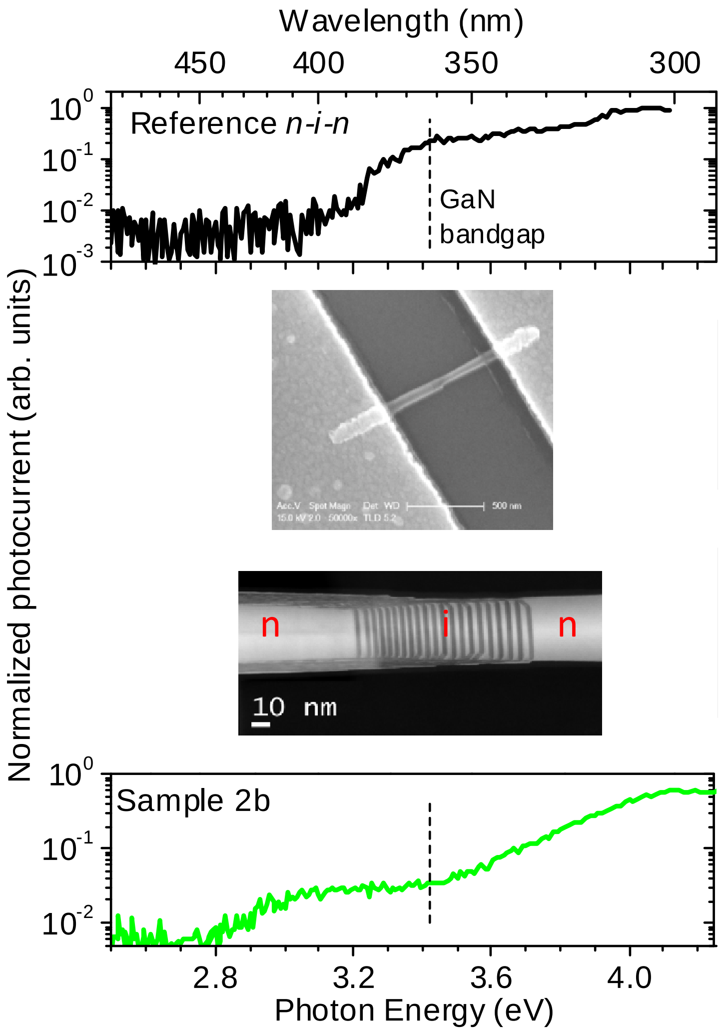

Device with GaN/AlN Qdiscs

Piezo electric nano-generators

Z. L. Wang et al 2006 Science 312 242 (2006)
Georgia Inst. Technol. , Atlanta

Xu et al, Nanotechnology 22, 105704 (2011)
IMEP, Grenoble

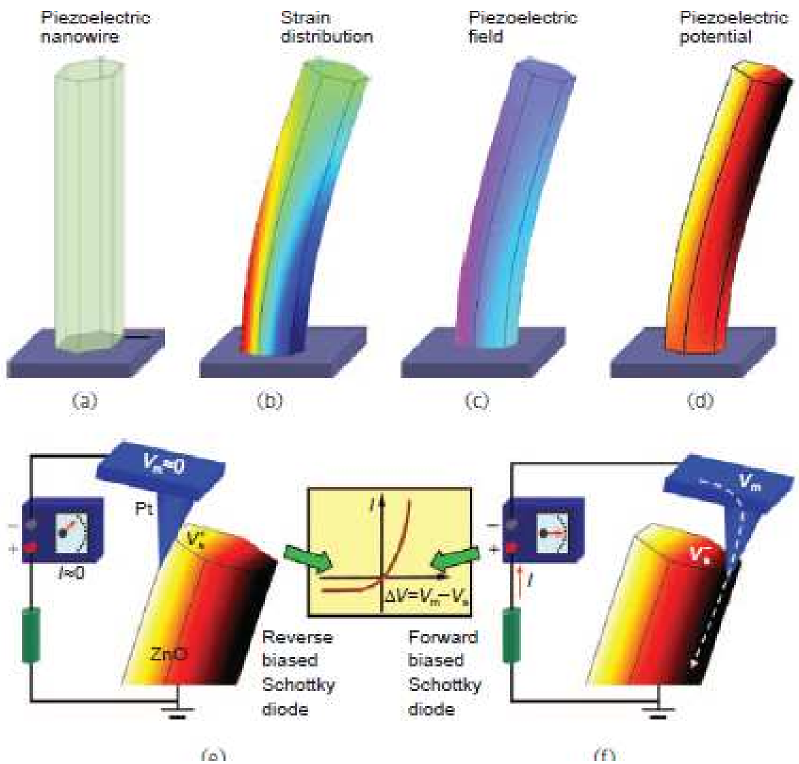

Power generation from bending NWs

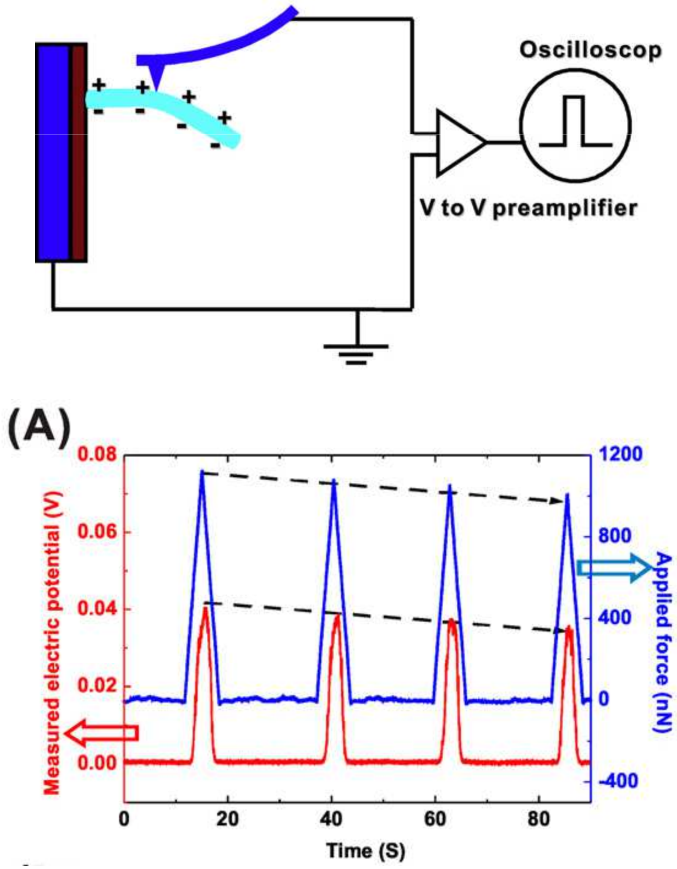

Spontaneous electric potential measured in GaN nanowires

Application→ self-powering of nano-systems

Photonic properties

Kölper , Phys. Status Solidi C 8, 2305 (2011)
Osram Opto Semiconductors, Regensburg

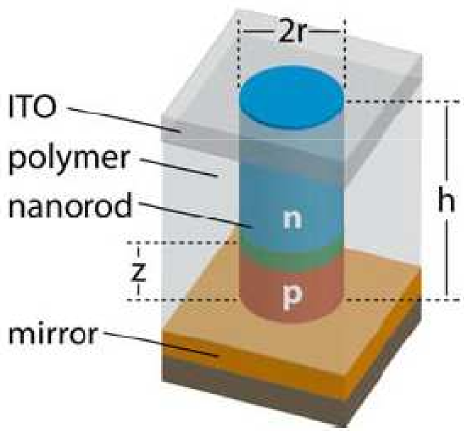

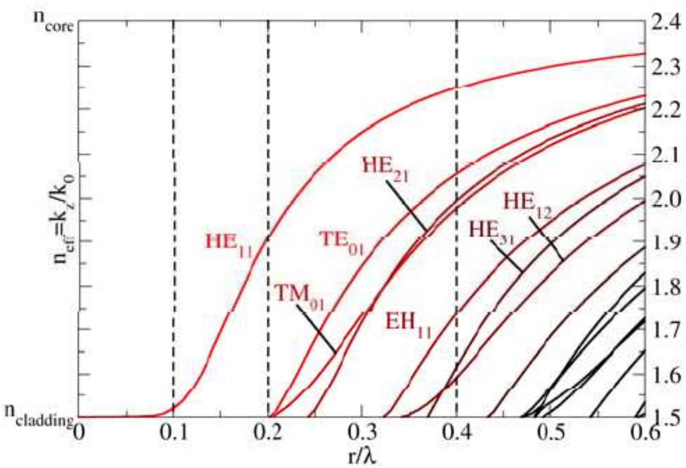

a NW can act as a monomode waveguide
for r/λ<0.2

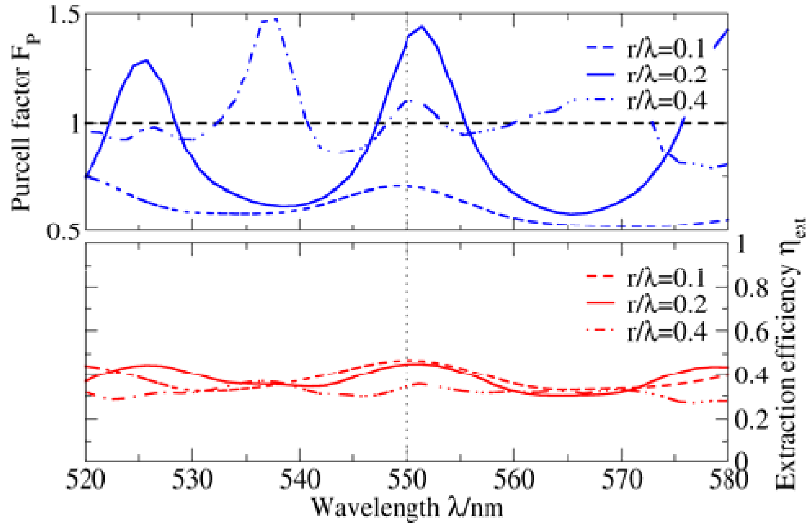

Purcell factor and light extraction efficiency

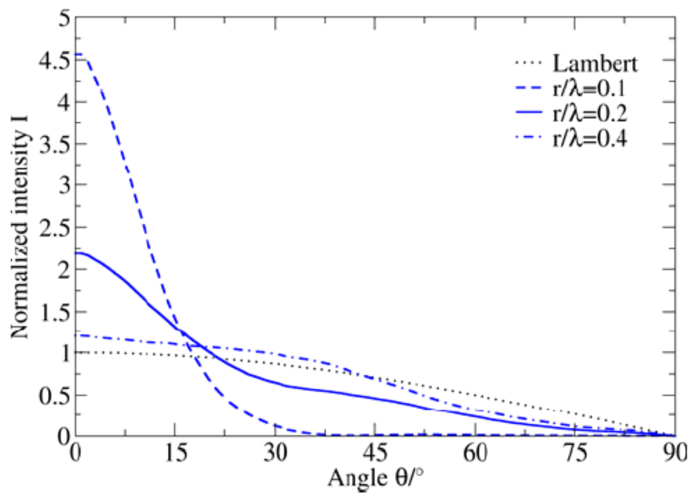

Directivity of the light emission

Brief outlook on III-N NW devices

NW ensembles

A few promising characteristics

Very challenging competition with established technologies based 2D layers

Advantage of the large choice of substrates

Uniform injection/collection in NW ensembles is necessary (regular arrays)

Single NWs

More academic studies

Single photon emitter

Sensors in micro-systems